IOWA STATE UNIVERSITY
Digital Repository

Graduate Theses and Dissertations

Iowa State University Capstones, Theses and Dissertations

2020

Resilience-oriented design and proactive preparedness of electrical distribution system

Shanshan Ma
Iowa State University

Follow this and additional works at: https://lib.dr.iastate.edu/etd

Recommended Citation

Ma, Shanshan, "Resilience-oriented design and proactive preparedness of electrical distribution system" (2020). *Graduate Theses and Dissertations*. 17958.
https://lib.dr.iastate.edu/etd/17958

This Thesis is brought to you for free and open access by the Iowa State University Capstones, Theses and Dissertations at Iowa State University Digital Repository. It has been accepted for inclusion in Graduate Theses and Dissertations by an authorized administrator of Iowa State University Digital Repository. For more information, please contact digirep@iastate.edu.

www.manaraa.com

Resilience-oriented design and proactive preparedness of electrical distribution systems

by

Shanshan Ma

A dissertation submitted to the graduate faculty

in partial fulfillment of the requirements for the degree of

DOCTOR OF PHILOSOPHY

Major: Electrical Engineering

Program of Study Committee:
Zhaoyu Wang, Major Professor
Venkataramana Ajjarapu
Ian Dobson
James D. McCalley
Leigh Tesfatsion

The student author, whose presentation of the scholarship herein was approved by the program of study committee, is solely responsible for the content of this dissertation. The Graduate College will ensure this dissertation is globally accessible and will not permit alterations after a degree is conferred.

Iowa State University

Ames, Iowa

2020

Copyright © Shanshan Ma, 2020. All rights reserved.

المنارة للاستشارات

www.manaraa.com

DEDICATION

I would like to dedicate this thesis to my husband Yu Chen and to my little baby Marcus without their support I would not be able to complete this work. I would also like to thank my friends and family for their loving guidance and support during the writing of this work.

المنارة للاستشارات
www.manaraa.com

TABLE OF CONTENTS

Page

LIST OF TABLES v

LIST OF FIGURES vi

ACKNOWLEDGMENTS vii

ABSTRACT ix

CHAPTER 1. OVERVIEW 1
- 1.1 Research Motivation and Problem Statement 1
- 1.2 Research Objective 3
- 1.3 Organization of the Dissertation 3

CHAPTER 2. REVIEW OF LITERATURE 5
- 2.1 Overview 5
- 2.2 Resilience-oriented Design Measures 5
- 2.3 Resilience-oriented Operational Measures 7
- 2.4 Summary 10

CHAPTER 3. RESILIENCE-ORIENTED DESIGN OF DISTRIBUTION SYSTEMS USING STOCHASTIC PROGRAMMING 11
- 3.1 Overview 11
- 3.2 Stochastic Decision Process Modeling 12
  - 3.2.1 The First Stage Decisions 13
  - 3.2.2 Uncertainty Modeling 14
  - 3.2.3 The Second Stage Decisions 18
  - 3.2.4 Probability of sampled scenarios 19
  - 3.2.5 Scenario Generation 19
- 3.3 Two-Stage Stochastic MILP ROD Formulation 21
  - 3.3.1 The First Stage Problem 22
  - 3.3.2 The Second Stage Problem 25
- 3.4 Solution Algorithm 34
  - 3.4.1 A Compact Notation Form of ROD Model 34
  - 3.4.2 Dual Decomposition Algorithm 34
- 3.5 Simulation and Results 36
  - 3.5.1 Test Case: IEEE-123 Distribution Feeder 36
  - 3.5.2 Case1: Comparison with and without ROD 38
  - 3.5.3 Case2: The Self-Healing Operation 40

المنارة للاستشارات
www.manaraa.com

3.5.4 Computational Results . . . 41
3.5.5 Solution Validation . . . 42
3.6 Summary . . . 43

CHAPTER 4. RISK-AVERSE PROACTIVE PREPAREDNESS OF ELECTRICAL DISTRIBUTION SYSTEMS WITH CONDITIONAL VALUE-AT-RISK . . . 45
4.1 Overview . . . 45
4.2 Proposed Methodology . . . 45
4.2.1 Uncertainty Estimation under Extreme Weather Events . . . 46
4.2.2 Proactive Energy Management and Preparation . . . 48
4.3 Two-stage Stochastic Mixed-Integer Programming Formulation with CVaR Constraints 49
4.3.1 Conditional Value-at-Risk as a Risk Measure . . . 49
4.3.2 Conditional Value-at-Risk in Optimization . . . 50
4.3.3 Mathematical Formulation . . . 53
4.4 Solution Algorithm . . . 66
4.4.1 The Compact Notation of Pre-Event Preparation Problem . . . 66
4.4.2 Progressive Hedging Algorithm . . . 66
4.4.3 Lower Bounds on CVaR-Based Stochastic Integer Programs . . . 67
4.5 Numerical Results . . . 69
4.5.1 Input Data . . . 69
4.5.2 Pre-event Resource Preparation Results with $\alpha = 95\%$ . . . 70
4.5.3 Resilience Analysis . . . 71
4.5.4 Risk Analysis . . . 73
4.6 Summary . . . 76

CHAPTER 5. CONCLUSIONS AND FUTURE WORK . . . 77
5.1 Conclusion . . . 77
5.2 Research Contribution . . . 79
5.2.1 Resilience-Oriented Design of Distribution Systems . . . 79
5.2.2 Risk-Averse Proactive Preparedness of Distribution Systems with Conditional Value-at-Risk . . . 79
5.3 Future Work . . . 80
5.3.1 Resilience Assessment of Distribution Systems . . . 80
5.3.2 Resilience-oriented Design of Distribution Systems Using Risk Measures . . . 81
5.3.3 Proactive Preparedness . . . 81
5.4 Publications . . . 81

REFERENCES . . . 83

المنارة للاستشارات
www.manaraa.com

LIST OF TABLES

		Page
Table 3.1	Nomenclature for the SMILP ROD model	23
Table 3.2	Evaluation of the on-off status variable	29
Table 3.3	The investment cost of different ROD measures	38
Table 3.4	The solution quality statics for DD algorithm solving ROD problems	42
Table 4.1	Nomenclature for the CVaR-based SMILP model	53
Table 4.2	The cost parameters for simulation	69
Table 4.3	The amount of load served, average outage duration and pre-event allocation cost with different confidence level α	73

المنارة للاستشارات
www.manaraa.com

LIST OF FIGURES

		Page
Figure 1.1	The number, type, and annual cost of U.S. billion-dollar disasters from 1980 to 2018, based on NCEI data in 2019 [1]	2
Figure 3.1	Decision process for ROD problem.	12
Figure 3.2	Pole types.	13
Figure 3.3	The structure of uncertainty space: independent observable random variables/processes (highlighted in red) + deterministic casual connections (parameterized by the first-stage decision).	15
Figure 3.4	Multipliers of load profiles at the substation (root node), with the peak values as the bases.	17
Figure 3.5	The illustrative example for isolating a contingency	27
Figure 3.6	Simulating a distribution pole's damage status in a hurricane	39
Figure 3.7	The optimal ROD methods implementation	40
Figure 3.8	The second stage cost comparison with and without ROD under different scenarios	41
Figure 3.9	The system resilience curve comparison	41
Figure 3.10	System's self-healing operation at $t = 10$	42
Figure 3.11	System's self-healing operation at $t = 21$	43
Figure 4.1	The sequential actions of the distribution system operator for an upcoming extreme weather event	46
Figure 4.2	Line damage status simulation procedure	47
Figure 4.3	The VaR_α and CVaR_α of damage loss $\pi(\boldsymbol{x}, \boldsymbol{\xi})$	51
Figure 4.4	The optimal pre-event resource preparation at confidence level $\alpha = 95\%$	70
Figure 4.5	The optimal pre-event resource preparation at different confidence level α	71
Figure 4.6	The damaged lines in the additional random scenario with $\alpha = 95\%$	72
Figure 4.7	Load served percentage comparison for different confidence level α	73
Figure 4.8	The value of CVaR_α solutions over ER solutions	75
Figure 4.9	The value of ER solutions over CVaR_α solutions	75

المنارة للاستشارات
www.manaraa.com

ACKNOWLEDGMENTS

I would like to take this opportunity to express my thanks to those who helped me with various aspects of conducting research and the writing of this thesis. First and foremost, Dr. Zhaoyu Wang for his guidance, patience, and support throughout this research and the writing of this thesis. His insights and words of encouragement have often inspired me to explore new approaches for solving my research problems and renewed my hopes for completing my graduate education. He helped me to become a strongly self-motivated researcher.

Secondly, I would like to thank my committee members for their efforts and contributions to this work: Dr. Venkataramana Ajjarapu, Dr. Ian Dobson, Dr. James D. McCalley, and Dr. Leigh Tesfatsion. It is my honor to take those famous professors' classes at Iowa State University. Dr. Ajjarapu's lecture on the steady study of power system enhanced my fundamental knowledge of the power system. In Dr. McCalley's power system planning class, I got some instrumental conceptions on the planning optimization problems. Dr. Dobson's resilience lecture helped me to rethink the definition of resilience. With cooperation with Dr. Tesfatsion, I learned how to describe my idea logically. I would additionally like to thank Dr. Lizhi Wang for his inspirational teaching of linear programming and optimization. His lecture inspired me to mathematically model my research problems and find practical algorithms to solve them. I also tremendously appreciated Dr. Sarah M Ryan's guidance in the stochastic programming.

Thirdly, I would like to thank my collaborators: Dr. Bokan Chen, Dr. Liu Su, Dr. Ge Guo, Dr. Anmar Arif, and Dr. Shiyang Li. Dr. Chen helped me to get into my research quickly, and with his help, I published my first transaction journal. Dr. Liu strengthened my understanding of decision-dependent uncertainty. Dr. Guo taught me how to use high-performance computation and formulate stochastic programming problems in the Pyomo, which are very useful for my research. Dr. Li always gave me the robust support for my research. Each time's discussion always sharpened

المنارة للاستشارات
www.manaraa.com

my intelligence and inspired me to generate new ideas. He can explain the problems in the power system in a mathematically way and gave me very good suggestions for my research.

Fourthly, I would like to thank my friends: Dr. Qian Zhang, Dr. Xian Guo, Dr. Yihua Li., Dr. Dan Hu, Kai Zhou, Nichelle'Le Carrington and my labmates. Their accompanying let me know I am not alone as a Ph.D. student.

Finally, I want to express my thanks to my family for their support. Without my husband's help, I even can not start my Ph.D. life. Thanks to my parents' understanding and support as it has been five years that I did not go back home and missed so many important family events. I do appreciate my parents-in-law's taking care of my new-born baby, especially my mother-in-law Mrs. Emei Tang. Without her help, I cannot finish my thesis writing and come back to my research.

المنارة للاستشارات

www.manaraa.com

ABSTRACT

Extreme weather events, such as hurricanes and ice storms, pose a top threat to power distribution systems as their frequency and severity increase over time. Recent severe power outages caused by extreme weather events, such as Hurricane Harvey and Hurricane Irma, have highlighted the importance and urgency to enhance the resilience of electric power distribution systems. The goal of enhancing the resilience of distribution systems against extreme weather events can be fulfilled through upgrading and operating measures. This work focuses on investigating the impacts of upgrading measures and preventive operational measures on distribution system resilience. The objective of this dissertation is to develop a multi-timescale optimization framework to provide some actionable resilience-enhancing strategies for utility companies to harden/upgrade power distribution systems in the long-term and do proactive preparation management in the short-term.

In the long-term resilience-oriented design (ROD) of distribution system, the main challenges are i) modeling the spatio-temporal correlation among ROD decisions and uncertainties, ii) capturing the entire failure-recovery-cost process, and iii) solving the resultant large-scale mixed-integer stochastic problem efficiently. To deal with these challenges, we propose a hybrid stochastic process with a deterministic casual structure to model the spatio-temporal correlations of uncertainties. A new two-stage stochastic mixed-integer linear program (MILP) is formulated to capture the impacts of ROD decisions and uncertainties on system responses to extreme weather events. The objective is to minimize the ROD investment cost in the first stage and the expected costs of loss of load, DG operation, and damage repairs in the second stage. A dual decomposition (DD) algorithm with branch-and-bound is developed to solve the proposed model with binary variables in both stages. Case studies on the IEEE 123-bus test feeder have shown the proposed approach can improve the system resilience at minimum costs.

المنارة للاستشارات
www.manaraa.com

For an upcoming extreme weather event, we develop a pre-event proactive energy management and preparation strategy such that flexible resources can be prepared in advance. In order to explicitly materialize the trade-off between the pre-event resource allocation cost and the damage loss risk associated with an event, the strategy is modeled a two-stage stochastic mixed-integer linear programming (SMILP) with Conditional Value at-Risk (CVaR) constraints. The progressive algorithm is used to solve the proposed model and obtain the optimal proactive energy management and preparation strategy. Numerical studies on the modified IEEE 123-bus test feeder show the effectiveness of the proposed approach to improve the system resilience at different risk levels.

المنارة للاستشارات
www.manaraa.com

CHAPTER 1. OVERVIEW

1.1 Research Motivation and Problem Statement

The extreme weather-caused outages have resulted in substantial economic losses in recent years in the United States. Between 2003 and 2012, roughly 679 power outages, each affecting at least $50,000$ customers, occurred due to weather events in the United States, and 80%-90% of these outages were due to failures in distribution systems [2]. For example, Hurricane Sandy in 2012 paralyzed the power systems of several coastal states and resulted in outages that affected over 8.5 million customers [3]. Moreover, the number and cost of extreme weather events have increased over time due to a combination of increased exposure, vulnerability, and the fact the climate change is increasing the frequency of some types of extreme weather events that have led to billion-dollar disasters [1]. A summary for the number, type, and annual cost of U.S. billion-dollar disasters from 1980 to 2018 is shown in Figure 1.1. In the Figure 1.1, the number of severe storm events accounts for more than 50% of the total number of extreme events, and they have brought more than $150 billion/year in damage costs over the last three years. For example, Hurricane Irma in 2017 knocked out power to 6.7 million electricity customers—64% of all customers accounts in the state of Florida— and its overall damage cost reached to approximately 50 billion [4, 5].

However, most existing distribution systems are designed and maintained for normal weather conditions and cannot withstand extensive damages caused by the low-probability but high-intense extreme weather events [6]. Moreover, U.S. power grids are now old and outdated, making them more vulnerable to extreme weather events. Although the majority of utilities have recognized the necessity of taking actions to upgrade the grid against extreme weather events, they still make grid upgrading decisions based on experiences, patrols, and observations instead of leveraging systematic and rigorous optimization techniques that are based on risk and consequence analysis. A common approach is to upgrade previously damaged facilities or perform targeted components hardening

المنارة للاستشارات
www.manaraa.com

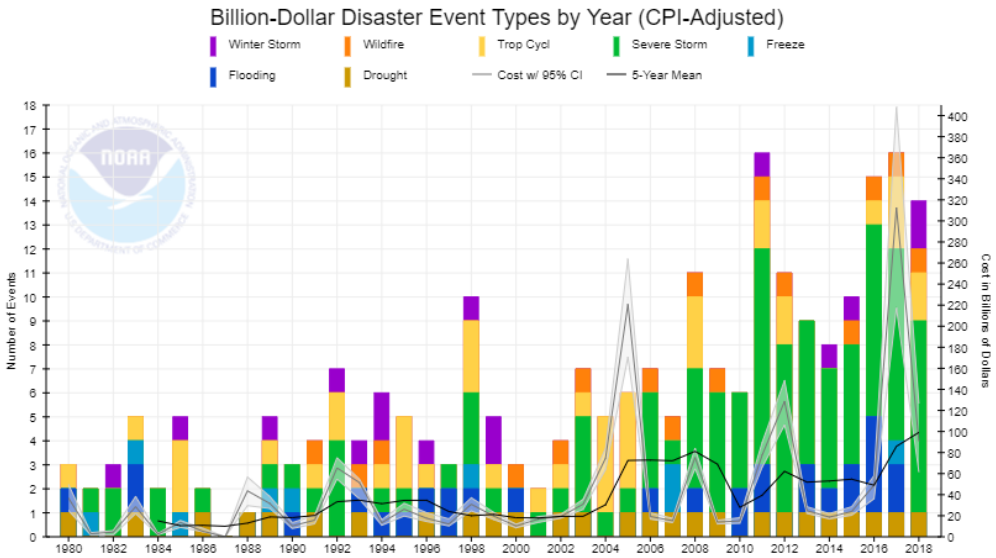

Figure 1.1 The number, type, and annual cost of U.S. billion-dollar disasters from 1980 to 2018, based on NCEI data in 2019 [1]

based on experience. In addition, it is economically infeasible to harden/upgrade all the systems and take all potential extreme events into account. On the other hand, advanced weather forecasting methodologies and damage estimation process provide utilities the ability to predict the severity of damage to distribution systems before extreme weather events. If the utility can pre-allocating the available flexible resources such as mobile emergency generator and energy storage, and repair crews in advance, it can reduce the potential damage loss and decrease the restoration time. Therefore, the need is to develop a decision support tool for long-term designing resilient distribution systems and short-term preparing flexible resources for upcoming extreme weather events.

Power grid resilience is the ability to prepare for, absorb, recover from, or more successfully adapt to actual or potential adverse events [7]. The resilience-enhancement goals can be fulfilled through upgrading and operating measures [8]. This work focuses on investigating the impacts of upgrading measures and preventive operational measures on distribution system resilience.

المنارة للاستشارات
www.manaraa.com

1.2 Research Objective

The objectives of the dissertation are listed as follows:

- Develop a new modeling and solution methodology for the long-term resilience-oriented design of power distribution systems against wind-induced extreme weather events. The objective is to take optimal ROD measures, namely, line hardening, installing backup distributed generators (DGs), and adding automatic switches, to make distribution systems more resilient to wind-induced extreme weather events. This methodology should consider the spatial-temporal correlations among ROD measures, uncertainty space, and system operations during and after extreme weather events. It is also supposed to model the entire failure-recover-cost process of distribution systems during and after extreme weather events so that both investment and restoration costs can be modeled.

- Develop a short-term pre-event proactive energy management and preparation strategy such that flexible resources can be prepared for an upcoming event. The objective is to strategically prepare and coordinate various flexible resources, such as mobile emergency generator (MEG), mobile energy storage (MES), back-up diesel DGs, network reconfiguration, and repair crews to improve resilience during and after the event, while treats the trade-off between the damage loss risk and pre-event allocation cost.

1.3 Organization of the Dissertation

The rest of the dissertation is organized as follows:

Chapter 2 reviews the important literature and background information for enhancing the resilience of electric distribution systems under extreme weather events. It presents the general resilience-oriented operational measures and ROD measures and the relevant research works for boosting the resilience of distribution systems. Chapter 3 presents the methodology for long-term resilience-oriented design of power distribution systems. The chapter starts with the stochastic decision process to model the uncertainties under the extreme weather events. Then a two-stage stochas-

المنارة للاستشارات
www.manaraa.com

tic programming formulation and solution algorithm for ROD problems are presented. Chapter 4 presents a short-term proactive energy management and preparation approach for an upcoming extreme weather event. A two-stage stochastic mixedinteger linear programming (SMILP) with Conditional Valueat-Risk (CVaR) constraint is modeled for preallocating flexible resources and the Progressive Hedging algorithm is introduced. Chapter 5 presents the conclusions and contributions of this work and includes a discussion of possible future works.

المنارة للاستشارات
www.manaraa.com

CHAPTER 2. REVIEW OF LITERATURE

2.1 Overview

This chapter presents a review of the literature and background information for enhancing the resilience of electric distribution systems under extreme weather events. The efforts to enhance distribution system resilience can be classified into two broad categories [8, 9, 10]: resilience-oriented design measures and operational measures. Section 2.2 presents the current ROD measures and related studies for designing resilience-oriented distribution systems. Section 2.3 introduces the current main operational measures and related research for boosting system operational resilience.

2.2 Resilience-oriented Design Measures

ROD measures for enhancing distribution system resilience refer to physical changes of the utility's infrastructure to make it less susceptible to extreme weather event damages, such as high winds, flooding, or flying debris [11]. It aims to improve the grid infrastructures' durability and stability and allow the system to withstand the impacts of extreme weather events with minimal damage. The general ROD measures used by utilities include grid hardening, installing DGs, and adding line switches.

Various grid hardening strategies can protect systems against extreme weather events. These include overhead structure reinforcement, vegetation management, undergrounding distribution lines, and the relocation of facilities. Overhead structure reinforcement constitutes a primary hardening strategy that involves upgrading distribution poles to a stronger class, enhancing guying, and refurbishing poles. Extensive vegetation management also can contribute to distribution system hardening, as fallen trees and debris are credited with the majority of power outages that occur during severe storms in the Northeastern part of the United States [12]. Undergrounding distribution lines can reduce system susceptibility to wind-induced damages, lightning, and vegetation contacts,

المنارة للاستشارات
www.manaraa.com

but they extend restoration time with a high installation and repair cost. Elevating substations and relocating facilities to areas that are less prone to extreme weather can help protect against floods.

The installation of back-up DGs can provide on-site power for critical facilities and load centers and contribute to energizing MGs to restore load after an extreme weather event [13, 14, 15]. Installing automatic switches enables network reconfiguration that can reroute power to on-outage portions of distribution networks, shorten the restoration time, and enhance the restoration capability [16]. Although resilience-oriented planning measures could reduce physical infrastructure failures and restoration efforts, hardening and upgrading the entire distribution systems are potentially expensive.

A few optimization models have been proposed to optimally implement those resilience-oriented planning measures to protect against extreme weather events, which in general apply two types of modeling techniques: robust and stochastic modeling. Yuan *et al.* [17] proposed a new robust optimization model to solve the resilient distribution network planning problem under the worst scenario of extreme weather events. However, their study used a polyhedral set to represent damage uncertainty, where grid fragility models for specific extreme weather events were ignored in calculating the uncertainty budget. Moreover, only one hardening measure (line hardening) was taken into consideration. In addition, it was assumed that hardened lines would not be damaged in future events, which is impractical. In [18], the authors proposed a power distribution system hardening framework using robust tri-level optimization. Three hardening strategies are considered in [18]: upgrading distribution poles, managing vegetation, and the combination of the two. A greedy algorithm was proposed to deal with the coupling issue of the hardening decisions at the first level and the damage uncertainty in the second level. However, some important ROD measures were missed, such as the installation of DGs and automatic tie switches. A tri-level robust optimization model was presented in [19] to explore optimal network hardening strategies for enhancing the resilience of integrated electricity and natural gas distribution systems against natural disasters. Authors considered the distinct failure probabilities of overhead distribution lines and underground

المنارة للاستشارات
www.manaraa.com

gas pipelines and applied DGs and gas storage facilities as effective emergency response resources to supply critical loads.

Another approach to manage uncertainty in ROD problems is stochastic programming. Stochastic programming is an extension of standard deterministic mathematical programming, in which the space of possible outcomes (e.g., line failure uncertainty) is represented by a probability-weighted scenario tree. Yamangil *et al.* [20] proposed a scenario-based variable neighborhood decomposition search algorithm to design resilient electrical distribution grids. This work improved previous studies by assuming that the hardened lines could be damaged at the rate of $\frac{1}{10}$ of unhardened counterparts. However, the interrelation between the first-stage line hardening decisions and the uncertain line damage status was not taken into account. The decision-dependent uncertainty is inherent in infrastructure resilience enhancement. This is because resilience enhancement can only change the failure probability of system components, but cannot reduce it to zero. To manage the risk more realistically, it is necessary to model the failure of system components as a decision-dependent uncertainty. Arab et al. [21] proposed a proactive resource allocation model for the repair and restoration of potential damages to power system components in the traveling paths of upcoming hurricanes. They used Bender's decomposition to solve the two-stage stochastic integer program. However, the quality of the solutions was not evaluated. Moreover, Bender's decomposition is efficient in solving stochastic programs with linear programming problems, but not for mixed-integer programs in the second stage. A two-stage stochastic program model was introduced in [22] to design resilient distribution grids and simultaneously considers hardening options, redundancy options, MGs, and networked MGs.

2.3 Resilience-oriented Operational Measures

Operational measures refer to "smart" control-based actions taken to provide preventive and corrective operational flexibility for effectively dealing with unfolding extreme weather events [9]. They aim to make the distribution system "bend" rather than "break" in the face of an extreme weather event [23]. The potential operational measures include network reconfiguration, distributed gen-

المنارة للاستشارات
www.manaraa.com

eration (DG) rescheduling, conservation voltage regulation (CVR), defensive islanding, microgrid-assisted control actions, and priority-based load shedding. Those operational measures contribute to conservatively anticipating and coping with the adverse impacts of extreme weather events.

In the context of operational measures for preventive preparation in the resilience enhancement of electric distribution systems, many researchers have investigated pre-event resource allocation problems. A pre-hurricane generation resource allocation approach was presented in [13] to enhance the capability of microgrids (MGs) and DGs to serve outage critical load during the post-hurricane restoration. A novel defensive islanding algorithm was proposed in [24] to split the distribution system into stable and self-adequate islands in order to isolate vulnerable components before extreme weather events, as the failure of these items could trigger cascading events. The role of MGs has become important in establishing proactive measures for enhancing distribution system resilience. A MG proactive management framework was presented in [23] to cope with the adverse impacts of extreme windstorms. The schedule ensures the normal operation of MG before a windstorm while reducing the MG vulnerability at the event onset. A proactive scheduling methodology of MGs was proposed in [25] to run the resilience-constrained optimal power flow in the pre-event phase to minimize the adverse impacts of an upcoming flood. The authors in [26] employed a two-stage adaptive robust optimization model for scheduling MG in advance to reduce the damaging consequences of extreme weather events. Other researchers in [27] presented a preventive resource allocation methodology to form MGs to restore critical loads after a large external disturbance while satisfying post-disaster and operational constraints within each MG. A two-stage framework that comprises pre-positioning and real-time allocation was proposed in [28] to dispatch mobile energy generators to some nodes to restore critical loads after extreme weather events by forming multiple MGs. Authors in [29] developed a two-stage stochastic mathematical model to select staging locations, and allocate crews and equipment for disaster preparation. However, there remains some limitations in the above studies on the short-term preparation and response for an upcoming extreme weathe event: (1) Coordination of multiple flexible resources, such as mobile generators and pre-staging repair crews, is not comprehensive; (2) Weather-induced uncertainties

المنارة للاستشارات
www.manaraa.com

are oversimplified; (3) Approximation of three-phase unbalanced power flow model is not tight; (4) The trade-off between pre-event allocation cost and risk associated with damage loss under the upcoming event is not considered.

In the context of operational measures for corrective strategies after extreme weather events, many types of repair and restoration techniques have been explored. Various algorithms of network reconfiguration have been proposed for load restoration, including heuristic techniques, dynamic programming, and multi-agent systems [30]. Recently, some studies have shown the potential to use DGs and MGs to assist restoration process. A resilience-oriented service restoration method by using MGs with limited generation resources was proposed in [14] to serve critical loads on distribution feeders after an extreme event. The authors in [31] proposed a hierarchical outage management scheme comprised of multi-microgrids to enhance the resilience of a smart distribution system against unexpected disaster events. An optimal critical service restoration strategy was presented in [32] to integrate MG formation and load switching sequence, and exploit the mobility, flexibility, and resilience of MGs to address the risk of service restoration in extended extreme events. The authors in [33] proposed a decentralized multi-agent system (MAS) approach for service restoration using controlled DG islanding. A novel distribution system operational approach by forming multiple microgrids energized by DGs was presented in [34] to restore critical loads in distribution systems after the power outages.

In the literature mentioned above regarding restoration techniques, the repair process of damaged components was either assumed to be specific, or the repair time was assumed to be known. However, a faster or an optimal crew repair process can reduce the duration and size of power outage and accelerate the restoration process. Some researches have explored the importance of crew dispatch assignments in the optimality of the restoration sequence. Xu *et al.* in [35] proposed a stochastic integer program to determine how to schedule the inspection, damage assessment, and repair tasks of a set of substations to optimize the post-earthquake restoration of electric power systems. A dynamic programming model was presented in [36] to determine the optimal sequence of manual switch operations for distribution system restoration, taking the dynamic crew dispatch-

المنارة للاستشارات
www.manaraa.com

ing into consideration. The authors in [37] proposed a methodology using concepts of queuing theory and stochastic point processes to determine the repair schedules in each service territory of a power distribution system. A mixed-integer linear programming model was introduced in [38] for scheduling maintenance vehicles under emergency scenarios in electrical distribution systems to minimize the dispatch time.

Other attempts have been made to integrate repair scheduling with restoration to enhance the resilience of electric distribution systems. The authors in [30] formulated the distribution system repair and restoration problem as a two-stage mixed integer linear program, considering constraints of system operation and repair crew routing. Then, Arif *et al.* in [39] extended the deterministic formulation in [30] to a two-stage stochastic mixed-integer program model to solve the repair and restoration problem considering the stochastic nature of the repair time and the customer load demand. Other researchers in [40] proposed a synthetic model that was introduced to co-optimize service restoration and crew dispatch problems. The proposed optimal synthetic restoration solution includes the optimal switching sequence of remote-controlled and manually operated switches, an optimal routing sequence of operation and repair crews, and an optimal load energization sequence. A mixed-integer nonlinear programming (MINLP) model was developed in [41] to co-optimize the routing and scheduling of repair crews and mobile power sources, and dynamic network reconfiguration for disaster recovery logistics.

2.4 Summary

This chapter provided a description and literature review for the research topics covered in this dissertation. The general ROD measures were discussed in section 2.2, and the optimization frameworks for optimally implementing them were covered in section 2.2. Section 2.3 summarized the general resilience-oriented operational measures and related research on the problems related to pre-event resource allocation, crew repair, and restoration.

المنارة للاستشارات
www.manaraa.com

CHAPTER 3. RESILIENCE-ORIENTED DESIGN OF DISTRIBUTION SYSTEMS USING STOCHASTIC PROGRAMMING

3.1 Overview

A distribution system is considered to be resilient if it is able to anticipate, absorb, adapt to, and/or rapidly recover from a disruptive event [7]. The resilience enhancement goals can be fulfilled through resilience-oriented operational and design measures [8].This chapter focuses on exploring the impacts of ROD measures on system resilience. The primary challenge of distribution system ROD is to model the entire failure-recovery-cost process. Specifically, evaluating the damage states requires the modeling of various spatial-temporal uncertainties in weather events and structural strengths, and some of them are decision-dependent. The recovery phase is usually neglected in the existing literature on ROD. However, the ROD decisions affect the system recovery and the associated outage/repair costs. For example, adding DGs and switches offer self-healing capabilities such as reconfiguration and automatic microgrid formation. These self-healing actions are time-varying. In addition, there is an interaction between structural damages and electric outage propagation, as the outage induced by physical damages may propagate in the network until a sectionalizer isolates the fault. To overcome these challenges, section 3.2 propose a novel stochastic decision process to describe the spatio-temporal correlations among ROD decisions, uncertainties of extreme weather events, and system operation. A two-stage stochastic MILP formulation is proposed in section 3.3 to describe these spatial-temporal correlations of ROD decisions and uncertainty space with the operation behavior during extreme weather events. Section 3.4 introduces the DD algorithm to achieve the exact optimal solutions for the two-stage stochastic MILP of the ROD problem. The proposed methodology is validated on a modified IEEE 123-bus distribution test system in section 3.5.

المنارة للاستشارات
www.manaraa.com

3.2 Stochastic Decision Process Modeling

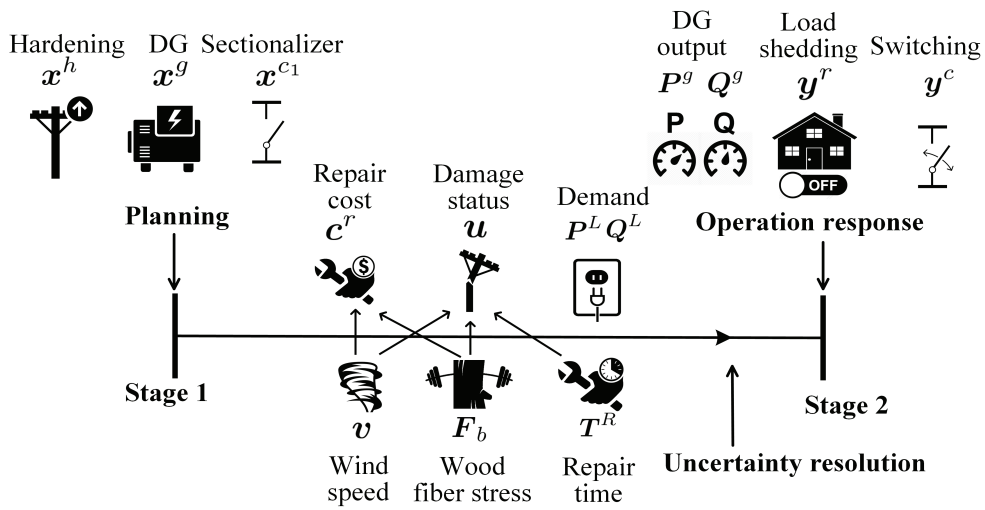

Figure 3.1 Decision process for ROD problem.

The goal of ROD for a distribution system is to optimally apply ROD measures to prevent system from extensive damages caused by extreme weather events. However, the operation condition of distribution systems during an extreme weather event is affected by many random factors and some of them are coupled with ROD decisions. It results in the complexity of uncertainty modeling. As depicted in Figure 3.1, the ROD problem is modeled as a two-stage stochastic decision process: (i) the planner makes ROD decisions, i.e., pole hardening, installing backup DGs and adding sectionalizers in the first stage; (ii) then the operational uncertainties are resolved during the hazards, which include (a) power demand, (b) line damage statuses, and (c) line repair costs; (iii) the operator makes the recourse decisions (i.e., DG re-dispatch, load shedding, and reconfiguration) to minimize the operational cost during an extreme weather event in the second stage. Notice that the line statuses are determined by wind speeds, pole strengths, and repair times, all of which are stochastic. In particular, pole strengths and repair times are decision-dependent. Note that as the wind-induced extreme weather events pose the top resilience-related threat to distribution system, we focus on the uncertainty modeling caused by wind-induced extreme weather events.

المنارة للاستشارات
www.manaraa.com

3.2.1 The First Stage Decisions

The resilience of distribution systems can be effectively enhanced by (i) strengthening vulnerable components, (ii) increasing adequacy of power supply, and (iii) increasing topological flexibility. Accordingly, this dissertation considers the following resilience-enhancing methods: (a) upgrading pole classes, (b) adding transverse guys, (c) installing backup DGs, and (d) adding sectionalizers. Thus, the first-stage decisions are represented by a row vector $\boldsymbol{x} = \left[\boldsymbol{x}^h, \boldsymbol{x}^g, \boldsymbol{x}^{c_1}\right]$, which is explained as follows.

3.2.1.1 Hardening poles

For illustration, three commonly used pole types are considered: Southern Yellow Pine pole 40-2, 40-3, and 40-4, each with or without guying [42]. Thus, there are $2 \times 3 = 6$ pole types (see Figure 3.2). For each line section, 6 binary decision variables are used to represent which pole type is used for this line: let $\boldsymbol{x}^h_{ij} = \left[x^h_{ij,1}, x^h_{ij,2}, x^h_{ij,3}, x^h_{ij,4}, x^h_{ij,5}, x^h_{ij,6}\right] \in \{\mathbf{1}, \mathbf{2}, \mathbf{3}, \mathbf{4}, \mathbf{5}, \mathbf{6}\}$ denote the selected pole type for line (i, j). For example, $\boldsymbol{x}^h_{ij} = \left[x^h_{ij,1}, x^h_{ij,2}, x^h_{ij,3}, x^h_{ij,4}, x^h_{ij,5}, x^h_{ij,6}\right] = \mathbf{1} = [1, 0, 0, 0, 0, 0]$ indicates pole type 1 (40-2 with guying) is used. We have $\boldsymbol{x}^h = \left[\boldsymbol{x}^h_1, \boldsymbol{x}^h_2, \ldots, \boldsymbol{x}^h_{|\Omega_B|}\right] \in \{0, 1\}^{6|\Omega_B|}$ denoting pole types and implying pole hardening decisions of all lines. The formulation can be easily extended to include more pole types.

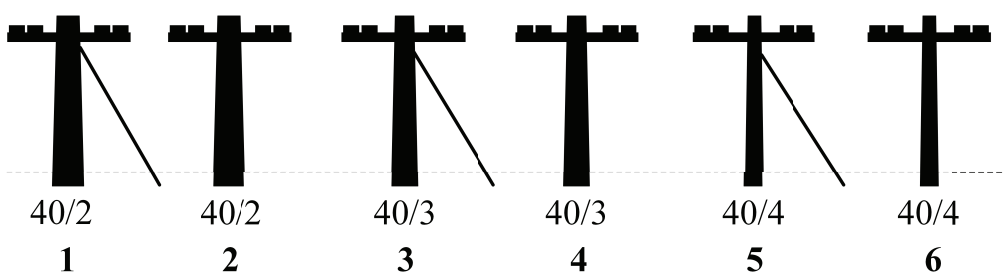

Figure 3.2 Pole types.

المنارة للاستشارات
www.manaraa.com

3.2.1.2 Installing Backup DGs

This paper considers backup DGs that are dispatchable during hazards. Let $\boldsymbol{x}^g = \left[x_1^g, x_2^g, \ldots, x_{|\Omega_N|}^g\right] \in \{0,1\}^{|\Omega_N|}$ denote the DG deployment decisions, where a DG will be installed at node i if $x_i^g = 1$.

3.2.1.3 Adding sectionalizers

The automatic sectionalizers can be added at both ends of a line. They can be used to reroute the power flow, and isolate the faulted or damaged network sections. Let $\boldsymbol{x}_{ij}^{c_1} = \left[x_{ij,i}^{c_1}, x_{ij,j}^{c_1}\right] \in \{0,1\}^2$, where a sectionalizer is added at the end i of line (i,j) if $x_{ij,i}^{c_1} = 1$, and a sectionalizer is deployed at the end j of line (i,j) if $x_{ij,j}^{c_1} = 1$. We have $\boldsymbol{x}^{c_1} = \left[\boldsymbol{x}_1^{c_1}, \boldsymbol{x}_2^{c_1}, \ldots, \boldsymbol{x}_{|\Omega_B|}^{c_1}\right] \in \{0,1\}^{2|\Omega_B|}$ denoting the decisions of deploying sectionalizers.

3.2.2 Uncertainty Modeling

The key challenge of uncertainty modeling in a ROD problem is the spatial-temporal correlations among ROD decisions, extreme weather event uncertainties, and system operations. Besides, the hazards and system operations are time-varying. It is challenging to model these uncertainties by formulating a high-dimensional joint distribution. Therefore, a hybrid of independent stochastic processes and deterministic causal structure is proposed as shown in Figure 3.3. Based on this structure, we firstly sample independent random variables individually and then generate the correlated latent variables using the causal structure. Finally, three groups of random variables that have direct impacts on the evolution of the system operation state can be obtained (highlighted in blue): (a) line damage statuses $\boldsymbol{u}(t;\boldsymbol{x}^h) \in \{0,1\}^{|\Omega_B|}$ for $t \in \mathcal{T}_H$, where $\mathcal{T}_H$ is the time horizon set of a climatic hazard, and $|\mathcal{T}_H|$ equals the hazard duration plus the longest line repair time; (b) repair costs $\boldsymbol{c}^r \in \mathbb{R}_+^{|\Omega_B|}$; and (c) load demands $\boldsymbol{P}^L(t)$, $\boldsymbol{Q}^L(t)$, for $t \in \mathcal{T}_H$. We use $\xi = \left[\boldsymbol{u}, \boldsymbol{c}^r, \boldsymbol{P}^L, \boldsymbol{Q}^L\right] : \Omega \to \Omega_{\mathcal{S}}$ to denote the random variable associated to a scenario.

المنارة للاستشارات
www.manaraa.com

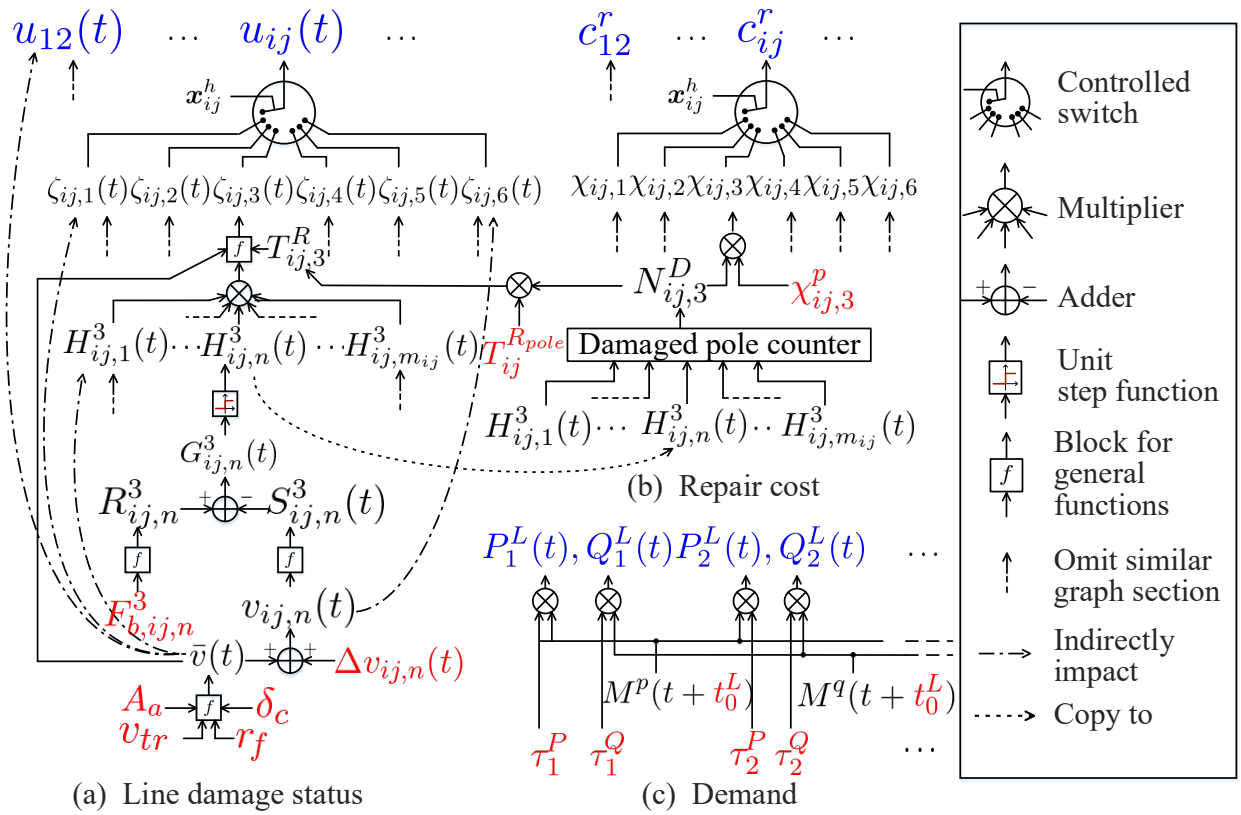

Figure 3.3 The structure of uncertainty space: independent observable random variables/processes (highlighted in red) + deterministic casual connections (parameterized by the first-stage decision).

3.2.2.1 Line Damage Status

Notice that the first-stage decision variable $\boldsymbol{x}^h$ is a parameter in $\boldsymbol{u}(t;\boldsymbol{x}^h)$ as hardening poles reduces the probability of line damage. This raises the challenge of sampling the random variables, since the distribution of $\boldsymbol{u}(t)$ cannot be determined before the decision $\boldsymbol{x}^h$ is known. It is reasonable to assume that a line's damage status is related to its own pole type, i.e., $u_{ij}(t;\boldsymbol{x}^h)=u_{ij}(t;\boldsymbol{x}^h_{ij})$ for all $(i,j)\in\Omega_B, t\in\mathcal{T}_H$, and the number of possible values of $\boldsymbol{x}^h_{ij}$ is small (6 in this dissertation) compared to the number of possible values of $\boldsymbol{x}^h$ ($6^{|\Omega_B|}$). Thus, each $u_{ij}(t)$ can be sampled in advance for all possible values of $\boldsymbol{x}^h_{ij}$, which are $\zeta_{ij,1}(t),\ldots,\zeta_{ij,6}(t)$ in Figure 3.3(a). We can regard them as different *versions* of $u_{ij}(t)$ in six "parallel universes", and only one of them will finally realize

المنارة للاستشارات
www.manaraa.com

according to the value of x_{ij}^h in the ROD solution. This selection logic is represented by constraint (3.14) in Section 3.

A line is damaged when at least one pole of the line section is damaged, and it remains damaged status until the repair is finished. We assume all the repair starts after the wind-induced hazard ends (the wind speed drops to a certain level). Take $\zeta_{ij,3}(t)$ in Figure 3.3(a) as an example. Each version of $u_{ij}(t)$ is determined by whether any pole of line (i,j) can be damaged, i.e., $H_{ij,1}^3(t),\ldots,H_{ij,m_{ij}}^3(t)$ under this version, the wind speed trend $\bar{v}(t)$ (detailed later), and the repair time of line (i,j), i.e., $T_{ij,3}^R$. It is assumed that $T_{ij,k}^R = N_{ij,k}^D \cdot T_{ij}^{R_{pole}}$, where $N_{ij,k}^D$ is the total number of damaged poles of line (i,j) under version k, and $T_{ij}^{R_{pole}}$ is the repair time for a single pole. For all $(i,j) \in \Omega_B$, $T_{ij}^{R_{pole}}$ is a random variable with an independent identical Weibull distribution:

$$f_{T_{ij}^{R_{pole}}}(t) = \begin{cases} \frac{\beta_T}{\alpha_T}(\frac{t}{\alpha_T})^{\beta_T-1}\exp[-(\frac{t}{\alpha_T})^{\beta_T}] & \text{if } \ t \geqslant 0 \\ 0 & \text{otherwise,} \end{cases} \tag{3.1}$$

where $\beta_T = 10$ and $\alpha_T = 4$ [21]. $N_{ij,3}^D$ can be obtained given $H_{ij,1}^3(t),\ldots,H_{ij,m_{ij}}^3(t)$.

Fragility models have been used to determine whether a pole will be damaged by a hurricane, e.g., a fragility model that uses a log-normal distribution to express a pole's failure probability as a function of wind speed [23, 18]. It represents the probability that a pole will reach a defined limit state within a given period. But it cannot model the temporal correlation of damages or provide the exactly damaged time. In Figure 3.3(a), a pole's status (damaged or functional) in each version is simulated at every time instant based on the structural limit state function $G(t)$=R–$S(t)$ in [43]. Here the scalar quantities R and $S(t)$ are functions of a number of more basic parameters corresponding to a reliability formulation of high dimension in the structural design of civil engineering. Take the n-th pole as an example, $H_{ij,n}^3(t)$ is determined by comparing the pole resistance under current version, i.e., $R_{ij,n}^3$, and the wind load under current version, i.e., $S_{ij,n}^3(t)$:$H_{ij,n}^3(t)$=0 iff $R_{ij,n}^3 \leqslant S_{ij,n}^3(t)$, which implies that the nth pole of line (i,j) can be damaged by the wind-induced hazard at time t under version 3; $H_{ij,n}^3(t)$=1 iff $R_{ij,n}^3 > S_{ij,n}^3(t)$. $R_{ij,n}^3$ captures the impact of pole types. The discrepancy among different poles of the same type is described by $F_{ij,n}^3$, which is modeled by a normal distribution with mean of 8000 psi and standard deviation of

المنارة للاستشارات
www.manaraa.com

1600 psi [44]. According to the pole type (which is 3 here), $S^3_{ij,n}(t)$ is a function of the time-varied wind speed that the nth pole of line (i, j) experiences (detailed in [43]). The wind speed can be decomposed into two components: the slow varying part $\bar{v}(t)$ (trend) and the fast varying part $\Delta v_{ij,n}(t)$ (volatility). Since the geographic range of a distribution system is usually much smaller compared to the areas being affected by a wind-induced hazard, it is assumed: (i) $\bar{v}(t)$ (detailed in [45]) is shared by all versions, all lines and all poles; and (ii) $\Delta v_{ij,n}(t)$ follows an independent and identical normal distribution for all poles of all lines [45]. The dot-dashed lines in Figure 3.3(a) illustrate these assumptions.

3.2.2.2 Repair cost

Similarly, $\chi_{ij,1}, \ldots, \chi_{ij,6}$ represent the 6 versions of the repair cost of line (i, j), for the 6 pole types. Take version 3 as an example [see Figure 3.3(b)], we assume $\chi_{ij,3} = N^D_{ij,3} \cdot \chi^p_{ij,3}$, where $\chi^p_{ij,3}$ is the repair cost for a single pole in the current version, which is assumed to be constant.

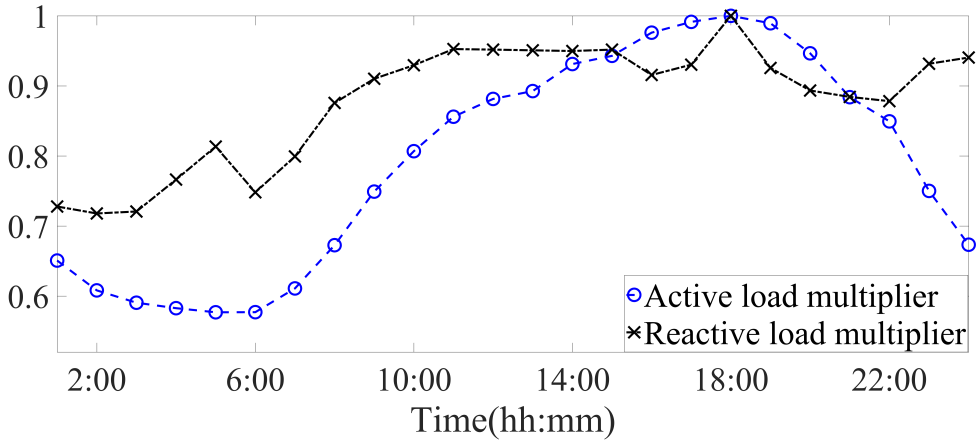

Figure 3.4 Multipliers of load profiles at the substation (root node), with the peak values as the bases.

المنارة للاستشارات
www.manaraa.com

3.2.2.3 Demand

The power demand of load $i \in \Omega_L$ is assumed to be the product of a random multiplier, τ_i^P or τ_i^Q, and the hourly normalized load profile. For the multipliers, assume

$$\tau_i^P \sim N(\overline{P}_i, (0.02\overline{P}_i)^2), \forall i \in \Omega_L \tag{3.2}$$

$$\tau_i^Q \sim N(\overline{Q}_i, (0.02\overline{Q}_i)^2), \forall i \in \Omega_L \tag{3.3}$$

are independent for all i, where $\overline{P}_i$ and $\overline{Q}_i$ represent the mean values of daily peak active and reactive power of load i over a year, respectively. We use $M^p(t)$ and $M^q(t)$ to make load profile shapes change with time. Figure 3.4 shows the multipliers of active and reactive load profiles at a substation on a typical day in summer [46, 47]. In this dissertation, all loads are assumed to share the same $M^p(t)$ and $M^q(t)$. Since the wind-induced hazard could happen at any time, let assume a uniformly distributed time offset, t_0^L, for the load profiles. Thus, it will have

$$P_i^L(t) = \tau_i^P \cdot M^p(t + t_0^L), \forall i \in \Omega_L, t \in \mathcal{T}_H \tag{3.4}$$

$$Q_i^L(t) = \tau_i^Q \cdot M^q(t + t_0^L), \forall i \in \Omega_L, t \in \mathcal{T}_H. \tag{3.5}$$

Notice that all variables at the source nodes in Figure 3.3 (highlighted in red) are independent. Thus, they can be independently sampled, which can be performed in parallel with a small computational burden.

3.2.3 The Second Stage Decisions

After the uncertainty is resolved, the system operator makes the recourse decisions to minimize operation costs. The second-stage operation decisions can be represented by a vector $\boldsymbol{y}^{R,s} = [\boldsymbol{P}^{g,s}, \boldsymbol{Q}^{g,s}, \boldsymbol{y}^{c,s}, \boldsymbol{y}^{r,s}]$, where $\boldsymbol{P}_g^s$ and $\boldsymbol{Q}_g^s \in \mathbb{R}_+^{|\mathcal{T}_H| \times |\Omega_N|}$ denote the active and reactive power output of backup DGs for $t \in \mathcal{T}_H$; $\boldsymbol{y}^{c,s} \in \{0,1\}^{|\mathcal{T}_H| \times 2|\Omega_B|}$ denotes the status of all sectionalizers for $t \in \mathcal{T}_H$; $\boldsymbol{y}^{r,s} \in \mathbb{R}_+^{|\mathcal{T}_H| \times |\Omega_L|}$ denotes the load shedding ratios of all loads for all $t \in \mathcal{T}_H$.

المنارة للاستشارات
www.manaraa.com

3.2.4 Probability of sampled scenarios

In a formal formulation of stochastic programming, the space of random variable $\Omega_{\mathcal{S}}$ is sketched by a finite set of sampled scenarios, i.e. $\mathcal{S}$ (described by (3.12)). Accordingly, the distribution of all random variables must be discretized to fit $\mathcal{S}$ (otherwise the probability for any scenario depending on continuous distributions mentioned above is exactly zero). In practice, we first generate $\mathcal{S}$ according to the distributions given above, then use

$$\mathbb{P}(\xi) = 1/|\mathcal{S}|\,, \tag{3.6}$$

i.e. the frequency of scenario sample in $\mathcal{S}$, to replace the original probability measure given by the continuous distributions.

3.2.5 Scenario Generation

In summary, the procedure for scenario generation is as follows:

Input: network parameters (Ω_B, Ω_L, and m_{ij} for all $(i,j) \in \Omega_B$), operational parameters [$M^p(t)$ and $M^q(t)$], scenario parameter ($|\mathcal{S}|$), version (pole type) parameters (Ω_K, physical parameters), distribution parameters of independent random variables (A_a, δ_c, v_{tr}, r_f; $\Delta v_{ij,n}$, $F^k_{b,ij,n}$ and $T^{R_{pole}}_{ij}$, for all $1 \le n \le m_{ij}$, all $(i,j) \in \Omega_B$ and all $k \in \Omega_K$; τ^P_i and τ^Q_i for all $i \in \Omega_L$; t^L_0; $\chi ij, k$ for all $(i,j) \in \Omega_B$ and all $k \in \Omega_K$.

for scenario $s = 1, \ldots, |\mathcal{S}|$ **do**

  Sample A_a, δ_c, v_{tr} and r_f to generate $\bar{v}(t)$ for $t = 1, \ldots, \mathcal{T}^l$, where $\mathcal{T}^l$ is the time when $\bar{v}(t)$ drops back to normal level

  for $(i,j) \in \Omega_B$ **do**

    Sample $T^{R_{pole}}$ from (3.1)

    for $k = 1, \ldots, |\Omega_K|$ **do**

      for $n = 1, \ldots, m_{ij}$ **do**

        Sample $F^k_{b,ij,n}$

        Derive $R^k_{ij,n}$

المنارة للاستشارات
www.manaraa.com

```
    for t = 1, ..., T^l do
      Set H^k_{ij,n}(t) = 1
      for t' = -60/60, -59/60, ..., -1/60 do
        if k = 1 then
          Sample v_{ij,n}(t+t')
        end if
        Derive S^k_{ij,n}(t+t')
        Get G^k_{ij,n}(t+t') = R^k_{ij,n} - S^k_{ij,n}(t+t')
        Get H^k_{ij,n}(t+t') = { 1  G^k_{ij,n}(t+t') ≥ 0
                               { 0  G^k_{ij,n}(t+t') < 0
        if H^k_{ij,n}(t+t') = 0 then
          Set H^k_{ij,n}(t) = 0
          break
        end if
      end for
      if H^k_{ij,n}(t) = 0 then
        Set H^k_{ij,n}(t+1) = ... = H^k_{ij,n}(T^l) = 0
        break
      end if
    end for
  end for
  Get N^D_{ij,k} = Σ_{n=1}^{m_ij} ( 1 - Π_{t=1}^{T^l} H^k_{ij,n}(t) )
  Get T^R_{ij,k} = N^D_{ij,k} · T^{R_pole}
  Get T^c_{ij,k} = T^l + T^R_{ij,k}
  for t = 1, ..., T^l do
    ζ_{ij,k}(t) = 1 - Π_{n=1}^{m_ij} H^k_{ij,n}(t)
    if ζ_{ij,k}(t) = 1 then
```

المنارة للاستشارات
www.manaraa.com

Set $\zeta_{ij,k}(t+1) = \ldots = \zeta_{ij,k}(\mathcal{T}^c_{ij,k}) = 1$

break

end if

end for

Get $\chi_{ij,k} = N^D_{ij,k} \cdot \chi_{ij,k}$

end for

end for

Get $\mathcal{T}^c = \max\limits_{\substack{k \in \Omega_T \\ (i,j) \in \Omega_B}} \mathcal{T}^c_{ij,k}$

for $(i,j) \in \Omega_B$ **do**

for $k = 1, \ldots, |\Omega_T|$ **do**

Set $\zeta_{ij,k}(t) = 0$ for $\mathcal{T}^c_{ij,k} \leq t \leq \mathcal{T}^c$

end for

end for

Sample t^L_0 from discrete uniform distribution on [0, 23]

for $i = 1, \ldots, \Omega_L$ **do**

Sample τ^P_i and τ^Q_i by (3.2) and (3.3)

Calculate $P^L_i(t)$ and $Q^L_i(t)$ by (3.4) and (3.5)

end for

Output: $\zeta_{ij,k}(t)$ for all $k \in \Omega_K$, $(i,j) \in \Omega_B$, $1 \leq t \leq \mathcal{T}^c$; $\chi_{ij,k}$ for all $k \in \Omega_K$, $(i,j) \in \Omega_B$; $P^L_i(t)$ and $Q^L_i(t)$ for all $i \in \Omega_L$, $1 \leq t \leq \mathcal{T}^c$

end for

Notice that to obtain more authentic simulation of wind, $\Delta v_{ij,n}(t)$, and therefore $H^k_{ij,n}(t)$ is first sampled minutely (see t' above), then $H^k_{ij,n}(t)$ is down-sampled to hourly resolution.

3.3 Two-Stage Stochastic MILP ROD Formulation

A two-stage stochastic mixed-integer ROD formulation is developed. The objective of the first stage is to minimize the costs of hardening lines, installing backup DGs, adding sectionalizers, and

المنارة للاستشارات
www.manaraa.com

the expected cost of the second stage. The second stage is to minimize the costs of loss of load, DG operation and damage repair. The first-stage problem is a linear integer program, and the second stage is a mixed-integer linear program. The nomenclature for the proposed ROD model is shown in the Table 3.1.

3.3.1 The First Stage Problem

$$\min \sum_{(i,j)\in\Omega_B}\sum_{k\in\Omega_K} c_{ij,k}x^h_{ij,k} + \sum_{i\in\Omega_N} c^g_i x^g_i + \sum_{(i,j)\in\Omega_B} c^c_{ij}(x^{c_1}_{ij,i} + x^{c_1}_{ij,j}) + \mathcal{Q}(x) \tag{3.7}$$

$$s.t. \sum_{k\in\Omega_K} x^h_{ij,k} = 1, \forall (i,j)\in\Omega_B \tag{3.8}$$

$$\sum_{i\in\Omega_N} x^g_i \leqslant N_G \tag{3.9}$$

$$x^{c_0}_{ij,n} + x^{c_1}_{ij,n} = x^c_{ij,n}, \forall (i,j)\in\Omega_B, n\in\{i,j\} \tag{3.10}$$

$$\begin{gathered} x^h_{ij,k}, x^{c_1}_{ij,n}, x^c_{ij,n}, x^g_i \in \{0,1\}, \forall i\in\Omega_N, (i,j)\in\Omega_B, \\ k\in\Omega_H, n\in\{i,j\} \end{gathered} \tag{3.11}$$

$$\text{where} \quad \mathcal{Q}(x) = w_H \cdot \mathbb{E}_{\boldsymbol{\xi}}\phi(x,\boldsymbol{\xi}) \cong w_H \cdot \sum_{s\in\mathcal{S}} p_r(s)\phi(x,s) \tag{3.12}$$

In the objective function, $c_{ij,k}$ represents the hardening cost of line (i,j) with k-th pole type, which is also related to the original pole type before hardening. If the original pole type at line (i,j) is assumed to be **3**, then $c_{ij,3} = 0$. For example, $c_{ij,2}$ equals the cost of replacing all poles associated with line section (i,j) to pole type 2, and $c_{ij,1}$ equals the cost of upgrading all poles at line (i,j) to pole type 2 with pole guying. Constraint (3.8) indicates that only one hardening strategy can be selected for each line. Constraint (3.9) restricts the number of DGs that can be installed. $x^c_{ij,n}$ in constraint (3.10) represents whether line (i,j) has a switch or not at the end of n, which is used in the second-stage problem. The second-stage expected cost is given by equation

المنارة للاستشارات
www.manaraa.com

Table 3.1 Nomenclature for the SMILP ROD model

Indices and sets	
Ω_B	Set of line indices (i, j)
Ω_K	Set of hardening pole type indices k
Ω_L	Set of loads indices i
Ω_N	Set of nodes indices i
$\Omega_{\mathcal{S}}$	Probability space of stochastic scenarios
$\mathcal{S}$	Set of sampled scenario indices s
$\mathcal{T}_H$	Time duration set of climatic hazard indices t
ξ	A random event
Parameters	
α_L	Penalty coefficient of virtual load
B'_{ij}	Virtual reactance for line (i, j)
c^c_{ij}	Cost of installing sectionalizer at line (i, j)
$c^h_{ij,k}$	Cost of hardening line (i, j) with k-th pole type
c^g_i	Cost of installing a DG at bus i
c^L_i	Cost of shedding $1kWh$ of i-th load
c^o_i	Cost of operating DG at bus i
m_{ij}	The total number of poles at line (i, j)
M_1, M_2	Sufficiently large positive numbers
M_3, M_4	Sufficiently large positive numbers
N_G	The limit for total number of newly installed DGs
$P^{L,s}_{i,t}, Q^{L,s}_{i,t}$	Stochastic parameter indicating active/reactive load demand at time t
$P^{\max}_{ij,t}, Q^{\max}_{ij,t}$	Maximum Active/reactive line flow at time t
$P^{g\max}_i, Q^{g\max}_i$	Active/reactive power limits of DG
R^e_{ij}, X^e_{ij}	Resistance/reactance of line (i, j)
S_0	Positive base power

المنارة للاستشارات
www.manaraa.com

Table 3.1 (Continued)

V_0	Reference voltage magnitude
$V_i^{\max}, V_i^{\min}$	Maximum/minimum voltage magnitude
$\varepsilon_1, \varepsilon_2, \varepsilon_3$	Sufficiently small positive numbers
w_H	The total occurrence of climatic hazards in a year
$\chi_{ij,k}^s$	Stochastic parameter indicating repair cost of line (i,j) with k-th pole type
$x_{ij,i}^{c_0}$	Binary parameter indicating whether line (i,j) has an existing sectionalizer (1) or not (0) at the end i
$\zeta_{ij,k,t}^s$	Stochastic parameter indicating status of line (i,j) with k-th pole type, damaged (1) or functional (0) at time t
$c_{ij}^{r,s}$	Repair cost of line (i,j)

Decision Variables

$\lambda_{a,ij,t}^s, \lambda_{b,ij,t}^s$	Dual variable
$\lambda_{c,i,t}^s$	Dual variable
$\mu_{d,i,t}^s, \mu_{e,i,t}^s$	Dual variable
$P_{ij,t}^s, Q_{ij,t}^s$	Active/reactive power flow of line (i,j) at time t
$P_{i,t}^{g,s}, Q_{i,t}^{g,s}$	Active/reactive power output of DGs at time t
$\mathcal{P}_{l,ij,t}^s$	Virtual line flow of line (i,j) at time t
$\mathcal{P}_{L,i,t}^s$	Virtual load of bus i at time t
$\theta_{i,t}^s$	Voltage angle (radians) at bus i at time t
$u_{ij,t}^s$	Binary variable indicating whether line (i,j) is damaged (1) or not (0) at time t
$V_{i,t}^s$	Voltage magnitude of bus i at time t
$w_{i,t}^{a,s}$	Binary variable indicating whether voltage angle is zero (1) or not (0) at bus i at time t
$w_{ij,t}^{b,s}$	Binary variable indicating whether line (i,j) is an active branch (1) or not (0) at time t
$w_{i,t}^{m,s}$	Auxiliary binary variable for setting different restriction on the voltage magnitude at bus i at time t
$w_{ij,t}^{o,s}$	Binary variable indicating whether line is on (1) or off (0) at time t

المنارة للاستشارات
www.manaraa.com

Table 3.1 (Continued)

$x^{c_1}_{ij,i}$	Binary variable indicating whether a new sectionalizer is deployed (1) or not (0) at the end i of line (i,j)
$x^{c}_{ij,i}$	Binary variable indicating whether line (i,j) has a sectionalizer (1) or not (0) at the end i of line (i,j)
$x^{h}_{ij,k}$	Binary variable indicating whether line (i,j) is hardened with k-th pole type (1) or not (0)
x^{g}_{i}	Binary variable indicating whether a new DG is placed at bus i (1) or not (0)
$y^{c,s}_{ij,t}$	Binary variable indicating whether the sectionalizer at line (i,j) is open (1) or not (0) at time t
$y^{r,s}_{i,t}$	Load shedding percentage of load at bus i at time t

(3.12), where w_H is the total number of the wind-induced hazards occurring in a year and $p_r(s)$ is the scenario sample probability, which equals $\frac{1}{|\mathcal{S}|}$.

3.3.2 The Second Stage Problem

In the second stage, the sectionalizers isolate damaged lines with the minimal service interruption. Since the distribution network is assumed to be radial in this dissertation, the opening of sectionalizers can separate the network into a few *islands*. The "healthy islands", i.e., islands without damaged lines and with power supply from the substation and/or DGs, are supposed to operate as stand-alone microgrids; the "unhealthy islands" will be de-energized until they are gradually recovered in the repair stage. During the repair stage, if a part of the de-energized island becomes healthy and there exists a breaker or sectionalizer that can isolate it from the remaining unhealthy part, this part will be prioritized in the repair, and operate as a MG. Finally, when all damaged lines are repaired, the system will return to normal operating condition. For each healthy island, DG dispatching and load shedding will be used to meet the load demand as much as possible. It is necessary to develop a mathematic formulation that can model self-healing operations mentioned above. For this purpose, there are two main challenges: (i) the sectionalizers

المنارة للاستشارات
www.manaraa.com

and breakers only exist in certain line sections, which poses the challenge to isolate the damaged part with the minimum customer interruptions; and (ii) the energized networks should keep radial topologies to reduce potential operation issues, and facilitate the system to return to the normal operation topology when all damaged lines are repaired.

3.3.2.1 Modeling strategy

A novel modeling method is proposed to meet the challenge (i). The idea is to add a *fictitious fault* at a damaged line. A line damage will not necessarily lead to a fault, but the damaged line should be isolated as if it was faulted. Therefore, the system model is modified by inserting a virtual node in the middle of each line, then a symmetric ground fault at the virtual node is applied if the line is damaged. The virtual node is also included in power flow constraints. The second key modification is to set the bus voltage magnitude feasible region to be $\{0\} \cup [V^{\min}, V^{\max}]$ in (3.27), where $[V^{\min}, V^{\max}]$ is the safe range, i.e., $0.9 \sim 1.1p.u$. If the voltage magnitude of a faulted line is within $0.9 \sim 1.1p.u$ and there is no switch on that line, it causes a large fault current, which violates the power flow constraints (3.20)-(3.21). Consequently, the voltage magnitude at the two ends of the faulted line is forced to be zero. This fictitious faulting logic propagates to the rest of the network until a switch can break it. It results in a de-energized island with zero voltages, which is formed by all line sections that are directly connected to the faulted line without switches in between. In this case, there is no power flow in the island, given constraint (3.24). Constraint (3.30) disconnects the DGs on a faulted bus. The load shedding is minimized in the objective (3.13), which encourages all sectionalizers to block the fault propagation, and maximizes the load service in the healthy islands.

Take the network shown in Figure 3.5 as an example. Suppose branch AB is damaged, and each actual node has loads. According to the above-mentioned settings, the virtual node F_{AB} is faulted. Notice that there is no switch at any end of branch AB. If the voltage magnitude of A is within $0.9 \sim 1.1$ p.u., it will cause a large fault current on branch AF_{AB}, which will exceed the loading limit of branch AB (this can be ensured in advance, and we can add more virtual nodes if needed).

المنارة للاستشارات
www.manaraa.com

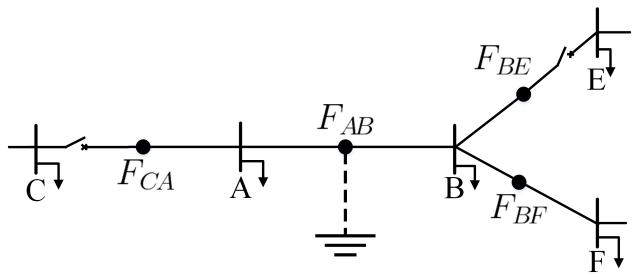

Figure 3.5 The illustrative example for isolating a contingency

Thus, the voltage magnitude of node A is forced to be 0 according to its feasible region. That is to say, node A is faulted. The same process happens to node B. In this way, the fault propagates to the whole network, until some switches can break it. In this example, there is a switch at the left end of branch CA. It must be open in the optimal solution, otherwise, the load at node C would lost power as the fault propagates to node C. Similarly, the switch that is close to node E must be open in the optimal solution, and the fault will further propagate through node F until there is a switch. Finally, all line sections that are directly connected to branch AB (i.e., no switches in between) are de-energized and have zero voltage.

To solve the challenge (ii), the network is represented as a forest. The radiality constraint for a forest can be constructed according to a theorem in graph theory [48]: A forest of N nodes has exactly $N - N_c$ edges, where N_c is the number of connected network components. Thus, the radiality constraint is satisfied *iff* the number of active branches equals $N - N_c$. The calculation of N_c is based on the fact that when power flow equations are satisfied, the voltage angles of a connected network component (healthy island) have exactly one degree of freedom counted. Hence, the number of components can be calculated by the degree of freedom of voltage angles. To obtain this degree of freedom, a virtual DC optimal power flow (VDCOPF) subproblem is formulated. The optimal solution of this subproblem satisfies that the virtual loads in the same energized island are nearly equally distributed at active nodes and each energized island has and only has an active node with zero angle. Since the continuous VDCOPF subproblem has a positive definite quadratic objective and linear constraints, it can be equivalently replaced by the corresponding Karush-Kuhn-Tucker (KKT) condition in MILP form. The dual variable of voltage angle in KKT condition is

المنارة للاستشارات
www.manaraa.com

used as the indicator of zero angle. The formulation of the above modeling strategies is detailed below.

Let Ω_{B_F} denote the line set considering virtual nodes (each line is divided into two parts by its virtual node), Ω_F denotes the set of virtual nodes, and $\Omega_{N_F} = \Omega_N \cup \Omega_F$. For $(i,j) \in \Omega_{B_F}$, i is assumed to represent the original node, where $i \in \Omega_N$, and j is assumed to represent the virtual node, where $j \in \Omega_F$. The power injection direction at node i is assumed to be flowing out, and the power injection direction at node j is flowing in.

3.3.2.2 Problem Formulation

Least-cost objective

The objective (3.13) is to minimize the total cost of the loss of load, DG operation, repair, and the weighted penalty cost of voltage angles and the relaxation of line flows given a specific scenario s and fixed first-stage decisions.

$$\phi(\boldsymbol{x}, s) = \min \sum_{i \in \Omega_N} \sum_{t \in \mathcal{T}_H^s} c_i^L y_{i,t}^{r,s} P_{i,t}^{L,s} \Delta t + \sum_{i \in \Omega_N} \sum_{t \in \mathcal{T}_H^s} c_i^o P_{i,t}^{g,s} \Delta t + \sum_{(i,j) \in \Omega_B} c_{ij}^{r,s} \tag{3.13}$$

Line damage status constraint

$$u_{ij,t}^s = \sum_{k \in \Omega_K} x_{ij,k}^h \zeta_{ij,k,t}^s, \forall (i,j) \in \Omega_B, t \in \mathcal{T}_H^s \tag{3.14}$$

As mentioned in Section 3.2.2.1, we only need to sample $\zeta_{ij,k,t}^s$ for all (i,j) independently in the phase of scenario generation. The line damage status $u_{ij,t}^s$ will be decided by $x_{ij,k}^h$ and $\zeta_{ij,k,t}^s$.

Line repair cost constraint

$$c_{ij}^{r,s} = \sum_{k \in \Omega_K} x_{ij,k}^h \chi_{ij,k,}^s, \forall (i,j) \in \Omega_B \tag{3.15}$$

As mentioned in Section 3.2.2.2, the line repair cost $c_{ij}^{r,s}$ can be decided by $x_{ij,k}^h$ and $\chi_{ij,k}^s$.

Line's on-off status constraints

A line's on-off status is controlled by two decision variables, x_{ij}^c, and $y_{ij,t}^{c,s}$, $\forall (i,j) \in \Omega_{B_F}$. Here $x_{ij}^c, \forall (i,j) \in \Omega_{B_F}$ is the same expression of $x_{ij,n}^c, \forall n \in \{i,j\}, (i,j) \in \Omega_B$. It is beneficial to introduce a

المنارة للاستشارات
www.manaraa.com

new decision variable $w_{ij,t}^{o,s}, \forall (i,j) \in \Omega_{B_F}, t \in \mathcal{T}_H^s$ to represent the line's on-off status (e.g. $w_{ij,t}^{o,s} = 1$ means line (i,j) is on at time t). Table 3.2 lists the desired values of $w_{ij,t}^{o,s}$ given all possible combinations of x_{ij}^c and $y_{ij,t}^{c,s}$.

Table 3.2 Evaluation of the on-off status variable

x_{ij}^c	$y_{ij,t}^{c,s}$	$w_{ij,t}^{o,s}$	x_{ij}^c	$y_{ij,t}^{c,s}$	$w_{ij,t}^{o,s}$
0	0	1	1	0	1
0	1	N/A	1	1	0

*N/A: the case should be infeasible.

This evaluation table can be formulated by

$$y_{ij,t}^{c,s} \leqslant x_{ij}^c, \forall (i,j) \in \Omega_{B_F}, t \in \mathcal{T}_H^s \tag{3.16}$$

$$x_{ij}^c + y_{ij,t}^{c,s} + 2w_{ij,t}^{o,s} \geqslant 2, \forall (i,j) \in \Omega_{B_F}, t \in \mathcal{T}_H^s \tag{3.17}$$

$$w_{ij,t}^{o,s} + y_{ij,t}^{c,s} \leqslant 1, \forall (i,j) \in \Omega_{B_F}, t \in \mathcal{T}_H^s \tag{3.18}$$

$$y_{ij,t}^{c,s}, w_{ij,t}^{o,s} \in \{0,1\}, \forall (i,j) \in \Omega_{B_F}, t \in \mathcal{T}_H^s \tag{3.19}$$

Constraint (3.16) indicates that closing a sectionalizer is feasible only if it exits. If a line has no sectionalizer or breaker on it ($x_{ij}^c = y_{ij,t}^c = 0$), the line's status will be on as shown in (3.17); if a line has a sectionalizer ($x_{ij}^c = 1$), the line's status will be controlled by $y_{ij,t}^c$ in (3.18).

Line flow limits

$$-w_{ij,t}^{o,s} P_{ij}^{\max} \leqslant P_{ij,t}^s \leqslant w_{ij,t}^{o,s} P_{ij}^{\max}, \forall (i,j) \in \Omega_{B_F}, t \in \mathcal{T}_H^s \tag{3.20}$$

$$-w_{ij,t}^{o,s} Q_{ij}^{\max} \leqslant Q_{ij,t}^s \leqslant w_{ij,t}^{o,s} Q_{ij}^{\max}, \forall (i,j) \in \Omega_{B_F}, t \in \mathcal{T}_H^s \tag{3.21}$$

Constraints (3.20)-(3.21) approximate the line flow limits. If $w_{ij,t}^{o,s} = 0$, the state of line (i,j) is off, and there is no power flow through i node to j node.

المنارة للاستشارات
www.manaraa.com

Linearized DistFlow equations

Constraints (3.22)-(3.24) represent the linearized DistFlow equations, which have been widely used in distribution systems [49, 17, 34].

$$\sum_{\{j|(i,j)\in\Omega_{B_F}\}} P^s_{ij,t} = P^{g,s}_{i,t} - (1-y^{r,s}_{i,t})P^L_{i,t} - \varepsilon_1 V^s_{i,t}, \forall i \in \Omega_N, t \in \mathcal{T}^s_H \tag{3.22}$$

$$\sum_{\{j|(i,j)\in\Omega_{B_F}\}} Q^s_{ij,t} = Q^{g,s}_{i,t} - (1-y^{r,s}_{i,t})Q^L_{i,t}, \forall i \in \Omega_N, t \in \mathcal{T}^s_H \tag{3.23}$$

$$\begin{aligned} V^s_{i,t} - \frac{R^e_{ij}P^s_{ij,t} + X^e_{ij}Q^s_{ij,t}}{V_0} - (1-w^{o,s}_{ij,t})M_1 \leqslant V^s_{j,t} \leqslant V^s_{i,t} \\ - \frac{R^e_{ij}P^s_{ij,t} + X^e_{ij}Q^s_{ij,t}}{V_0} + (1-w^{o,s}_{ij,t})M_1, \forall i \in \Omega_{N_F}, t \in \mathcal{T}^s_H \end{aligned} \tag{3.24}$$

Equations (3.22)-(3.23) represent power balance at each node. Constraint (3.24) indicates the relationship of voltage magnitudes of neighboring buses. A big M approach is used to decouple voltages of two buses connected by a line that is off. The network connectivity, which is affected by line on-off status, is represented by constraints (3.20)-(3.24).

Virtual node power injection constraints

$$-u^s_{ij,t}M_2 \leqslant \sum_{k\in\{i,j\}} P^s_{kf_{ij},t} + \varepsilon_1 \cdot V^s_{i,t} \leqslant u^s_{ij,t}M_2, \forall (i,j) \in \Omega_B, f_{ij} \in \Omega_{N_F}, t \in \mathcal{T}^s_H \tag{3.25}$$

$$-u^s_{ij,t}M_2 \leqslant \sum_{k\in\{i,j\}} Q^s_{kf_{ij},t} \leqslant u^s_{ij,t}M_2, \forall (i,j) \in \Omega_B, f_{ij} \in \Omega_{N_F}, t \in \mathcal{T}^s_H \tag{3.26}$$

Constraint (3.25)-(3.26) indicate that if line (i,j) is not damaged, the power injection at the virtual node f_{ij} is zero; if line (i,j) is damaged, constraint (3.25)-(3.26) is canceled off, and if its voltage is within the normal range, it will cause a large short current.

Voltage magnitude limits

$$w^{m,s}_{i,t} V_i^{\min} \leqslant V^s_{i,t} \leqslant w^{m,s}_{i,t} V_i^{\max}, \forall i \in \Omega_{N_F}, t \in \mathcal{T}^s_H \tag{3.27}$$

$$u^s_{ij,t} + w^{m,s}_{f_{ij},t} \leqslant 1, \forall (i,j) \in \Omega_B, f_{ij} \in \Omega_F, t \in \mathcal{T}^s_H \tag{3.28}$$

$$w^{m,s}_{i,t} \in \{0,1\}, \forall i \in \Omega_{N_F}, t \in \mathcal{T}^s_H \tag{3.29}$$

المنارة للاستشارات
www.manaraa.com

The auxiliary binary variable $w_{i,t}^{m,s}$ in (3.27) is introduced to give different restrictions on the voltage magnitude: if $w_{i,t}^{m,s}=1$, the voltage magnitude will be restricted to be within the safe range; if $w_{i,t}^{m,s}=0$, then $V_{i,t}^{s}=0$. When line (i,j) is damaged, constraints (3.27)-(3.28) are used to force the voltage magnitude at the virtual node to be zero ($V_{f_{ij},t}=0$).

Load shedding ratio limit

$$1-w_{i,t}^{m,s} \leqslant y_{i,t}^{r,s} \leqslant 1, \forall i \in \Omega_N, t \in \mathcal{T}_H^s \tag{3.30}$$

The load shedding ratio limit is shown in constraint (3.30). If the voltage magnitude of a node is zero, load shedding ratio at that node will be 1. In the objective function, the cost of load shedding is used as a severity index for a climatic hazard.

DG capacity limits and operation status

$$0 \leqslant P_{i,t}^{g,s} \leqslant x_i^g P_i^{g,\max}, \forall i \in \Omega_N, t \in \mathcal{T}_H^s \tag{3.31}$$

$$0 \leqslant Q_{i,t}^{g,s} \leqslant x_i^g Q_i^{g,\max}, \forall i \in \Omega_N, t \in \mathcal{T}_H^s \tag{3.32}$$

Constraints (3.31)-(3.32) represent the generation capacity limits of DG at node i if it has been installed in the first stage.

Radiality constraints

$$\sum_{(i,j)\in\Omega_{B_F}} w_{ij,t}^{b,s} = \sum_{i\in\Omega_{N_F}} w_{i,t}^{m,s} - \sum_{i\in\Omega_{N_F}} w_{i,t}^{a,s} \tag{3.33}$$

$$w_{ij,t}^{o,s} + w_{i,t}^{m,s} - 1 \leqslant w_{ij,t}^{b,s} \leqslant 0.5 w_{ij,t}^{o,s} + 0.5 w_{i,t}^{m,s}, \forall i \in \Omega_{N_F}, (i,j) \in \Omega_{B_F}, t \in \mathcal{T}_H^s \tag{3.34}$$

$$w_{i,t}^{a,s}, w_{ij,t}^{b,s} \in \{0,1\}, \forall i \in \Omega_{N_F}, (i,j) \in \Omega_{B_F}, t \in \mathcal{T}_H^s \tag{3.35}$$

The radiality constraint can be expressed by (3.33), where the number of active branches equals the total number of active nodes minus the number of active nodes with zero angles [50]. Here a new binary variable $w_{ij,t}^{b,s}$ is introduced to represent the active branch since $w_{ij,t}^{o,s}$ cannot fully indicate

المنارة للاستشارات
www.manaraa.com

whether that line is energized. For example, if line (i,j) is damaged, its connected lines without a sectionalizer or breaker will also be de-energized although their line statuses are on. Constraint (3.34) indicates whether line (i,j) is an active line, is decided by two decision variables, $w^{o,s}_{ij,t}$ and $w^{m,s}_{i,t}$. $w^{m,s}_{i,t}=1$ can be regarded as an indicator of active node. If line's status is on ($w^{o,s}_{ij,t}=1$) and node i is an active node ($w^{m,s}_{i,t}=1$), it must be an active branch. Since a small constant current load ($\varepsilon_1 \cdot V^s_{i,t}$) in constraint (3.22) and (3.25) can impose all the nodes' voltage magnitude in the de-energized but no fault areas be zero.

The minimality condition of VDCOPF subproblem

$$\left(\mathcal{P}^{s,\star}_{L,t}, \mathcal{P}^{s,\star}_{l,t}, \theta^{s,\star}_t\right) = \underset{\mathcal{P}^s_{L,t},\mathcal{P}^s_{l,t},\theta^s_t}{\arg\min} \left\{ \sum_{i\in\Omega_{N_F}} (\theta^s_{i,t} + \frac{\alpha_L}{2}(\mathcal{P}^s_{L,i,t})^2) \right.$$

$$\text{s.t.} \quad \left. \begin{aligned} a:\ & -\left(1-w^{o,s}_{ij,t}\right)M_3 \leqslant \mathcal{P}^s_{ij,t} - S_0 B'_{ij}\left(\theta^s_{i,t} - \theta^s_{j,t}\right) \\ & \qquad \leqslant \left(1-w^{o,s}_{ij,t}\right)M_3, \forall (i,j)\in\Omega_{B_F} \\ b:\ & -w^{o,s}_{ij,t}M_3 \leqslant \mathcal{P}^s_{ij,t} \leqslant w^{o,s}_{ij,t}M_3, \forall (i,j)\in\Omega_{B_F} \\ c:\ & \sum_{\{j|(i,j)\in\Omega_{B_F}\}} \mathcal{P}^s_{ij,t} - P^{g,s}_{i,t} + \mathcal{P}^s_{L,i,t} = 0, \forall i\in\Omega_{N_F} \\ d:\ & -\theta^s_{i,t} \leq 0, \quad \forall i\in\Omega_{N_F} \\ e:\ & -\mathcal{P}^s_{L,i,t} \leq 0, \quad \forall i\in\Omega_{N_F} \end{aligned} \right\}, \tag{3.36}$$

$$\forall t \in \mathcal{T}^s_H$$

VDCOPF subproblem is modeled to realize that a connected network component (healthy MG) has one and only one degree of freedom of voltage angle under the condition of full DC power flow equations. The non-negative constraint on voltage angles and the corresponding summation penalty function in the objective force the minimum value of voltage angles in active components to be zero. Meanwhile, minimizing the sum of squares of virtual loads in the objective encourages the virtual loads to be equally distributed on active nodes in healthy MGs. Such a load distribution plus the standardized B'_{ij} (with random noise) ensure the bus of minimum angle (i.e., zero angle) is unique for each active component. In this way, the number of zero angles in active components is equal to the number of healthy MGs. Notice that the DC power flow equations (3.36).a-c are isolated from the actually power flow constraints, i.e., the DisFlow equations in (3.22)-(3.24), by

المنارة للاستشارات
www.manaraa.com

the subproblem. Only line on-off status and DG output are passed to the VDC OFF subproblem, as to avoid the potential conflicts between two suits of power flow equations.

Equation (3.36) can be equivalently replaced by its KKT condition:

Primal feasibility

$$\begin{aligned}
&-\left(1-w_{ij,t}^{o,s}\right)M_3 \leqslant \mathcal{P}_{ij,t}^{s,\star} - S_0 B_{ij}^{'}\left(\theta_{i,t}^{s,\star}-\theta_{j,t}^{s,\star}\right) \leqslant \left(1-w_{ij,t}^{o,s}\right)M_3, \forall (i,j)\in\Omega_{B_F}, t\in\mathcal{T}_H^s \\
&-w_{ij,t}^{o,s}M_3 \leqslant \mathcal{P}_{ij,t}^{s,\star} \leqslant w_{ij,t}^{o,s}M_3, \forall (i,j)\in\Omega_{B_F}, t\in\mathcal{T}_H^s \\
&\sum_{\{j|(i,j)\in\Omega_{B_F}\}} \mathcal{P}_{ij,t}^{s,\star} - P_{i,t}^{g,s} + \mathcal{P}_{L,i,t}^{s,\star} = 0, \forall i\in\Omega_{N_F}, t\in\mathcal{T}_H^s
\end{aligned} \tag{3.37}$$

Stationarity

$$\begin{aligned}
&\partial\mathcal{L}\Big/\partial\mathcal{P}_{L,i,t}^{s,\star} : \alpha_L \mathcal{P}_{L,i}^{s,\star} + \lambda_{c,i,t}^s - \mu_{e,i,t}^s = 0, \forall i\in\Omega_{N_F}, t\in\mathcal{T}_H^s \\
&\partial\mathcal{L}\Big/\partial\mathcal{P}_{ij,t}^{s,\star} : -\lambda_{a,ij,t}^s + \lambda_{b,ij,t}^s + \lambda_{c,i,t}^s - \lambda_{c,j,t}^s = 0, \forall (i,j)\in\Omega_{B_F}, t\in\mathcal{T}_H^s \\
&\partial\mathcal{L}/\partial\theta_{i,t}^{s,\star} : \sum_{\{j|(i,j)\in\Omega_{B_F}\}} \lambda_{a,ij,t}^s B_{ij} S_0 + 1 - \mu_{d,i,t}^s = 0, \forall i\in\Omega_{N_F}, t\in\mathcal{T}_H^s
\end{aligned} \tag{3.38}$$

Complementary slackness and dual feasibility

$$\begin{aligned}
&0 \leqslant \mu_{d,i,t}^s \perp \theta_{i,t}^{s,\star} \geqslant 0, \qquad \forall i\in\Omega_{N_F}, t\in\mathcal{T}_H^s \\
&0 \leqslant \mu_{e,i,t}^s \perp \mathcal{P}_{L,i,t}^{s,\star} \geqslant 0, \quad \forall (i,j)\in\Omega_{N_F}, t\in\mathcal{T}_H^s
\end{aligned} \tag{3.39}$$

On-off line status

$$\begin{aligned}
&-\left(1-w_{ij,t}^{o,s}\right)M_4 \leqslant \lambda_{a,ij,t}^s \leqslant \left(1-w_{ij,t}^{o,s}\right)M_4, \forall i\in\Omega_{N_F}, t\in\mathcal{T}_H^s \\
&-w_{ij,t}^{o,s}M_4 \leqslant \lambda_{b,ij,t}^s \leqslant w_{ij,t}^{o,s}M_4, \forall i\in\Omega_{N_F}, t\in\mathcal{T}_H^s
\end{aligned} \tag{3.40}$$

Zero angle indicator constraints

$$w_{i,t}^{a,s} - 1 \leqslant \frac{1}{2|\Omega_{N_F}|}(\mu_{d,i,t}^s - 1 + \varepsilon_3) \leqslant w_{i,t}^{a,s}, \forall i\in\Omega_N, t\in\mathcal{T}_H^s \tag{3.41}$$

Constraint (3.41) imposes $w_{i,t}^{a,s} = 1$ if $\mu_{d,i,t}^s > 1$, as $\mu_{d,i,t}^s$ has strong duality on $\theta_{i,t}^s$. If node i has zero angle ($\theta_{i,t}^s = 0$) in the healthy and active MG, its corresponding shadow price $\mu_{d,i,t}^s$ must be larger than 1 when each component has at least 2 buses (indicated by the coefficients of α_L in the objective).

المنارة للاستشارات
www.manaraa.com

3.4 Solution Algorithm

3.4.1 A Compact Notation Form of ROD Model

For brevity, the proposed ROD model is written in a compact notation form. The first-stage problem is expressed as

$$\min_{\boldsymbol{x}} \quad \left\{ \boldsymbol{c}^\top \boldsymbol{x} + \mathcal{Q}(\boldsymbol{x}) : \boldsymbol{A}\boldsymbol{x} = \boldsymbol{b} \right\} \tag{3.42}$$

where the vector $\boldsymbol{c}$ represents the cost for ROD methods; $\mathcal{Q}(\boldsymbol{x}) = \sum_{s \in \mathcal{S}} p_r(s)\phi(\boldsymbol{x}, s)$ is the recourse function of the second stage, which computes the expected value of taking decision $\boldsymbol{x}$. (3.42) is a vector form representation of first-stage constraints (3.8)-(3.10), where inequality constraints can be handled by the introduction of appropriate slack variables. The second stage value function $\phi(\boldsymbol{x}, s)$ is defined as follows:

$$\min \quad \left\{ \boldsymbol{q}(s)^\top \boldsymbol{y}^R : \ \boldsymbol{T}(s)\boldsymbol{x} + \boldsymbol{W}(s)\boldsymbol{y}^R = \boldsymbol{h}(s) \right\} \tag{3.43}$$

The objective function in (3.43) is a compact expression of the objective function (3.13). Constraints (3.14)-(3.35) and (3.37)-(3.41) of the second-stage problem are written as an equality constraint in (3.43) by introducing appropriate slack variables for those inequality constraints.

3.4.2 Dual Decomposition Algorithm

The simplest approach to solve (3.7)-(3.32) is to apply a standard MIP solver, e.g., CPLEX, to directly solve its extensive form (EF). However, there is a computational challenge for solving the EFs of large-scale ROD problems by MIP solvers. Since both first and second stages contain integer variables, scenario-based decomposition methods, such as progressive hedging and dual decomposition (DD) have better performance than stage-based methods, such as integer L-shaped method, since they can reduce the computational difficulty by decomposing the problem into scenario-based subproblems and solving subproblems in parallel [51]. Although the PH algorithm can find high-quality approximate solutions, it cannot guarantee optimality convergence [52]. We present a customized DD algorithm combined with branch-and-bound to obtain the optimal solutions of ROD problems.

المنارة للاستشارات
www.manaraa.com

The main idea of DD algorithm is to obtain lower bounds from Lagrangian dual by relaxing non-anticipativity constraints and using branch-and-bound to re-establish non-anticipativity [52]. Before we give the pseudocode of the proposed algorithm, it is better to explain the procedure of obtaining the best lower bound from Lagrangian dual, which will be used in the algorithm.

The deterministic equivalent of ROD problem can be written:

$$z = \min \left\{ \boldsymbol{c}^\top \boldsymbol{x} + \sum_{s \in S} p_r(s) \boldsymbol{q}^\top \boldsymbol{y}^{R,s} : (\boldsymbol{x}, \boldsymbol{y}^{R,s}) \in \boldsymbol{K}^s, \forall s \in S \right\} \tag{3.44}$$

where $\boldsymbol{K}^s = \{(\boldsymbol{x}, \boldsymbol{y}^{R,s}) : \boldsymbol{A}\boldsymbol{x} = \boldsymbol{b}, \boldsymbol{T}(s)\boldsymbol{x} + \boldsymbol{W}(s)\boldsymbol{y}^{R,s} = \boldsymbol{h}(s), \boldsymbol{x} \in \{0,1\}, \boldsymbol{y}^{R,s} = (\boldsymbol{y}^s_B, \boldsymbol{y}^s_C), \boldsymbol{y}^s_B \in \{0,1\}, \boldsymbol{y}^s_C \geqslant 0\}, \forall s \in \mathcal{S}$. Eq (3.44) is a large-scale deterministic MILP with a block-angular structure, which can lead decomposition methods to split it into more manageable scenario-based subproblems. To induce a scenario-based decomposable structure, the copies $\boldsymbol{x}^s, s \in \mathcal{S}$ of the first-stage variables $\boldsymbol{x}$ are introduced to create the following reformulation of (3.44):

$$\min \quad \left\{ \sum_{s \in S} p_r(s)(\boldsymbol{c}^\top \boldsymbol{x}^s + \boldsymbol{q}^\top \boldsymbol{y}^{R,s}) : \boldsymbol{x}^1 = \cdots = \boldsymbol{x}^{|S|},\ (\boldsymbol{x}^s, \boldsymbol{y}^{R,s}) \in \boldsymbol{K}^s, \forall s \in S \right\} \tag{3.45}$$

where $\boldsymbol{x}^1 = \cdots = \boldsymbol{x}^{|S|} = \overline{\boldsymbol{x}}$ represents the non-anticipativity constraint, which forces the first-stage decision not to be dependent on scenarios. The problem (3.45) can be decomposed when the non-anticipativity constraint is relaxed.

The Lagrangian relaxation with respect to the non-anticipativity constraint is the problem of finding $\boldsymbol{x}^s, \boldsymbol{y}^{R,s}, \forall s \in S$, such that

$$L(\boldsymbol{\mu}) = \min \left\{ \sum_{s \in S} \left[p_r(s)(\boldsymbol{c}^\top \boldsymbol{x}^s + \boldsymbol{q}^\top \boldsymbol{y}^{R,s}) + \boldsymbol{\mu}^s (\boldsymbol{x}^s - \overline{\boldsymbol{x}}) \right] : (\boldsymbol{x}^s, \boldsymbol{y}^{R,s}) \in \boldsymbol{K}^s \right\} \tag{3.46}$$

with the condition $\sum_{s \in \mathcal{S}} \boldsymbol{\mu}^s = 0$ required for boundness of the Lagrangian. Here $\boldsymbol{\mu} = (\boldsymbol{\mu}^1, \cdots, \boldsymbol{\mu}^{|S|})$ is the vector of multipliers of the relaxed constraints $\boldsymbol{x}^s = \overline{\boldsymbol{x}}, \forall s \in S$.

The Lagrangian dual function in (3.46) can be separated into

$$L(\boldsymbol{\mu}) = \sum_{s \in \mathcal{S}} L_s(\boldsymbol{\mu}^s) \tag{3.47}$$

$$\text{where } L_s(\boldsymbol{\mu}^s) = \min_{\boldsymbol{x}^s, \boldsymbol{y}^{R,s}} \left\{ p_r(s)(\boldsymbol{c}^\top \boldsymbol{x}^s + \boldsymbol{q}^\top \boldsymbol{y}^{R,s}) + \boldsymbol{\mu}^s \boldsymbol{x}^s : (\boldsymbol{x}^s, \boldsymbol{y}^{R,s}) \in \boldsymbol{K}^s \right\}, \forall s \in S \tag{3.48}$$

المنارة للاستشارات
www.manaraa.com

The Lagrangian dual of Eq. (3.45) then becomes the problem of finding the best lower bound:

$$z_{LD} = \max_{\boldsymbol{\mu}} \left\{ \sum_{s \in \mathcal{S}} L_s(\boldsymbol{\mu}^s) : \sum_{s \in \mathcal{S}} \boldsymbol{\mu}^s = 0 \right\} \tag{3.49}$$

The Lagrangian dual (3.49) is a convex non-smooth program and can be solved using subgradient methods.

According to Theorem 6.2 in [53], p. 327, we can get

$$z_{LD} = min \left\{ \sum_{s \in S} p_r(s)(\boldsymbol{c}^\top \boldsymbol{x}^s + \boldsymbol{q}^\top \boldsymbol{y}^{R,s}) : \boldsymbol{x}^1 = \cdots = \boldsymbol{x}^{|S|}, (\boldsymbol{x}, \boldsymbol{y}^R) \in \text{conv} \times_{j=1}^{|S|} \boldsymbol{K}^s, \forall s \in S \right\} \tag{3.50}$$

As the fact that $\text{conv} \times_{j=1}^{|S|} \boldsymbol{K}^s = \times_{j=1}^{|S|} \text{conv} \boldsymbol{K}^s$, the optimal value z_{LD}^* of the Lagrangian dual (3.49) equals the optimal value of the linear program (3.51)

$$z_{LB} = \min \quad \left\{ \sum_{s \in S} p_r(s)(\boldsymbol{c}^\top \boldsymbol{x}^s + \boldsymbol{q}^\top \boldsymbol{y}^{R,s}) : \boldsymbol{x}^1 = \cdots = \boldsymbol{x}^{|S|}, (\boldsymbol{x}^s, \boldsymbol{y}^{R,s}) \in \text{conv} \boldsymbol{K}^s, \forall s \in S \right\} \tag{3.51}$$

Then $z \geqslant z_{LD}^* = z_{LB}^*$.

At the same time, the upper bound on z provided by Eq. (3.46) is not bigger than the value of solving LP-relaxation of Eq. (3.44) [52], written as

$$z_{UB} = \min \quad \left\{ \sum_{s \in S} p_r(s)(\boldsymbol{c}^\top \boldsymbol{x}^s + \boldsymbol{q}^\top \boldsymbol{y}^{R,s}) : \boldsymbol{x}^1 = \cdots = \boldsymbol{x}^{|S|}, (\boldsymbol{x}^s, \boldsymbol{y}^{R,s}) \in \boldsymbol{K}_{LP}^s, \forall s \in S \right\} \tag{3.52}$$

where $\boldsymbol{K}_{LP}^s$ arises from $\boldsymbol{K}^s$ without the integer requirements.

As a result,

$z_{UB} \geqslant z \geqslant z_{LD} := \max_{\boldsymbol{\mu}} \left\{ \sum_{s \in \mathcal{S}} L_s(\boldsymbol{\mu}^s) : \sum_{s \in \mathcal{S}} \boldsymbol{\mu}^s = 0 \right\}$.

A duality gap may occur between the optimal Lagrangian dual and the optimal value due to the integer requirements. The steps of the modified DD algorithm are shown as Algorithm 1.

3.5 Simulation and Results

3.5.1 Test Case: IEEE-123 Distribution Feeder

The numerical experiments are performed on IEEE 123-bus distribution system [54]. The capital costs of the proposed ROD methods are shown in Table 3.3, whose life time are assumed to be 30

المنارة للاستشارات
www.manaraa.com

Algorithm 1 The customized DD algorithm

1: ***Initialization:*** Set $z^* = \infty$ and let $\mathcal{G}$ consists of problem (3.42).
2: ***Termination:*** **If** $\mathcal{G} = \emptyset$, **then** output $\boldsymbol{x}^\star$ with $z^\star = \boldsymbol{c}^\top \boldsymbol{x}^\star + \mathcal{Q}(\boldsymbol{x}^\star)$ is optimal.
3: ***Node Selection:***
a) Select and delete a problem $\mathcal{G}_i$ from $\mathcal{G}$
b) Solve its corresponding Lagrangian dual (3.49) and its optimal value yields $z_{LD} = z_{LD}(\mathcal{G}_i)$
c) **If** the associated $z_{LD}(\mathcal{G}_i) = \infty$ (infeasibility of subproblem i) **then** Go to 2.
4: ***Bounding:*** **If** $z_{LD}(\mathcal{G}_i) \geqslant z^\star_{LD}$, Go to 2. Otherwise proceed as follows:
If the first-stage solutions $\boldsymbol{x}^s, s \in \mathcal{S}$ of subproblems are
a) The scenario solutions $x^s, \forall s \in S$ are identical, then set $z^* := \min\{z^*, \boldsymbol{c}^\top \boldsymbol{x}^s + \mathcal{Q}(\boldsymbol{x}^s)\}$ and delete all problems $\mathcal{G}_i^{'}$ with $z_{LD}(\mathcal{G}_i^{'}) \geqslant z^\star_{LD}$ from $\mathcal{G}$. Go to 2.
b) The scenario solutions $x^s, \forall s \in S$ are different, then compute a suggestion $\hat{\boldsymbol{x}} := Heu(\boldsymbol{x}^1, \ldots, \boldsymbol{x}^{|S|})$ using heuristic (Try solutions of all scenarios). This heuristic is applied in the first 11 nodes to facilitate dicovery of an incumbent early in the B&B tree. **If** $\hat{\boldsymbol{x}}$ is feasible, **then** let $z^* := \min\{z^*, \boldsymbol{c}^\top \hat{\boldsymbol{x}} + \mathcal{Q}(\hat{\boldsymbol{x}})\}$ and delete all problems $\mathcal{G}_i^{'}$ with $z_{LD}(\mathcal{G}_i^{'}) \geqslant z^\star_{LD}$ from $\mathcal{G}$, Go to 5.
5: ***Branching:*** Select a component $\boldsymbol{x}_{(j)}$ of $\boldsymbol{x}$ and add two new problems to $\mathcal{G}$ that differ from $\mathcal{G}_i$ by the additional constraints $\boldsymbol{x}_{(j)} \leqslant \lfloor \hat{\boldsymbol{x}}_{(j)} \rfloor$ and $\boldsymbol{x}_{(j)} \geqslant \lfloor \hat{\boldsymbol{x}}_{(j)} \rfloor + 1$, respectively (as $\boldsymbol{x}_{(j)}$ is integer). Go to 3.

years. Without considering the interest rate, the annual capital cost for purchasing and installing of each ROD option is 1/30 of the initial investment cost. It is assumed that the backup DGs are connected in three phase and cannot be installed at the nodes just connected to single or two-phase lines. The basic load shedding cost is assumed to be $\$14/kWh$ [55] and the load shedding cost parameter c_i^L in equation (3.7) is the product of the basic load shedding cost and the load priority. The repair cost of a single pole for 6 pole types is assumed to be the same ($\chi^p_{ij,1} = \ldots = \chi^p_{ij,6} = \$4000$). The operation cost of backup DGs is assumed to be $\$8kW/h$. The time step is $\Delta t = 2$ hour. It is assumed that there are 5 load priorities, and the voltage range is set to be $0.95p.u \sim 1.05p.u$. 20 scenarios are randomly generated for experiments. Each scenario is assigned with a probability $p_r(s) = 1/20$. All experiments are implemented on the Iowa State University Condo cluster, whose individual blade consists of two 2.6 GHz 8-Core Intel E5-2640 v3 processors and 128GB of RAM. All models and algorithms are implemented using the software DDSIP [56].

المنارة للاستشارات
www.manaraa.com

Table 3.3 The investment cost of different ROD measures

#No.	Methods	Cost($)
1	Upgrading pole class	$6,000$/pole
2	Adding transverse guys to pole	$4,000$/pole
3	The combination of upgrading and guying pole	$10,000$/pole
3	Installing a natural gas-fired CHPs as DG with 400kW capacity	$1,000/kW$
4	Adding an automatic sectionlizer	$15,000$

*Assume the span of two consecutive poles is 150 ft.

3.5.2 Case1: Comparison with and without ROD

The IEEE 123-bus system is mapped into a coastal city in Texas. According to the histogram of landfall hurricane frequency in Texas [45], it is assumed w_H=2. Figure 3.6(a) represents the wind speed experienced by poles, which varies with the pole's distance to the hurricane's eye. Figure 3.6(b) compares the pole resistance ($R^3_{ij,n}$) and the wind load $S^3_{ij,n}(t)$. Wind load is determined by the sustained wind speed on the pole. Once $R^3_{ij,n} < S^3_{ij,n}(t_d)$, the pole would be damaged at time t_d and remain damaged until it is repaired, as shown in Figure 3.6(c). When the pole is damaged at time t_d, the entire line is out of service.

We compare the cases with and without ROD under 20 different scenarios to quantify the impact of ROD methods on system resilience. By solving our proposed model, the optimal ROD decisions are shown in Figure3.7, with a total investment cost of $\$5,048,000$. Consider the budget limitation, the total number of backup DGs is limited to be 5. We compare the second stage cost from the hurricane hits the system to the point when all damaged lines are repaired as shown in Figure 3.8. The expected second-stage cost with optimal ROD is 8.93% of that without ROD. It can seen that the optimal ROD can directly reduce the economic losses during hurricanes.

المنارة للاستشارات
www.manaraa.com

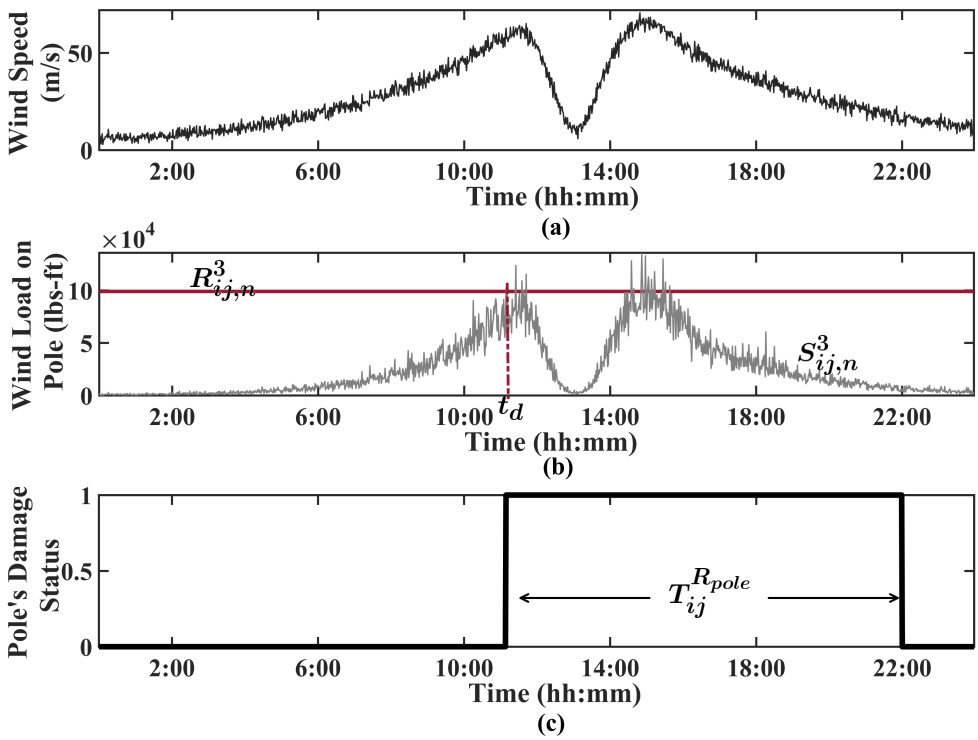

Figure 3.6 Simulating a distribution pole's damage status in a hurricane

To further illustrate the effectiveness of ROD, the percentage of power-served (POPS(t)) which can depict the resilience curve against time t is expressed as:

$$\text{POPS}(t) = \sum_{s \in \mathcal{S}} p_r(s) \frac{\sum_{i \in \Omega_N} (1 - y^{r,s}_{i,t}) P^{L,s}_{i,t}}{\sum_{i \in \Omega_N} P^{L,s}_{i,t}}, \forall t \in \mathcal{T}_H \tag{3.53}$$

Figure 3.9 compares system resilience curves with and without ROD. Compared to 93% POPS drop in the original system, the system with only optimal line hardening experiences a 84.1% POPS drop and the system after optimal ROD with multiple coordinated ROD options only experiences a 23.9% POPS drop. In addition, the POPS drop starts earlier in the original system. Moreover, systems with optimal ROD have shorter restoration time. For example, the original system needs 112 hours to recover from hurricane, but the systems after optimal ROD only need 20 hours. These results indicate the system with optimal ROD has stronger surviving ability to withstand hurricane and faster recovery. The results also indicate that the DGs and automatic sectionalizers

المنارة للاستشارات
www.manaraa.com

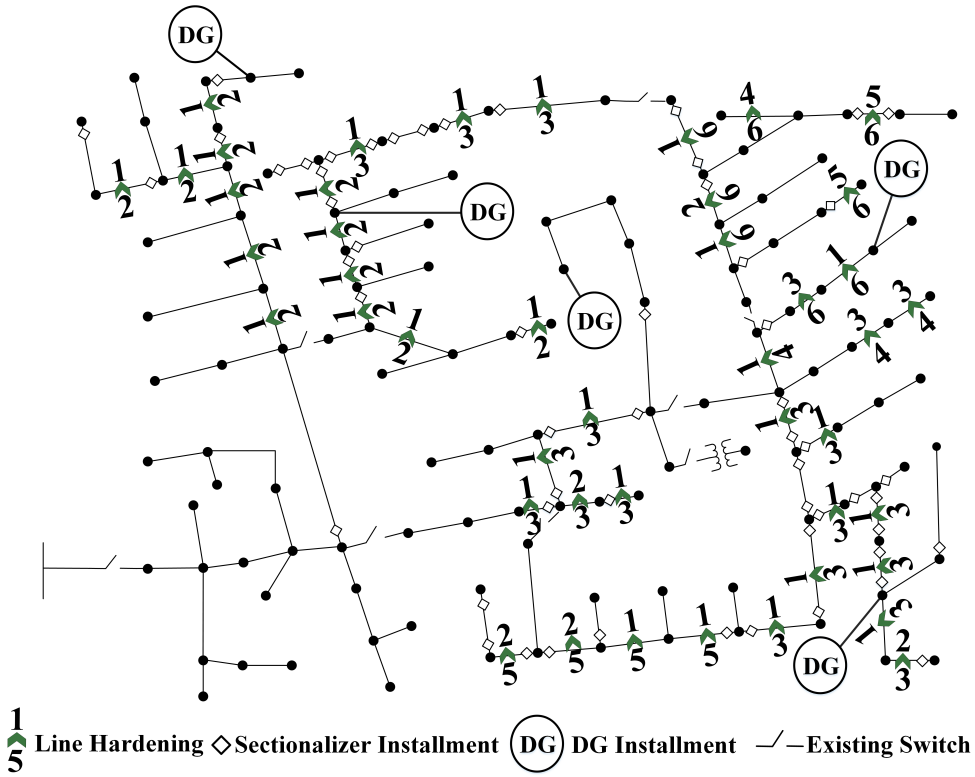

Figure 3.7 The optimal ROD methods implementation

can contribute to mitigating the hurricane's impact on the system. Hence, an optimal ROD should coordinate multiple resilience-enhancing methods.

3.5.3 Case2: The Self-Healing Operation

In order to validate the novelty of our MILP formulation strategy to solve the challenges of self-healing operation mentioned in section 3.3.2, the time varying system reactions to a hurricane are analyzed. It is assumed that the distribution system has implemented the optimal ROD measures as Figure 3.7 shown. We take two operation points at $t = 10$ and $t = 21$ in a scenario as illustrative example. In Figure 3.10, there were 14 lines out of service and isolated by the sectionalizers. The distribution system itself sectionalized into 5 healthy islands, which operated as MGs. In each healthy island, there was an active node with zero angle and its network kept radial. The number of zero angles was equal to the number of healthy islands. At the operation point $t = 21$,

المنارة للاستشارات
www.manaraa.com

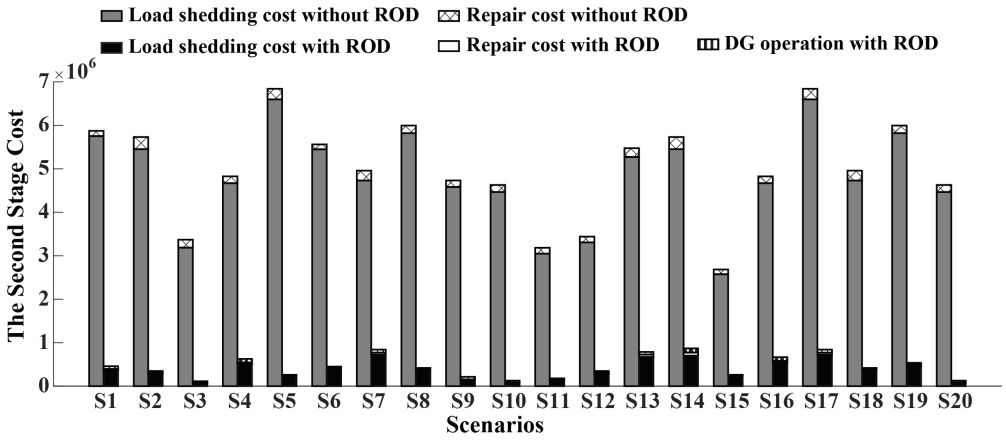

Figure 3.8 The second stage cost comparison with and without ROD under different scenarios

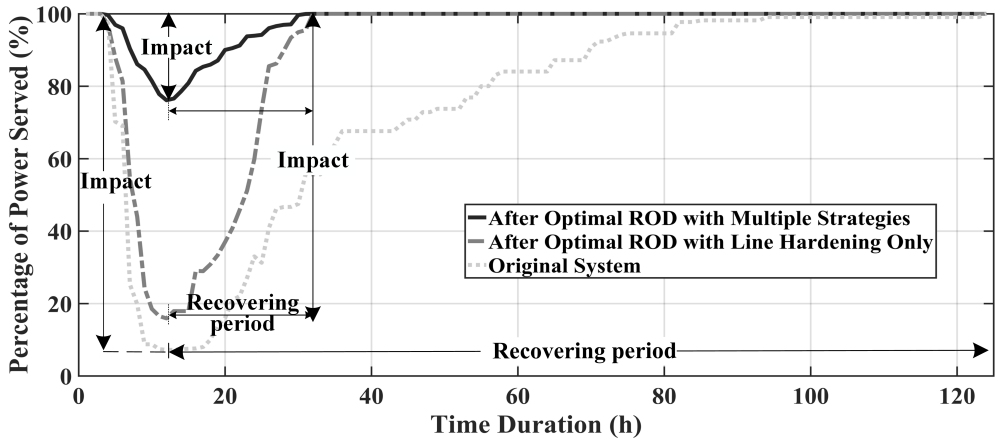

Figure 3.9 The system resilience curve comparison

6 damaged lines have been repaired. The distribution system reconfigured itself into 3 healthy islands, made some nodes in the de-energized islands become healthy and isolated them from the remaining outage areas as shown in Figure 3.11. These results indicate that the proposed modeling strategy can achieve self-healing operation.

3.5.4 Computational Results

Although the DD algorithm can use the branch and bound to converge eventually to any desired gap, it may takes days or weeks for the large scale scale ROD problem to get relative gap at 1% [51].

المنارة للاستشارات
www.manaraa.com

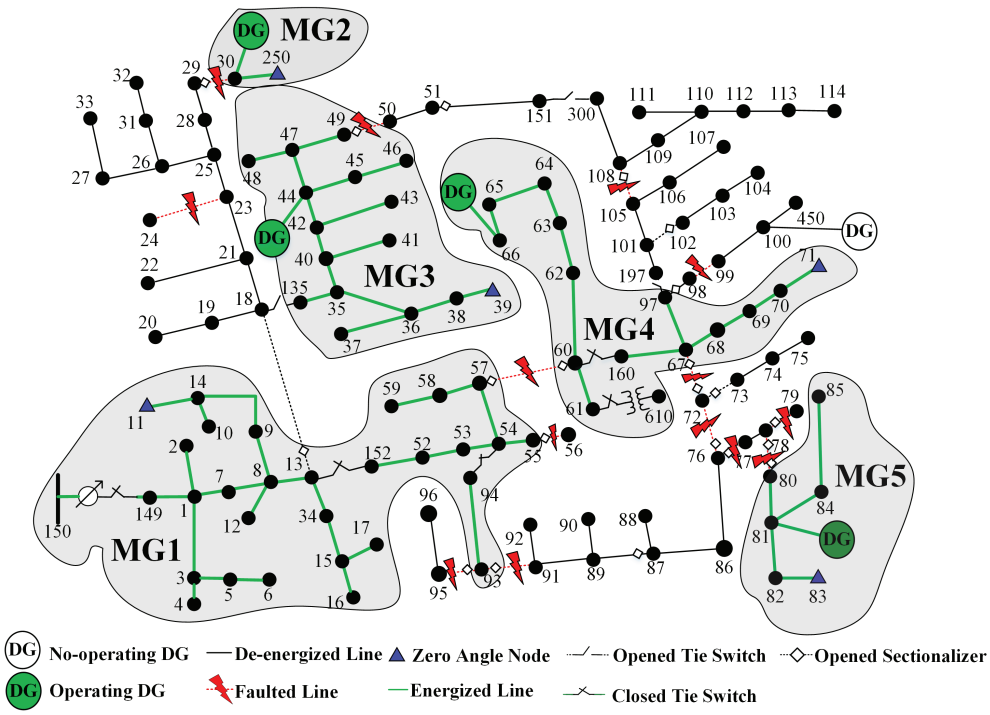

Figure 3.10 System's self-healing operation at $t = 10$

Here it is assumed the relative optimality gap is 8%. The computational results of ROD problem on the 123-bus test system under different scenarios are shown in the Table 3.4. From Table 3.4, it can been seen that the case with 20 scenarios takes longer computational time to solve but it still can converge to the relative optimality gap 8%.

Table 3.4 The solution quality statics for DD algorithm solving ROD problems

#Scenario	Upper Bound	Lower Bound	Wall Time (h)
5	674,286.3	628,434.8	67
10	729,310.1	671,694.6	115
20	1,057,962.1	976,499.1	156

3.5.5 Solution Validation

A multiple replication procedure (MRP) [57] is used to test the stability and quality of the candidate solutions shown in Figure 3.7. We generate 30 sets of scenarios, and each set has 20

المنارة للاستشارات
www.manaraa.com

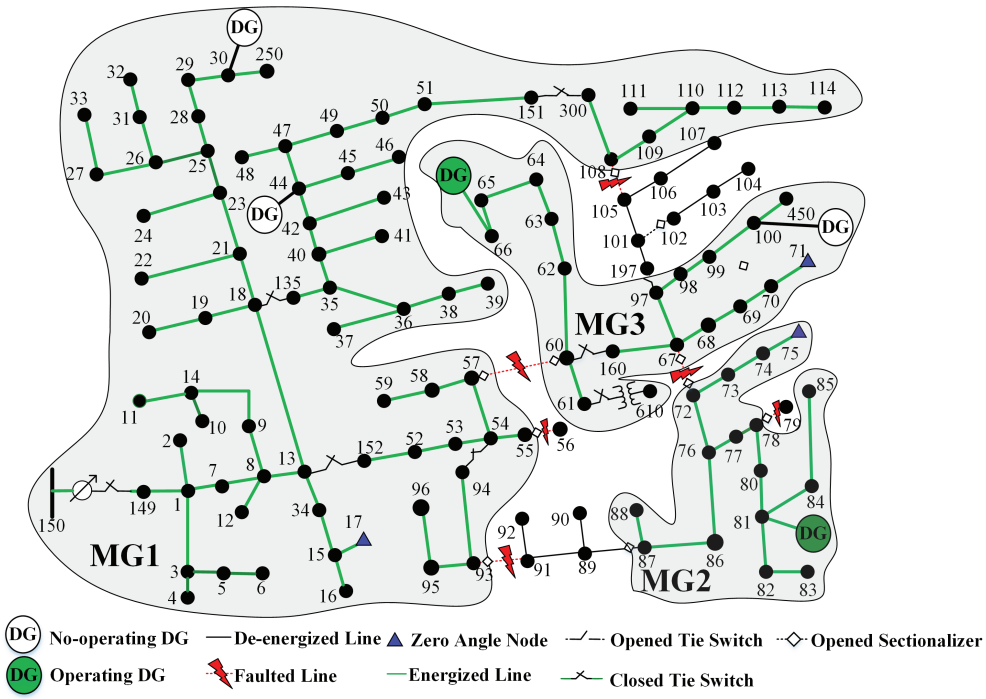

Figure 3.11 System's self-healing operation at $t = 21$

scenarios. The ROD problem is solved for the 30 sets of scenarios to construct the confidence interval (CI) for the optimality gap. The one-sided CI of the candidate solutions as shown in Figure 3.7 in the percentage term with regard to the objective value for the optimality gap is $[0, 10.54\%]$. This small gap shows the candidate solutions are stable and of high quality.

3.6 Summary

A new modeling and solution methodology for resilience-oriented design (ROD) of power distribution systems against wind-induced climatic hazards is proposed. The spatial-temporal correlations among ROD decisions, uncertainty space, and system operations during and after climatic hazards are well explored and established. A two-stage stochastic mixed-integer model is proposed with the objective to minimize the investment cost in the first-stage and the expected costs of the loss of loads, repairs and DG operations in the second stage. To solve this model, a scenario-based dual composition algorithm is developed. Numerical studies on the 123-bus distribution system

المنارة للاستشارات
www.manaraa.com

demonstrate the effectiveness of optimal ROD on enhancing the system resilience: 1) this model can build a resilience curve to represent the ROD decisions' effect on the evolving operation states; 2) the optimal solution of the second stage can model the outage propagation during faults while minimizing the outage areas and preserve radiality in each energized microgrid after reconfiguration.

المنارة للاستشارات
www.manaraa.com

CHAPTER 4. RISK-AVERSE PROACTIVE PREPAREDNESS OF ELECTRICAL DISTRIBUTION SYSTEMS WITH CONDITIONAL VALUE-AT-RISK

4.1 Overview

When an extreme weather event like a hurricane strikes an area, its corresponding distribution system may experience a failure-recovery-cost process: 1) some grid components are damaged; 2) power outages propagate and customers are out of service for several hours or even several days; 3) the utility makes full use of flexible resources, such as emergency generators and repair crews in the system to facilitate repair and service restoration. Moreover, this failure-recovery-cost process can be prolonged, as the damaged transportation network hinders the physical delivery of flexible resources and decreases crew mobility. Therefore, it is necessary for utilities to proactively prepare for extreme events to improve the system resilience and hasten the recovery process. This chapter proposes a two-stage SMILP with CVaR constraints that will strategically manage solar energy in coordination with various flexible resources to prepare for the forthcoming extreme weather events to improve distribution system resilience during and after the event. The proposed SMIP considers the uncertainty of load demand, line damage and solar irradiance. A modified progressive hedging algorithm is introduced to solve the proposed problem.

4.2 Proposed Methodology

For an upcoming extreme weather event, the distribution system operator can take some strategically sequential actions to enhance system resilience, as shown in Figure 4.1. Several days or hours before an extreme weather event (e.g., hurricane) hits a distribution system, a more accurate prediction of the event in terms of severity, affected areas, and trajectory path will be available from advanced weather foresting methodologies. With these weather data, the distribution system

المنارة للاستشارات
www.manaraa.com

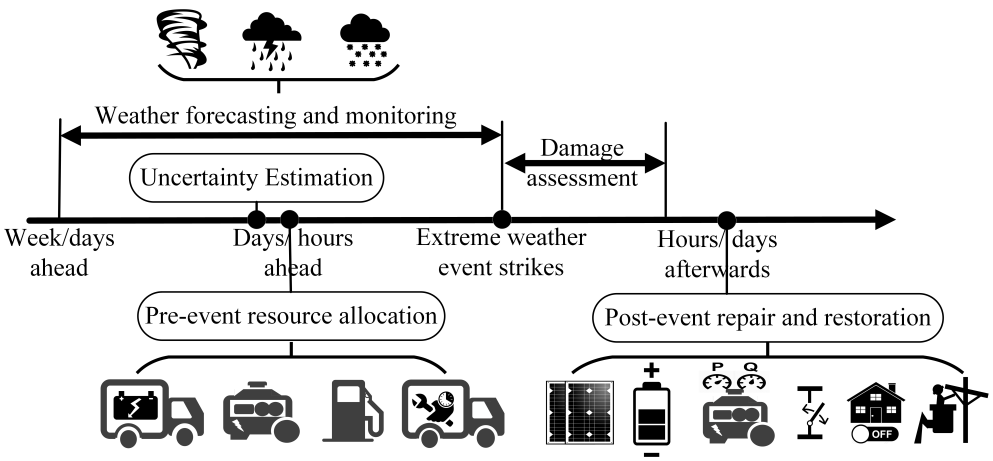

Figure 4.1 The sequential actions of the distribution system operator for an upcoming extreme weather event

operator can quantitatively estimate the impact of the upcoming extreme weather event on the distribution system through a specific stochastic process. After acquiring the estimated line damage information, the distribution system operator can strategically prepare and manage the flexible resources in the system within a given budget. During and after the event, the distribution system operator schedules and dispatches flexible resources, which are allocated in the pre-event proactive management and preparation module, to provide power for customers as fast as possible.

4.2.1 Uncertainty Estimation under Extreme Weather Events

We consider three kinds of uncertainties under the upcoming extreme weather events: line damage status, load profile and solar irradiance.

4.2.1.1 Line Damage Status

We simulate the line damage status and the repair times by modeling the complex interactions among weather, failures to physical infrastructure (e.g., distribution pole), and the repair time of damaged infrastructure. Figure 4.2 depicts the procedure taken to simulate the damage to the grid. It is assumed that a line damage status is determined by whether any pole of that line is damaged given the wind speed. From Figure 4.2, it can be seen that a line damage status, i.e.,

المنارة للاستشارات
www.manaraa.com

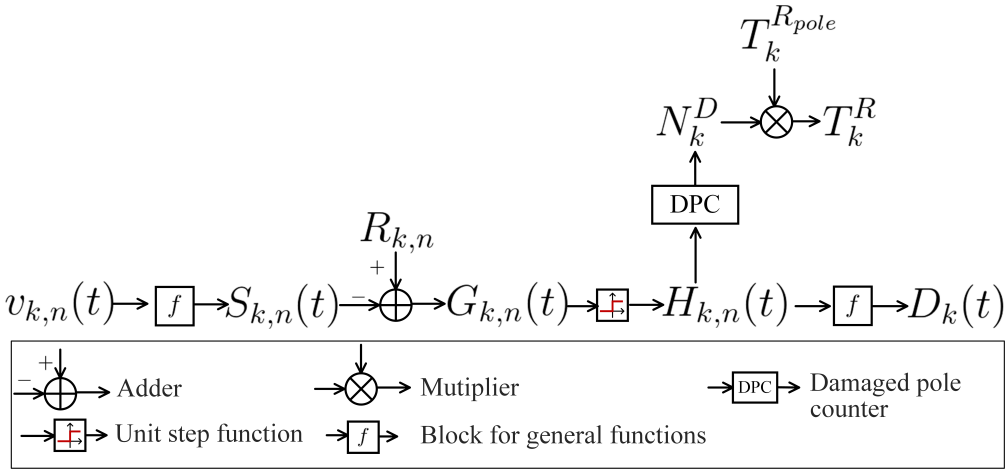

Figure 4.2 Line damage status simulation procedure

$D_k(t)$ is determined by whether any pole of line k is damaged ($H_{k,n}$=0). Line k's corresponding repair time is the product of the total number of damaged poles on the line N_k^D and repair time for a single pole $T_k^{R_{pole}}$. $T_k^{R_{pole}}$ follows the Weibull distribution [58]. The n-th pole's status (damaged or functional) is determined by comparing pole resistance $R_{k,n}$ and pole' wind load $S_{k,n}(t)$ according to the structural limit state function $G_{k,n}(t)$=$R_{k,n}$−$S_{k,n}(t)$ in [43].

4.2.1.2 Load Profile

It is assumed that the power demand of load is the product of the hourly forecast load profile denoted by $P_{i,\varphi,t}^L(t)/Q_{i,\varphi,t}^L(t)$ and the hourly forecast error $\tau(t)$:

$$P_{i,\varphi}^L(t) = P_{i,\varphi}^f(t)(1+\tau(t)), \forall i \in \Omega_N, \varphi, t \tag{4.1}$$

$$Q_{i,\varphi}^L(t) = Q_{i,\varphi}^f(t)(1+\tau(t)), \forall i \in \Omega_N, \varphi, t \tag{4.2}$$

where $\tau(t)$ follows a truncated normal distribution with ±15% bounding [59].

4.2.1.3 Solar Irradiance

In a solar-integrated distribution system, the power output of PVs depends on the incident solar irradiance. At the same time, solar irradiance is determined by the cloud coverage level during and

المنارة للاستشارات
www.manaraa.com

after the extreme weather event. So, it is necessary to model the uncertainty of solar irradiance under an extreme weather event. The value of solar irradiance can be expressed as follows [60]:

$$Ir_t = \overline{Ir}_t(1 - CCL_{co,t}) \tag{4.3}$$

where $\overline{Ir}$ represents the maximum solar irradiance at time t; and CCL_{co} represents the corrected cloud coverage level (CCL), which considers the variability of CCL. The value of the correctedd CCL follows a normal distribution with mean $\overline{CCL}_t$ and standard deviation 0.05 as follows:

$$CCL_{co,t} \sim \max\{0, N(\overline{CCL}_t, 0.05)\} \tag{4.4}$$

where $\overline{CCL}_t$ is determined by the forecast cloud type, which follows a uniform distribution:

$$CCL_t = U(CCL_{min}, CCL_{max}) \tag{4.5}$$

4.2.2 Proactive Energy Management and Preparation

Six kinds of flexible resources are considered for proactive energy management and preparation: 1) mobile emergency generators (MEG); 2) mobile energy storage (MES) devices; 3) fixed-installed distributed generators; 4) distributed solar energy resources; 5) repair crews; and 6) network reconfiguration. In the preparation stage, the distribution system operator preallocates mobile resources, fuels for diesel DGs, and repair crews. Pre-allocating mobile resources can ensure the earliest possible electric service recovery, and reduce the influence of road network damage and congestion. Pre-delivering fuel before an extreme event is critical to make emergency generators well prepared for islanded operation and service restoration. The repair crews should be pre-staged strategically to certain locations before the event, such that after the event, they can be dispatched to repair the damaged components efficiently. After the event strikes the system, the distribution system operator make full use of the dispatchable energy resources to provide energy for isolated areas that are not damaged, and to restore critical customers. Pre-assigned crews can provide a faster and more organized repair response. The flexibility of topology provided by network reconfiguration can make the distribution grid less prone to damage during the event and thus facilitate efficient

المنارة للاستشارات
www.manaraa.com

recovery after the event. As a result, the distribution system operator can perform the schedule and dispatch of pre-allocated flexible resources during and after the event to provide power for customers as fast as possible.

4.3 Two-stage Stochastic Mixed-Integer Programming Formulation with CVaR Constraints

The climatic hazards (e.g. hurricane, ice-storm, thunderstorm, etc) can significantly affect distribution system outage risk by increasing the frequency of failures of the power components and/or inducing severe damage [61]. In preparation for an upcoming extreme weather event, utility companies and governments are concerned about the monetary costs and benefits of proactive resource management. Therefore, it is necessary to find a trade-off between the preparation costs and the costs associated with the potential damage to the distribution system. At the same time, the natural property of the extreme weather event is low probability, but high damage consequence and the pre-event allocation decision is only specific for a single upcoming extreme weather event. These challenges indicate that we need to find a risk-averse approach to mitigate tail risks in the pre-event allocation problems. As CVaR is an averse risk measure that focuses on high consequence and can be flexibly determined between the mean loss and the maximum loss, depending on the value of α, we use CVaR as a track measure to provides different risk preference for the utility to make allocation decisions.

4.3.1 Conditional Value-at-Risk as a Risk Measure

Let $\pi(\boldsymbol{x}, \boldsymbol{\xi})$ be the damage loss associated with the pre-event allocation decision vector $\boldsymbol{x} \in \chi$, and the random vector $\boldsymbol{\xi}$. For each $\boldsymbol{x}$, the damage loss $\pi(\boldsymbol{x}, \boldsymbol{\xi})$ is a random variable having a distribution of $\boldsymbol{\xi}$ in $\mathbb{R}$. For each $\boldsymbol{x}$, we denote $\psi(\boldsymbol{x}, \cdot)$ as the cumulative distribution function of the damage loss $\pi(\boldsymbol{x}, \boldsymbol{\xi})$:

$$\psi(\boldsymbol{x}, \delta) = P[\boldsymbol{\xi} \,|\pi(\boldsymbol{x}, \boldsymbol{\xi}) \leq \delta] \tag{4.6}$$

المنارة للاستشارات
www.manaraa.com

Definition 1 Value-at-Risk (VaR). Given the confidence level $\alpha \in (0,1)$, the α-VaR of the damage loss associated with a decision $\boldsymbol{x}$ is the value

$$\begin{aligned}\delta_\alpha(\boldsymbol{x}) &= \min\{\delta \,|\psi(\boldsymbol{x},\delta) \geq \alpha\} \\ &= \min\{\delta \,|P[\boldsymbol{\xi}\,|\pi(\boldsymbol{x},\boldsymbol{\xi}) \leq \delta] \geq \alpha\}\end{aligned} \tag{4.7}$$

Given Definition 1, VaR is the minimum damage loss that will not be exceeded with probability α. It also can be interpreted as the smallest damage loss in the $(1-\alpha)\times 100\%$ worst cases.

The α-tail cumulative distribution function of $\pi(\boldsymbol{x},\boldsymbol{\xi})$ is defined as [62]:

$$\psi_\alpha(\boldsymbol{x},\delta) = \begin{cases} 0 & \text{if } \ \delta < \delta_\alpha(\boldsymbol{x}) \\ [\psi(\boldsymbol{x},\delta)-\alpha]/[1-\alpha] & \text{if } \ \delta \geq \delta_\alpha(\boldsymbol{x}) \end{cases} \tag{4.8}$$

Note that $\psi_\alpha(\boldsymbol{x},\cdot)$ is another distribution function, which is obtained by rescaling the function $\psi(\boldsymbol{x},\cdot)$ in the interval $[\alpha,1]$.

Definition 2 Conditional Value-at-Risk (CVaR). Given the confidence level $\alpha \in (0,1)$, the α-CVaR of the damage loss associated with a decision $\boldsymbol{x}$ is the value [62]

$$\begin{aligned}\phi_\alpha(\boldsymbol{x}) &= \text{mean of the } \alpha\text{-tail distribution of } \pi(\boldsymbol{x},\boldsymbol{\xi}) \\ &= \mathbb{E}\left[\delta \,|\delta \geq \delta_\alpha(\boldsymbol{x})\right]\end{aligned} \tag{4.9}$$

Figure 4.3 shows the VaR and CVaR for a specific continuous random variable $\pi(\boldsymbol{x},\boldsymbol{\xi})$. The cumulative distribution function of $\pi(\boldsymbol{x},\boldsymbol{\xi})$ can be used to find $\delta_\alpha(\boldsymbol{x})$, and $\delta_\alpha(\boldsymbol{x})$ can be used in turn to calculate $\phi_\alpha(\boldsymbol{x})$.

4.3.2 Conditional Value-at-Risk in Optimization

The function denoted by $F_\alpha(\boldsymbol{x},\delta)$ is defined to describe a characterization of $\phi_\alpha(\boldsymbol{x})$ and $\delta_\alpha(\boldsymbol{x})$:

$$F_\alpha(\boldsymbol{x},\delta) = \delta + \frac{1}{1-\alpha} E\left\{[\pi(\boldsymbol{x},\boldsymbol{\xi})-\delta]^+\right\}, \text{where } [t]^+ = \max\{0,t\} \tag{4.10}$$

$F_\alpha(\boldsymbol{x},\delta)$ can be approximated in various ways. For example, this can be done by sampling the probability distribution of $\boldsymbol{\xi}$ according to its density $p_r(\boldsymbol{\xi})$ [63]. If the sampling generates a

المنارة للاستشارات
www.manaraa.com

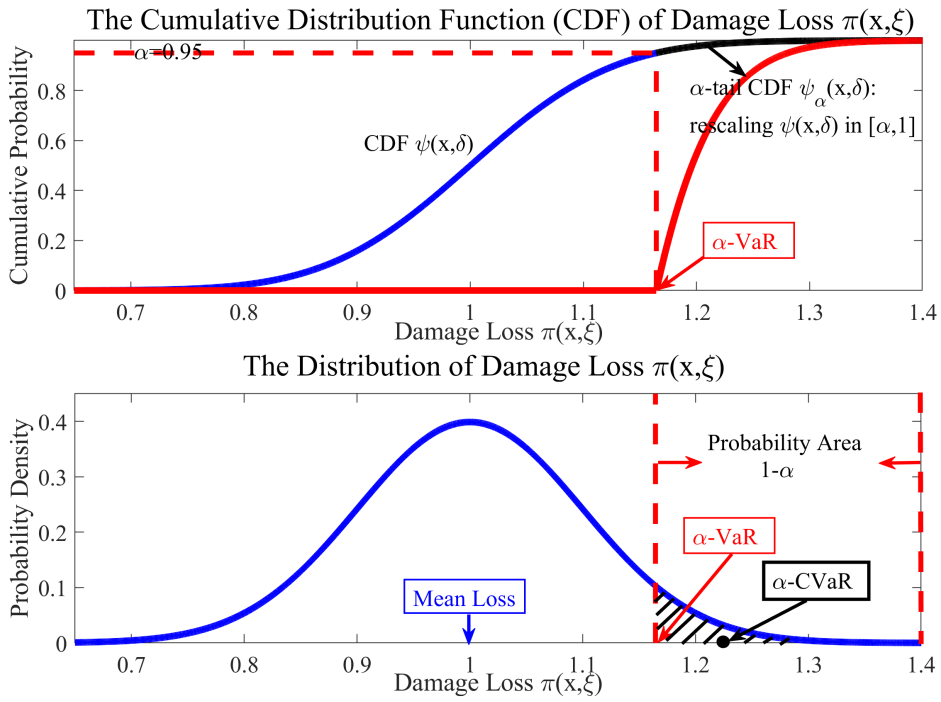

Figure 4.3 The VaR_α and CVaR_α of damage loss $\pi(\boldsymbol{x}, \boldsymbol{\xi})$

collection of vectors $\boldsymbol{\xi}_1, \ldots, \boldsymbol{\xi}_{|\mathcal{S}|}$, then the corresponding approximation to $F_\alpha(\boldsymbol{x}, \delta)$ is

$$\tilde{F}_\alpha(\boldsymbol{x}, \delta) = \delta + \frac{1}{1-\alpha} \sum_{\boldsymbol{\xi} \in \mathcal{S}} p_r(\boldsymbol{\xi})[\pi(\boldsymbol{x}, \boldsymbol{\xi}) - \delta]^+, \text{where } [t]^+ = \max\{0, t\} \tag{4.11}$$

Theorem 1 As a function of $\delta \in \mathbb{R}$, $F_\alpha(\boldsymbol{x}, \delta)$ is finite and convex. The α-CVaR of the loss associated with any $\boldsymbol{x} \in \chi$ can be determined from

$$\phi_\alpha(\boldsymbol{x}) = \min_\delta F_\alpha(\boldsymbol{x}, \delta) \tag{4.12}$$

and

$$\delta_\alpha(\boldsymbol{x}) = \text{lower endpoint of } \text{argmin}_\delta F_\alpha(\boldsymbol{x}, \delta) \tag{4.13}$$

In particular,

$$\delta_\alpha(\boldsymbol{x}) \in \text{argmin}_\delta F_\alpha(\boldsymbol{x}, \delta), \phi_\alpha(\boldsymbol{x}) = F_\alpha(\boldsymbol{x}, \delta_\alpha(\boldsymbol{x})) \tag{4.14}$$

المنارة للاستشارات
www.manaraa.com

Theorem 2 Minimizing $\delta_\alpha(\boldsymbol{x})$ with respect to $\boldsymbol{x} \in \chi$ is equivalent to minimizing $F_\alpha(\boldsymbol{x}, \delta)$ over all $(\boldsymbol{x}, \delta) \in \chi \times \mathbb{R}$, in the sense that

$$\min_{\boldsymbol{x} \in \chi} \phi_\alpha(\boldsymbol{x}) = \min_{(\boldsymbol{x},\delta) \in \chi \times \mathbb{R}} F_\alpha(\boldsymbol{x}, \delta) \tag{4.15}$$

where, moreover, a pair $(\boldsymbol{x}^*, \delta^*)$ achieves the second minimum if and only if $\boldsymbol{x}^*$ achieves the first minimum and $\delta^* \in \text{argmin}_\delta F_\alpha(\boldsymbol{x}^*, \delta)$. Therefore, in circumstances where the interval $\text{argmin}_\delta F_\alpha(\boldsymbol{x}^*, \delta)$ reduces to a single point, the minimization of $F_\alpha(\boldsymbol{x}, \delta)$ over $(\boldsymbol{x}, \delta) \in \chi \times \mathbb{R}$ produces a pair $(\boldsymbol{x}^*, \delta^*)$, such that $\boldsymbol{x}^*$ minimizes the α-CVaR and δ^* gives the corresponding α-VaR. Theorem 2 not only gives a way to express the CVaR minimization problem in a tractable form, but also allows to calculate α-CVaR without having to calculate α-VaR first.

Applying Theorem 2 and (4.11), the allocation decision $\boldsymbol{x}$ that minimizes the Conditional Value-at-Risk of the damage loss at the confidence level α can be expressed as:

$$\min_{\boldsymbol{x} \in \chi} CVaR_\alpha(\boldsymbol{x}) = \min_{(\boldsymbol{x},\delta) \in \chi \times \mathbb{R}} \delta + \frac{1}{1-\alpha} \sum_{\boldsymbol{\xi} \in \mathcal{S}} p_r(\boldsymbol{\xi})[\pi(\boldsymbol{x}, \boldsymbol{\xi}) - \delta]^+, \text{where } [t]^+ = \max\{0, t\} \tag{4.16}$$

In order to describe $[\pi(\boldsymbol{x}, \boldsymbol{\xi}) - \delta]^+$, the additional variables $\eta(\boldsymbol{\xi})$ are introduced subject to the conditions:

$$\pi(\boldsymbol{x}, \boldsymbol{\xi}) - \delta \leq \eta(\boldsymbol{\xi}), \eta(\boldsymbol{\xi}) \geq 0 \tag{4.17}$$

Therefore (4.16) is reformulated as following:

$$\begin{aligned} &\min_{(\boldsymbol{x},\delta) \in \chi \times \mathbb{R}} \delta + \frac{1}{1-\alpha} \sum_{\boldsymbol{\xi} \in \mathcal{S}} p_r(\boldsymbol{\xi}) \eta(\boldsymbol{\xi}) \\ &s.t.\ \pi(\boldsymbol{x}, \boldsymbol{\xi}) - \delta \leq \eta(\boldsymbol{\xi}), \eta(\boldsymbol{\xi}) \geq 0 \end{aligned} \tag{4.18}$$

The minimization of pre-event allocation cost and CVaR of potential damage loss in the proactive energy management and preparation optimization problem is formulated as:

$$\begin{aligned} &\min_{(\boldsymbol{x},\delta) \in \chi \times \mathbb{R}} c^\top \boldsymbol{x} + \delta + \frac{1}{1-\alpha} \sum_{s \in \mathcal{S}} p_r(s) \eta_s \\ &s.t.\ \pi(\boldsymbol{x}, s) - \delta \leq \eta_s, \eta_s \geq 0, \forall s \in \mathcal{S} \end{aligned} \tag{4.19}$$

where $\pi(\boldsymbol{x}, s)$ represents the damage loss associated with the pre-event allocation decision vector $\boldsymbol{x} \in \chi$ and the random scenario s; the optimal value of δ, δ^*, known as the value-at-risk (VaR)

المنارة للاستشارات
www.manaraa.com

represents the minimum value such that the probability that the damage loss cost exceeds or equal δ^* is less than or equal to $1-\alpha$; η_s is the difference between the damage loss cost of scenario s and VaR.

4.3.3 Mathematical Formulation

This subsection presents a two-stage stochastic mixed integer linear program (SMILP) with Conditional Value at Risk (CVaR) constraints, whose model with uncertainty considers the worse consequence of extreme events. In the first stage, we allocate mobile emergency generators and energy storage devices, fuel for diesel distributed generators (DGs), and repair crews with the minimum allocation cost. The second stage is to minimize the expected CVaR of damage loss, which includes the load shedding penalty cost, damaged line repair cost, fuel consumption cost and switch operation cost. The nomenclature of this chapter is provided in the Table 4.1.

Table 4.1 Nomenclature for the CVaR-based SMILP model

Indices and sets	
φ	Index for phase number
$\mathcal{S}$	Set of scenarios
Ω_C	Set of crews
Ω_{CN}	Set of candidate buses for MEG and MES
Ω_D	Set of damaged lines
$\Omega_{D(r)}$	Set of damaged lines in region r
Ω_{EG}	Set of buses with backup emergency generators
Ω_{ES}	Set of buses with energy storage
Ω_{ESC}	$\Omega_{ES} \cup \Omega_{CN}$
Ω_G	$\Omega_{EG} \cup \Omega_{CN}$
Ω_K	Set of lines

المنارة للاستشارات
www.manaraa.com

Table 4.1 (Continued)

$\Omega_{K(.,i)}$	Set of lines with bus i as the to bus
$\Omega_{K(i,.)}$	Set of lines with bus i as the from bus
$\Omega_{K(l)}$	Set of lines in loop l
Ω_{MEG}	Set of MEG
Ω_{MES}	Set of MES devices
Ω_{N}	Set of buses
Ω_{loop}	Set of possible loops in the distribution network
Ω_{PV}	Set of buses with solar cells
Ω_{PV}^{C}	Set of buses with on-grid PVs
Ω_{PV}^{G}	Set of buses with grid-forming PVs
Ω_{PV}^{H}	Set of buses with hybrid on-grid/off-grid PVs
Ω_{R}	Set of regions in the network
Ω_{Reg}	Set of voltage regulators
Ω_{Sub}	Set of substations
Ω_{SW}	Set of switches
$\mathcal{T}_b$	Set of time duration before repair
$\mathcal{T}_a$	Set of time duration after crews start to repair
$\mathcal{T}$	$\mathcal{T}_b \cup \mathcal{T}_a$

Parameters

a_f/b_f	Coefficients for calculating fuel consumption
C_i^D	Load shedding cost at bus i
C^{sw}	Switch operation cost
C^F/C^f	Fuel allocation/consumption cost
C_g^G/C_g^E	Allocation cost of MEG/MES
C^A/C^R	Crew allocation/repair cost
$D_{k,t,s}$	Line status before crews start to repair

المنارة للاستشارات
www.manaraa.com

Table 4.1 (Continued)

$P^L_{i,\varphi,t}/Q^L_{i,\varphi,t}$	Active/reactive power demand at bus i, phase φ and time t
F^T	The total amount of available fuel for the utility
F^C_i	Current amount of available fuel at bus i
F^{max}_i	Maximum amount of fuel allocated to bus i
$Ir_{t,s}$	Solar irradiance on PV at time t, and scenario s
M	Large positive number
N^C	Number of crews
$N^{C_{min/max}}_r$	Minimum/maximum number of crews at area r
$P/Q^{K_{max}}_k$	Active/reactive power limit of line k
$P/Q^{G_{max}}_i$	Active/reactive power limits of DGs
$P/Q^{PV_{max}}_i$	Rated active/reactive power of PV at bus i
$Pr(s)$	Probability of scenario s
$S^{ES/PV/K}$	Rated apparent power of energy storage device/PV/line
$\mathcal{T}^r_{k,s}$	The estimated time needed to repair damaged line k in scenario s
Z_k	The impedance matrix of line k
U_{min}/U_{max}	The squared voltage limits on each bus and phase
$\boldsymbol{p}_k$	Vector with binary entries for representing the phases of line k
$\boldsymbol{a}_k$	Vector representing the ratio between the primary and secondary voltages for each phase of the voltage regulator on line k
η_c/η_d	Charging/discharging efficiency
Δt	Time step

Decision Variables

A_r	Number of crews located at area r
$E_{i,t,s}$	Available energy of battery i at time t in scenario s
$FC_{i,s}$	Amount of fuel consumed at bus i in scenario s
$\gamma_{k,t,s}$	Binary variable indicates whether switch k is operated in time t in scenario s
$\boldsymbol{S}_{k,t,s}$	Vector representing the apparent power for line k at time t in scenario s

المنارة للاستشارات
www.manaraa.com

Table 4.1 (Continued)

$\boldsymbol{U}_{i,t,s}$	Vector representing the squared voltage magnitude for bus i at time t in scenario s
$w_{i,t,s}$	Binary variable equals to 0 if bus i is in an outage area at time t and scenario s
$h_{i,t,s}$	Charging/discharging state of the energy storage device
$P^{ch/dch}_{i,\varphi,t,s}$	Per-phase active power charged/discharged by the energy storage at bus i, phase φ, time t in scenario s
$P/Q^{G}_{i,\varphi,t,s}$	Active/reactive power generated by DG at bus i, phase φ, time t in scenario s
$P/Q^{K}_{k,\varphi,t,s}$	Active/reactive power flowing on line k, phase φ and time t in scenario s
$P/Q^{PV}_{i,\varphi,t,s}$	Active/reactive power generated by PV at bus i, phase φ, time t in scenario s
$Q^{ES}_{i,\varphi,t,s}$	Reactive power output of the energy storage device at bus i
$u_{k,t,s}$	Binary variables indicating the status of the line k at time t in scenario s
$u^{G}_{i,t,s}$	Binary variable indicating on/off status of generator at bus i, time t, and scenario s
$u^{M}_{g,i,t,s}$	Binary variable indicating on/off status of mobile generator g at bus i, time t in scenario s
$v^{f}_{k,\varphi,t,s}$	Virtual flow on line k
$v^{S}_{i,\varphi,t,s}$	Virtual flow from the virtual source to bus i, phase φ and time t in scenario s
x^{MEG}_{i}	Binary variable equals 1 if a mobile generator is staged at bus i
x^{MES}_{i}	Binary variable equals 1 if a mobile energy storage device is staged at bus i
x^{F}_{i}	Amount of fuel allocated to generator at bus i
$y_{i,t,s}$	Connection status of the load at bus i, time t, and scenario s
$z_{k,t,s}$	Binary variable equals 1 if line k is being repaired at time t in scenario s
$z^{a}_{k,t,s}$	Auxiliary variable used to ensure a damaged line is repaired in consecutive hours

المنارة للاستشارات
www.manaraa.com

4.3.3.1 Objective

The objective of the proactive resource management problem is to minimize the allocation cost of mobile emergency units, fuel and repair crews from other places, and the CVaR of the damage loss at the confidence level α:

$$\begin{aligned}\min \sum_{i\in\Omega_{CN}} \Big(\sum_{g\in\Omega_{MES}} C_g^E x_{g,i}^{MES} + \sum_{g\in\Omega_{MEG}} C_g^G x_{g,i}^{MEG} \Big) + \sum_{i\in\Omega_G} C^F x_i^F \\ + C^A \Big(\sum_{r\in\Omega_R} x_r^A - x_{fixed}^A \Big) + \delta + \frac{1}{1-\alpha} \sum_{s\in\mathcal{S}} p_r(s)\eta_s\end{aligned} \tag{4.20}$$

4.3.3.2 First-Stage Constraints

The constraints for the first stage are modeled as follows:

Mobile Sources Allocation

$$\sum_{i\in\Omega_{CN}} x_{g,i}^{MEG} \leqslant 1, \forall g \in \Omega_{MEG} \tag{4.21}$$

$$\sum_{i\in\Omega_{CN}} x_{g,i}^{MES} \leqslant 1, \forall g \in \Omega_{MES} \tag{4.22}$$

$$\sum_{g\in\Omega_{MES}} x_{g,i}^{MES} + \sum_{g\in\Omega_{MEG}} x_{g,i}^{MEG} \leqslant 1, \forall i \in \Omega_{CN} \tag{4.23}$$

Constraints (4.21) and (4.22) state that a MEG and MES can be placed at one bus, respectively. We assume that each bus can have only one mobile unit, which is enforced by (4.23).

Fuel Allocation

Define $\Omega_G = \Omega_{EG} \cup \Omega_{CN}$, where Ω_{EG} is the set of buses that have emergency generators, and Ω_{CN} is the set of candidate buses for mobile units. The fuel allocated to these buses must be limited to the amount of fuel available, as follows:

$$\sum_{i\in\Omega_G} x_i^F \leqslant F^T \tag{4.24}$$

Each location can have a limited number of fuel, and the location may already have fuel on site. The limits on the amount of fuel allocated to each bus are set by the following constraint:

$$F_i^C \leqslant x_i^F \leqslant F_i^{max}, \forall i \in \Omega_G \tag{4.25}$$

المنارة للاستشارات
www.manaraa.com

Crew Allocation

We assume that the distribution network is divided into different predefined regions, $r = \{1, 2, ..., |\Omega_R|\}$, and each region contains a set of distribution lines $\Omega_{K(r)}$. Each region r is assigned with a specific number of crews x_r^A. If the total number of crews is N^C, then the number of crews in each region is found using:

$$\sum_{r \in \Omega_R} x_r^A \leqslant N^C \tag{4.26}$$

The number of crews is limited in each region depending on the capacity of the staging locations.

$$N_r^{C_{min}} \leqslant x_r^A \leqslant N_r^{C_{max}}, \forall r \in \Omega_R \tag{4.27}$$

4.3.3.3 Second-Stage Constraints

The second-stage constraints include CVaR constraints, unbalanced power flow operation, energy storage constraints, network reconfiguration, PV system operation, and crew repair procedure.

CVaR Constraints

$$\begin{aligned} \pi_s = &\sum_{i \in \Omega_G} C^f FC_{i,s} + \sum_{\forall t} \sum_{\forall \varphi} \sum_{\forall i} C_i^D (1 - y_{i,t,s}) P_{i,\varphi,t,s}^L \\ &+ \sum_{t \in \mathcal{T}} \sum_{k \in \Omega_D} C_k^R (1 - u_{k,t,s}) + \sum_{\forall t} \sum_{k \in \Omega_{SW}} C^{sw} \gamma_{k,t,s}, \forall s \end{aligned} \tag{4.28}$$

$$\pi_s - \delta \leqslant \eta_s, \forall s \tag{4.29}$$

$$\eta_s \geqslant 0, \delta \in \mathbb{R}, \forall s \tag{4.30}$$

Constraint (4.28) represents the damage loss cost in a scenario, which includes load shedding penalty cost, fuel consumption cost, crew repair cost and switch operation cost. Constraint (4.29) and (4.30) impose the positive difference between the damage loss cost of scenario s and VaR.

Dispatchable Generators and Substation Limits

Two binary variables $u_{i,t,s}^G$ and $u_{g,i,t,s}^M$ are introduced to define the on-off status of emergency generators and mobile generators, respectively. These variables are necessary in order to evaluate

المنارة للاستشارات
www.manaraa.com

the amount of fuel consumed, which is discussed in section 4.3.3.3. Variable $u^{M}_{g,i,t,s}$ is correlated to $x^{MEG}_{g,i}$ using the following constraints:

$$u^{M}_{g,i,t,s} \leqslant x^{MEG}_{g,i}, \forall g \in \Omega_{MEG}, i \in \Omega_{CN}, t, s \tag{4.31}$$

The limits on generators are then imposed as follows:

$$0 \leqslant P^{G}_{i,\varphi,t,s} \leqslant u^{G}_{i,t,s} P^{G_{max}}_{i}, \forall i \in \Omega_{EG}, \varphi, t, s \tag{4.32}$$

$$0 \leqslant Q^{G}_{i,\varphi,t,s} \leqslant u^{G}_{i,t,s} Q^{G_{max}}_{i} \ , \ \forall i \in \Omega_{EG}, \varphi, t, s \tag{4.33}$$

$$0 \leqslant P^{G}_{i,\varphi,t,s} \leqslant \sum_{g \in \Omega_{MEG}} u^{M}_{g,i,t,s} P^{G_{max}}_{g} \ , \ \forall i \in \Omega_{CN}, \varphi, t, s \tag{4.34}$$

$$0 \leqslant Q^{G}_{i,\varphi,t,s} \leqslant \sum_{g \in \Omega_{MEG}} u^{M}_{g,i,t,s} Q^{G_{max}}_{g} \ , \ \forall i \in \Omega_{CN}, \varphi, t, s \tag{4.35}$$

The summation $\sum_{g \in \Omega_{MEG}} u^{M}_{g,i,t,s}$ is used to define the types of mobile DGs available with different power ratings. The formulations can be simplified in case of homogeneous mobile DGs. The limits on the substation active and reactive power are set by:

$$0 \leqslant P^{SS}_{i,\varphi,t,s} \leqslant P^{SS_{max}}_{i} \ , \ \forall i \in \Omega_{Sub}, \varphi, t, s \tag{4.36}$$

$$-Q^{SS_{max}}_{i} \leqslant Q^{SS}_{i,\varphi,t,s} \leqslant Q^{SS_{max}}_{i} \ , \ \forall i \in \Omega_{Sub}, \varphi, t, s \tag{4.37}$$

Line Limits

The linearized three phase power flow limit constraints are shown as follows [64]:

$$-u_{k,t,s} \ p_{k,\varphi} S^{K}_{k} \leqslant P^{K}_{k,\varphi,t,s} \leqslant u_{k,t,s} \ p_{k,\varphi} S^{K}_{k}, \forall k \in \Omega_{K}, \varphi, t, s \tag{4.38}$$

$$-u_{k,t,s} \ p_{k,\varphi} S^{K}_{k} \leqslant Q^{K}_{k,\varphi,t,s} \leqslant u_{k,t,s} \ p_{k,\varphi} S^{K}_{k}, \forall k \in \Omega_{K}, \varphi, t, s \tag{4.39}$$

المنارة للاستشارات
www.manaraa.com

$$-\sqrt{2}(u_{k,t,s}\ \ p_{k,\varphi})S_k^K \leqslant P_{k,\varphi,t,s}^K + Q_{k,\varphi,t,s}^K \leqslant \sqrt{2}(u_{k,t,s}\ \ p_{k,\varphi})S_k^K, \forall k \in \Omega_K, \varphi, t, s \quad (4.40)$$

$$-\sqrt{2}(u_{k,t,s}\ \ p_{k,\varphi})S_k^K \leqslant P_{k,\varphi,t,s}^K - Q_{k,\varphi,t,s}^K \leqslant \sqrt{2}(u_{k,t,s}\ \ p_{k,\varphi})S_k^K, \forall k \in \Omega_K, \varphi, t, s \quad (4.41)$$

Node Balance and Voltage Law

$$\sum_{\substack{\forall j \in \Omega_{Sub} \\ j=i}} P_{j,\varphi,t,s}^{ss} + \sum_{\forall k \in \Omega_{K(.,i)}} P_{b,\varphi,t,s}^K + \sum_{\substack{\forall j \in \Omega_G \\ j=i}} (P_{j,\varphi,t,s}^G - P_{j,\varphi,t,s}^{ch} + P_{j,\varphi,t,s}^{dch}) + \sum_{\substack{\forall j \in \Omega_{PV} \\ j=i}} P_{j,\varphi,t,s}^{PV} = \sum_{\forall k \in \Omega_{K(i,.)}} P_{k,\varphi,t,s}^K + P_{i,\varphi,t}^L y_{i,t,s},$$

$$\forall i \in \Omega_N, \varphi, t, s \quad (4.42)$$

$$\sum_{\substack{\forall j \in \Omega_{Sub} \\ j=i}} Q_{j,\varphi,t,s}^{ss} + \sum_{\forall k \in \Omega_{K(.,i)}} Q_{k,\varphi,t,s}^K + \sum_{\substack{\forall j \in \Omega_G \\ j=i}} (Q_{j,\varphi,t,s}^G + Q_{j,\varphi,t,s}^{ES}) + \sum_{\substack{\forall j \in \Omega_{PV} \\ j=i}} Q_{j,\varphi,t,s}^{PV} = \sum_{\forall k \in \Omega_{K(i,.)}} Q_{k,\varphi,t,s}^K + Q_{i,\varphi,t}^L\ y_{i,t,s},$$

$$\forall i \in \Omega_N, \varphi, t, s \quad (4.43)$$

$$\boldsymbol{U}_{j,t,s} - \boldsymbol{U}_{i,t,s} + \bar{\boldsymbol{Z}}_{k,s}\boldsymbol{S}_{k,t,s}^* + \bar{\boldsymbol{Z}}_{k,s}^*\boldsymbol{S}_{k,t,s} \leqslant (2 - \boldsymbol{p}_k - u_{k,t,s})M, \forall k \in \Omega_K \backslash \Omega_{Reg}, t, s \quad (4.44)$$

$$\boldsymbol{U}_{j,t,s} - \boldsymbol{U}_{i,t,s} + \bar{\boldsymbol{Z}}_{k,s}\boldsymbol{S}_{k,t,s}^* + \bar{\boldsymbol{Z}}_{k,s}^*\boldsymbol{S}_{k,t,s} \geqslant -(2 - \boldsymbol{p}_k - u_{k,t,s})M, \forall k \in \Omega_K \backslash \Omega_{Reg}, t, s \quad (4.45)$$

Constraints (4.42)-(4.43) are 3-phase active and reactive power node balance constraints. Constraints (4.44)-(4.45) represent Kirchhoff's voltage law. The detailed explanation for these two constraints can be found in [65].

Voltage Regulators

$$-(2 - u_{k,t,s} - \boldsymbol{p}_k)M \leqslant \boldsymbol{a}_k^2\boldsymbol{U}_{j,t,s} - \boldsymbol{U}_{i,t,s}, \forall k \in \Omega_{Reg}, t, s \quad (4.46)$$

$$\boldsymbol{a}_k^2\boldsymbol{U}_{j,t,s} - \boldsymbol{U}_{i,t,s} \leqslant (2 - u_{k,t,s} - \boldsymbol{p}_k)M, \forall k \in \Omega_{Reg}, t, s \quad (4.47)$$

Constraints (4.46) and (4.47) model the relationship between the voltage magnitudes on both sides for a three-phase voltage regulator, with i as the primary side and j as the secondary side.

المنارة للاستشارات
www.manaraa.com

The vector $\boldsymbol{a_k} \in \mathbb{R}^{3\times1}$ is the ratio between the primary and secondary winding for each phase, where the ratio is assumed to be constant [66].

Fuel Consumption

The fuel consumption for emergency DGs and MEG are calculated as follows [67]:

$$FC_{i,s} = \sum_{\forall t} b_f u^G_{i,t,s} P_i^{G_{max}} + a_f \sum_{\forall t} \sum_{\forall \varphi} P^G_{i,\varphi,t,s}, \forall i \in \Omega_{EG}, s \tag{4.48}$$

$$FC_{i,s} = \sum_{\forall t} \sum_{g \in \Omega_{MEG}} b_f u^M_{g,i,t,s} P_g^{G_{max}} + a_f \sum_{\forall t} \sum_{\forall \varphi} P^G_{i,\varphi,t,s}, \forall i \in \Omega_{CN}, s \tag{4.49}$$

where b_f and a_f are coefficients of the consumption in l/kWh. The fuel consumption coefficients are set to $a_f = 0.246$ l/kWh and $b_f = 0.08145$ l/kWh in this study [67]. The total amount of fuel consumed by a generator must be less than or equal to the available fuel:

$$FC_{i,s} \leqslant x_i^F, \forall i \in \Omega_G, s \tag{4.50}$$

Energy Storage System Constraints

The energy storage systems considered in this paper are batteries. Binary variable h represents the charging (1) and discharging (0) state of the energy storage device. If a battery is located in an area that have excess energy, the battery will be charged so that it can be later used to energize other locations as the system is repaired.

The charging and discharging limits for $i \in \Omega_{ES}$ are defined as follows:

$$0 \leqslant P^{ch}_{i,\varphi,t,s} \leqslant h_{i,t,s} P_i^{ch,\max}, \forall i \in \Omega_{ES}, \varphi, t, s \tag{4.51}$$

$$0 \leqslant P^{dis}_{i,\varphi,t,s} \leqslant (1 - h_{i,t,s}) P_i^{dis,\max}, \forall i \in \Omega_{ES}, \varphi, t, s \tag{4.52}$$

To avoid nonlinearity, we use the big M method to indicate whether a mobile storage device is charging or discharging:

$$0 \leqslant P^{ch}_{i,\varphi,t,s} \leqslant h_{i,t,s} M, \forall i \in \Omega_{CN}, \varphi, t, s \tag{4.53}$$

$$0 \leqslant P^{dis}_{i,\varphi,t,s} \leqslant (1 - h_{i,t,s}) M, \forall i \in \Omega_{CN}, \varphi, t, s \tag{4.54}$$

المنارة للاستشارات
www.manaraa.com

The charging/discharging limits are then represented by the following constraints:

$$0 \leqslant P^{ch}_{i,\varphi,t,s} \leqslant \sum_{g\in\Omega_{MES}} x^{MES}_{g,i} P^{dis,\max}_{g}, \forall i \in \Omega_{CN}, \varphi, t, s \tag{4.55}$$

$$0 \leqslant P^{dis}_{i,\varphi,t,s} \leqslant \sum_{g\in\Omega_{MES}} x^{MES}_{g,i} P^{dis,\max}_{g}, \forall i \in \Omega_{CN}, \varphi, t, s \tag{4.56}$$

where the sum of $x^{MES}_{g,i}$ is used similarly to constraint (4.34). The ESSs considered in this study can provide both active and reactive power. The reactive power is limited using the following constraints [68]:

$$-Q^{ES_{max}}_{i} \leqslant Q^{ES}_{i,\varphi,t,s} \leqslant Q^{ES_{max}}_{i}, \forall i \in \Omega_{ES}, \varphi, t, s \tag{4.57}$$

$$-\sum_{g\in\Omega_{MES}} x^{MES}_{g,i} Q^{ES_{max}}_{i} \leqslant Q^{ES}_{i,\varphi,t,s} \leqslant \sum_{g\in\Omega_{MES}} x^{MES}_{g,i} Q^{ES_{max}}_{i}, \forall i \in \Omega_{ES}, \varphi, t, s \tag{4.58}$$

The next set of constraints represents the energy level for each ESS:

$$E_{i,t,s} = E_{i,t-1,s} + \Delta t(\eta_c \sum_{\forall\varphi} P^{ch}_{i,\varphi,t,s} - \frac{\sum_{\forall\varphi} P^{dis}_{i,\varphi,t,s}}{\eta_d}), \forall i \in \Omega_{ESC}, t, s \tag{4.59}$$

$$E^{\min}_{i} \leqslant E_{i,t,s} \leqslant E^{\max}_{i}, \forall i \in \Omega_{ES}, t, s \tag{4.60}$$

$$E^{\min}_{g} \sum_{g\in\Omega_{MES}} x^{MES}_{g,i} \leqslant E_{i,t,s} \leqslant E^{\max}_{g} \sum_{g\in\Omega_{MES}} x^{MES}_{g,i}, \forall i \in \Omega_{CN}, t, s \tag{4.61}$$

Reconfiguration and Fault Isolation

$$w_{i,t,s} U_{min} \leqslant \boldsymbol{U}_{i,t,s} \leqslant w_{i,t,s} U_{max}\ ,\ \forall i \in \Omega_{N}, t, s \tag{4.62}$$

$$w_{i,t,s} + w_{j,t,s} \leqslant 2u_{k,t,s}, \forall k \in \Omega_{B} \backslash \Omega_{SW}, t, s \tag{4.63}$$

$$\sum_{k\in\Omega_{B(l)}} u_{k,t,s} \leqslant |\Omega_{B(l)}| - 1, \forall l \in \Omega_{loop}, t, s \tag{4.64}$$

المنارة للاستشارات
www.manaraa.com

$$\gamma_{k,t,s} \geq u_{k,t,s} - u_{k,t-1,s}, \forall k \in \Omega_{SW}, t, s \tag{4.65}$$

$$\gamma_{k,t,s} \geq u_{k,t-1,s} - u_{k,t,s}, \forall k \in \Omega_{SW}, t, s \tag{4.66}$$

Constraint (4.62) sets the different restrictions on the voltage: if $w_{i,t,s} = 0$, the bus node i is de-energized and $\boldsymbol{U}_{i,t,s} = 0$; otherwise, the voltage will be restricted to be within the safe range. If a line is damaged, constraint (4.63) will force the node voltages of that line to be zero. Combining with constraints (4.44)-(4.47), constraint (4.62) and (4.63) can model the outage propagation on the rest of the network until a circuit breaker or sectionalizer isolates the fault. Constraint (4.64) represents the radiality constraint. In this paper, it is assumed that all the possible loops in the network and lines associated with them have been identified by the depth-first search method. Constraint (4.65)-(4.66) restricts the number of switching operations.

PV System Constraints

Three types of PV systems are considered to facilitate the supply continuity during and after extreme weather events. Let $\Omega_{PV} = \Omega_{PV}^{G} \cup \Omega_{PV}^{H} \cup \Omega_{PV}^{C}$, where Ω_{PV}^{G} represents on-grid PV that will be switched off during an outage; Ω_{PV}^{H} represents hybrid on-grid/off-grid PV that operates on-grid in normal conditions and off-grid during an outage; Ω_{PV}^{C} represents grid-forming PV that can restore part of the undamaged network if the fault is isolated. As the active power output of a PV depends of the rating of solar cell and solar irradiancce, the output power from the PVs can be written using the following constraints [69]:

$$0 \leqslant P_{i,\varphi,t,s}^{PV} \leqslant \bar{P}_{i}^{PV}, \forall i \in \Omega_{PV} \backslash \Omega_{PV}^{G}, \varphi, t, s \tag{4.67}$$

$$0 \leqslant P_{i,\varphi,t,s}^{PV} \leqslant w_{i,t,s} \bar{P}_{i}^{PV}, \forall i \in \Omega_{PV}^{G}, \varphi, t, s \tag{4.68}$$

$$\text{where } \bar{P}_{i}^{PV} = \frac{Ir_{t,s}}{(1000W/m^2)} P_{i}^{PV_{max}}, \forall i \in \Omega_{PV}, \varphi, t, s \tag{4.69}$$

المنارة للاستشارات
www.manaraa.com

As advanced PV inverters enable PVs to provide reactive power support, the reactive output can be constrained by (4.70) and (4.71):

$$-Q_i^{PV_{max}} \leqslant Q_{i,\varphi,t,s}^{PV} \leqslant Q_i^{PV_{max}}, \forall i \in \Omega_{PV} \backslash \Omega_{PV}^G, \varphi, t, s \tag{4.70}$$

$$-w_{i,t,s} Q_i^{PV_{max}} \leqslant Q_{i,\varphi,t,s}^{PV} \leqslant w_{i,t,s} Q_i^{PV_{max}}, \forall i \in \Omega_{PV}^G, \varphi, t, s \tag{4.71}$$

As the different types of PVs have different connection restrictions during an outage, it is necessary to model the appropriate connection constraints for PVs. Authors in [59] constructed a set of connectivity constraints to identify the energized buses in the network by using virtual sources, load, and flow:

$$\sum_{\substack{j \in \Omega_{PV}^C \cup \Omega_G \cup \Omega_{Sub} \\ j=i}} v_{j,\varphi,t,s}^S + \sum_{k \in \Omega_{K(.,i)}} v_{k,\varphi,t,s}^f = w_{i,t,s} + \sum_{k \in \Omega_{K(.,i)}} v_{k,\varphi,t,s}^f, \forall i \in \Omega_N, \varphi, t, s \tag{4.72}$$

$$-(u_{k,t,s}\ p_{k,\varphi}) M \leqslant v_{k,\varphi,t,s}^f \leqslant (u_{k,t,s}\ p_{k,\varphi}) M, \forall k \in \Omega_K, \varphi, t, s \tag{4.73}$$

$$0 \leqslant v_{i,\varphi,t,s}^S \leqslant \Big(\sum_{\substack{\forall j \in \Omega_{Sub} \\ j=i}} P_{j,\varphi,t,s}^{ss} + \sum_{\substack{\forall j \in \Omega_G \\ j=i}} (P_{j,\varphi,t,s}^G + P_{j,\varphi,t,s}^{dch}) + \sum_{\substack{\forall j \in \Omega_{PV}^C \\ j=i}} P_{j,\varphi,t,s}^{PV}\Big) M, \forall i \in \Omega_N, \varphi, t, s \tag{4.74}$$

$$w_{i,t,s} \geq y_{i,t,s}, \forall i \in \Omega_N \backslash \{\Omega_G \cup \Omega_{PV}^C \cup \Omega_{PV}^H\}, t, s \tag{4.75}$$

$$w_{i,t,s} + \Big(\sum_{g \in \Omega_{MES}} x_{g,i}^{MES} + \sum_{g \in \Omega_{MEG}} x_{g,i}^{MEG}\Big) \geq y_{i,t,s}, \forall i \in \Omega_{CN}, t, s \tag{4.76}$$

Repair Process Constraints

To model the repair process, we solve an allocation problem where crews are allocated to damaged components at each time step.

$$u_{k,t,s} = D_{k,t,s}, \forall k \in \Omega_D, \forall t \in \mathcal{T}_b, s \tag{4.77}$$

المنارة للاستشارات
www.manaraa.com

$$\sum_{\forall k \in \Omega_{D(r)}} z_{k,t,s} \leqslant x_r^A, \forall r \in \Omega_R, \forall t \in \mathcal{T}_a, s \tag{4.78}$$

$$\sum_{\forall t} z_{k,t,s} = \mathcal{T}_{k,s}^r, \forall k \in \Omega_D, \forall t \in \mathcal{T}_a, s \tag{4.79}$$

$$\sum_{\tau=1}^{t-1} \frac{z_{k,\tau,s}}{\mathcal{T}_{k,s}^r} - 1 + \epsilon \leqslant u_{k,t,s} \leqslant \sum_{\tau=1}^{t-1} \frac{z_{k,\tau,s}}{\mathcal{T}_{k,s}^r}, \forall k \in \Omega_D, \forall t \in \mathcal{T}_a, s \tag{4.80}$$

$$z_{k,t,s}^a \geqslant z_{k,t,s} - z_{k,t-1,s}, \forall k \in \Omega_D, t > |\mathcal{T}_b| + 1, s \tag{4.81}$$

$$z_{k,|\mathcal{T}_b|+1,s}^a = z_{k,|\mathcal{T}_b|+1,s}, \forall k \in \Omega_D, s \tag{4.82}$$

$$\sum_{\forall t \in T_a} z_{k,t,s}^a = 1, \forall k \in \Omega_D, s \tag{4.83}$$

$$0 \leqslant z_{k,t,s}^a \leqslant 1, \forall k \in \Omega_D, \forall t \in \mathcal{T}_a, s \tag{4.84}$$

Constraint (4.77) represents line status before crews start to repair. Constraint (4.78) limits the number of repairs being conducted in each region according to the number of crews x_r^A available. Constraint (4.79) defines the repair time for each damaged line. Constraint (4.80) sets the status of the line to be 1 once it is repaired. For example, let $\mathcal{T}_{k,s}^r = 3$ and $z_{k,t,s} = \{0, 0, 1, 1, 1, 0, 0\}$, then $u_{k,t,s} = \{0, 0, 0, 0, 0, 1, 1\}$. For $t = 6$ and $\epsilon = 0.001$, constraint (4.80) becomes $0.668 \leqslant u_{k,6,s} \leqslant 1$, which forces $u_{k,6,s} = 1$. An auxiliary variable $z_{k,t,s}^a$ is introduced to ensure that the repairs are done in consecutive hours. For example, $z_{1,t,1} = [0, 0, 1, 1, 1, 0]$ is valid, but $z_{1,t,1} = [1, 0, 0, 1, 1, 0]$ is not valid, $\forall t = \{1, \ldots, 6\}$. Constraint (4.81) forces the value of $z_{k,t,s}^a$ to be 1 if $z_{k,t,s}$ goes from 0 to 1. Constraint (4.82) defines $z_{k,t,s}^a$ for the first time period, and constraint (4.83) ensures that $z_{k,t,s}^a$ is equal to 1 only once.

المنارة للاستشارات
www.manaraa.com

4.4 Solution Algorithm

4.4.1 The Compact Notation of Pre-Event Preparation Problem

In order to facilitate the solution discussion, the CVaR-based stochastic optimization model can be written in a compact notation form:

$$\begin{aligned} z_{\alpha-CVaR} = \min_{x,y,\delta,r} \{ & \boldsymbol{c}^\top \boldsymbol{x} + \delta + \frac{1}{1-\alpha} \sum_{s \in \mathcal{S}} p_r(s) \eta_s : \delta + \eta_s \\ & \geqslant q(s)^\top y(s), (x, y(s)) \in O_s, \delta \in \mathbb{R}, \eta_s \in \mathbb{R}_+, \forall s \in \mathcal{S} \}. \end{aligned} \tag{4.85}$$

where $O_s = \{(x, y(s)) : Ax = b, x \in X, Wy(s) = h(s) - T(s)x, y(s) \in Y\}$.

4.4.2 Progressive Hedging Algorithm

The general combination, NP-hard natural of mixed-integer problems and uncertainty, leads to the considerable difficulty in solving SMILP pre-event preparation models. For small-scale SMILP pre-event preparation problems, standard MILP solvers can be used to directly solve their extensive forms (EFs) presented in (4.85). However, for large-scale pre-event preparation problems, their EFs are too large to solve using in a reasonable run-time using available MIP solvers. In addition, the commonly used stage-based decomposition algorithm, Benders decomposition, relies heavily on the convexity of $\phi(\boldsymbol{x}, s)$ and cannot be directly applied to the case with integer variables in the second stage [70]. Rockafellar and Wets proposed the Progressive Hedging (PH) decomposition algorithm as a heuristic [71] to effectively solve stochastic mixed-integer problems. PH algorithm can reduce the computational difficulty by decomposing the EF in (4.85) into scenario-based subproblems and solving subproblems in parallel. PH has been successfully implemented in solving unit commitment problems [70, 72, 73].

For such a two-stage CVaR-based SMIP prevent preparation problem, the modified PH algorithm is sketched in Algorithm 1. The PH algorithm is initialized by solving the individual-scenario problems in Step 1. In each iteration, PH solves subproblems individually and aggregates the solutions to obtain the expected value $\widehat{\boldsymbol{x}}^k$. The estimates of multipliers $\boldsymbol{w}(s)^k$ are updated in Step 4 using a specific penalty parameter ρ to enforce the non-anticipative policy. The performance of

المنارة للاستشارات
www.manaraa.com

Algorithm 2 PH Algorithm for CVaR-base SMILP

1: ***Initialization:*** Let $k \leftarrow 0$ and $\boldsymbol{w}_s^k \leftarrow 0, \forall s \in \mathcal{S}$. For each $s \in \mathcal{S}$, compute:
$(\boldsymbol{x}_s^{k+1}, \boldsymbol{y}_s^{k+1}) := \underset{(\boldsymbol{x}_s, \boldsymbol{y}_s)}{\operatorname{argmin}} \left\{ \boldsymbol{c}^\top \boldsymbol{x}_s + \delta_s + \frac{1}{1-\alpha}\eta_s : \delta_s + \eta_s \geqslant \boldsymbol{q}_s^\top \boldsymbol{y}_s, (\boldsymbol{x}_s, \boldsymbol{y}_s) \in O_s, \delta_s \in \mathbb{R}, \eta_s \in \mathbb{R}_+ \right\}$

2: ***Iteration update:*** $k \leftarrow k+1$

3: ***Aggregation:*** $\widehat{\boldsymbol{x}}^k := \sum_{s \in \mathcal{S}} p_s \boldsymbol{x}_s^k$

4: ***Update multiplier:*** $\boldsymbol{w}_s^k = \boldsymbol{w}_s^{k-1} + \rho(\boldsymbol{x}_s^k - \widehat{\boldsymbol{x}}^k), s \in \mathcal{S}$

5: ***Decomposition:*** For each $s \in \mathcal{S}$, compute:
$(\boldsymbol{x}_s^k, \boldsymbol{y}_s^k) := \underset{(\boldsymbol{x}_s, \boldsymbol{y}_s)}{\operatorname{argmin}} \left\{ \boldsymbol{c}^\top \boldsymbol{x}_s + \delta_s + \frac{1}{1-\alpha}\eta_s + \boldsymbol{w}_s^{k-1}\boldsymbol{x}_s + \frac{\rho}{2}\|\boldsymbol{x}_s - \widehat{\boldsymbol{x}}_{k-1}\|^2 : \delta_s + \eta_s \geqslant \boldsymbol{q}_s^\top \boldsymbol{y}_s, (\boldsymbol{x}_s, \boldsymbol{y}_s) \in O_s, \delta_s \in \mathbb{R}, \eta_s \in \mathbb{R}_+ \right\}$

6: ***Termination:*** If all first-stage scenario solutions $\boldsymbol{x}_s^k$ agree, go to Stop; otherwise go to Step 2

PH depends on the value of ρ. The decomposition step (Step 5) of each iteration involves solving variants of subproblems that are augmented with a linear term proportional to the multiplier $\boldsymbol{w}(s)^k$ and a squared two norm term penalizing deviation of $\boldsymbol{x}(s)^k$ from $\widehat{\boldsymbol{x}}^{k-1}$.

4.4.3 Lower Bounds on CVaR-Based Stochastic Integer Programs

Although the convergence of PH is not guaranteed for stochastic mixed-integer problems, computational studies have shown that PH can find solutions with acceptable optimality gap for practical applications [73]. However, it is still necessary to evaluate the quality of PH solutions. Gade et al. [51] proposed an approach to calculate the lower bounds in any iteration of PH simply by solving an optimization problem. The lower bounds not merely allow us to assess the quality of the solutions in each iteration, but also can provide lower bounds for solution methods that rely on lower bounds like branch-and-bound. The proposition of lower bound in [51] can be restated as follows:

Proposition 1: Let $\boldsymbol{w}_\xi, \xi \in \mathcal{S}$, satisfies $\sum_{\xi \in \mathcal{S}} p_\xi \boldsymbol{w}_\xi = 0$. And $D_\xi(\boldsymbol{w}_\xi) := \min \left\{ p_\xi(\boldsymbol{c}^\top \boldsymbol{x}_\xi + \boldsymbol{q}_\xi^\top \boldsymbol{y}_\xi + \boldsymbol{w}_\xi \boldsymbol{x}_\xi) : (\boldsymbol{x}_\xi, \boldsymbol{y}_\xi) \in O_\xi \right\}$.

Then $D(\boldsymbol{w}) := \sum_{\xi \in \mathcal{S}} D_\xi(\boldsymbol{w}_\xi) \leqslant z^*$.

المنارة للاستشارات
www.manaraa.com

In each iteration, the lower bound $D(\boldsymbol{w})$ on the optimal objective value z^* is computed using the multiplier $\boldsymbol{w}_\xi^k$. These lower bounds are reported in our numerical results. The major advantage is that we can obtain the lower bounds for a stochastic mixed-integer problem even when the sub-problems are not solved to the optimality, and a lower bound can be easily calculated with approximately the same effort as one PH iteration.

By applying Proposition 1 to the two-stage CVaR optimization stochastic integer program (4.85), we show how the lower bounds on the optimal objective value of z^*_{CVaR} can be computed.

Proposition 2: Let $\boldsymbol{w}_\xi, \xi \in \mathcal{S}$, satisfies $\sum_{\xi\in\mathcal{S}} p_\xi \boldsymbol{w}_\xi = 0$ and $\boldsymbol{w}'_\xi, \xi \in \mathcal{S}$, satisfies $\sum_{\xi\in\mathcal{S}} p_\xi \boldsymbol{w}'_\xi = 0$. Let $D_\xi(\boldsymbol{w}_\xi, \boldsymbol{w}'_\xi) := \min_{x,y,\delta,\eta} \left\{ \boldsymbol{c}^\top \boldsymbol{x}_\xi + \delta_\xi + \frac{1}{1-\alpha}\eta_\xi + \boldsymbol{w}_\xi^\top \boldsymbol{x}_\xi + \boldsymbol{w}'_\xi \delta_\xi : \delta_\xi + \eta_\xi \geqslant \boldsymbol{q}_\xi^\top \boldsymbol{y}_\xi, (\boldsymbol{x}_\xi, \boldsymbol{y}_\xi) \in O_\xi, \delta_\xi \in \mathbb{R}, \eta_\xi \in \mathbb{R}_+ \right\}$.

Then $D(\boldsymbol{w}, \boldsymbol{w}') := \sum_{\xi\in\mathcal{S}} D_\xi(\boldsymbol{w}_\xi, \boldsymbol{w}'_\xi) \leqslant z^*_{CVaR}$.

However, solving problem $D(\boldsymbol{w}, \boldsymbol{w}')$ in Proposition 1 is not straightforward as solving problem $D(\boldsymbol{w})$ in Proposition 2. More challenges come along with the additional first stage variable δ and second stage variables $\eta_\xi, \forall \xi \in \mathcal{S}$ in the problem $D_\xi(\boldsymbol{w}_\xi, \boldsymbol{w}'_\xi)$. We find out problem $D(\boldsymbol{w}, \boldsymbol{w}')$ can turn out to be an unbounded optimization problem. In order to find valid lower bounds for two-stage CVaR optimization stochastic integer programs, we first need to make the CVaR variable δ to be bounded while maintaining the original set of feasible solutions. We now show upper and lower bounds for the optimal value of variable that lead to tight lower bounds of z^*_{CVaR} and can be obtained with least computational effort. Furthermore, the bounds on variable δ will speed up the convergence of Progressive Hedging algorithm at the same time.

Proposition 3: Let δ^* be the optimal solution of variable δ for problem (4.85), then

$$L = \min_{\xi\in\mathcal{S}} \left\{ \min_{\boldsymbol{x},\boldsymbol{y}} \left\{ \boldsymbol{c}^\top \boldsymbol{x} + \boldsymbol{q}_\xi^\top \boldsymbol{y} : (\boldsymbol{x}, \boldsymbol{y}) \in O_\xi \right\} \right\} \leq \delta^*$$

$$U = \max_{\xi\in\mathcal{S}} \left\{ \max_{\boldsymbol{x},\boldsymbol{y}} \left\{ \boldsymbol{c}^\top \boldsymbol{x} + \boldsymbol{q}_\xi^\top \boldsymbol{y} : (\boldsymbol{x}, \boldsymbol{y}) \in O_\xi \right\} \right\} \geq \delta^*$$

المنارة للاستشارات
www.manaraa.com

4.5 Numerical Results

4.5.1 Input Data

The modified IEEE 123-bus distribution feeder [65] is used as a test case for the pre-event resource allocation problem. The network is modified by including 2 dispatchable DGs, 18 new switches, 5 PVs and 2 BESSs. The 2 DGs are rated at 500 kW and 410 kVAr. PVs in on-grid and hybrid systems are rated at 50 kW, and the PV at bus 62 is rated at 900 kW. The BESSs at bus 2 and 62 are rated at 50 kW/132 kWh and 500 kW/ 2100 kWh, respectively. The basic load shedding cost is assumed to be $\$14/kWh$ and the load shedding cost parameter C_i^D in equation (4.28) is the product of the basic load shedding cost and the load priority. It is assumed the all the pre-allocated resources are transported from warehouses with 100 miles distance. The utility has 3 fixed repair crew and two crew depot in the system. The cost parameters for the simulation is shown in Table 4.2. The stochastic models and algorithms are implemented using the PySP package in Pyomo. IBM's CPLEX 12.6 mixed-integer solver is used to solve all subproblems. The experiments were performed on Iowa State University's Condo cluster, whose individual blades consist of two 2.6 GHz 8-Core Intel E5-2640 v3 processors and 128 GB of RAM.

Table 4.2 The cost parameters for simulation

Name	Value	Name	Value	Name	Value
C_g^E	\$500/unit	C^F	\$4/kwh	C^R	\$225/line
C_g^G	\$400/unit	C^A	\$4285/crew	C^{sw}	\$8

المنارة للاستشارات
www.manaraa.com

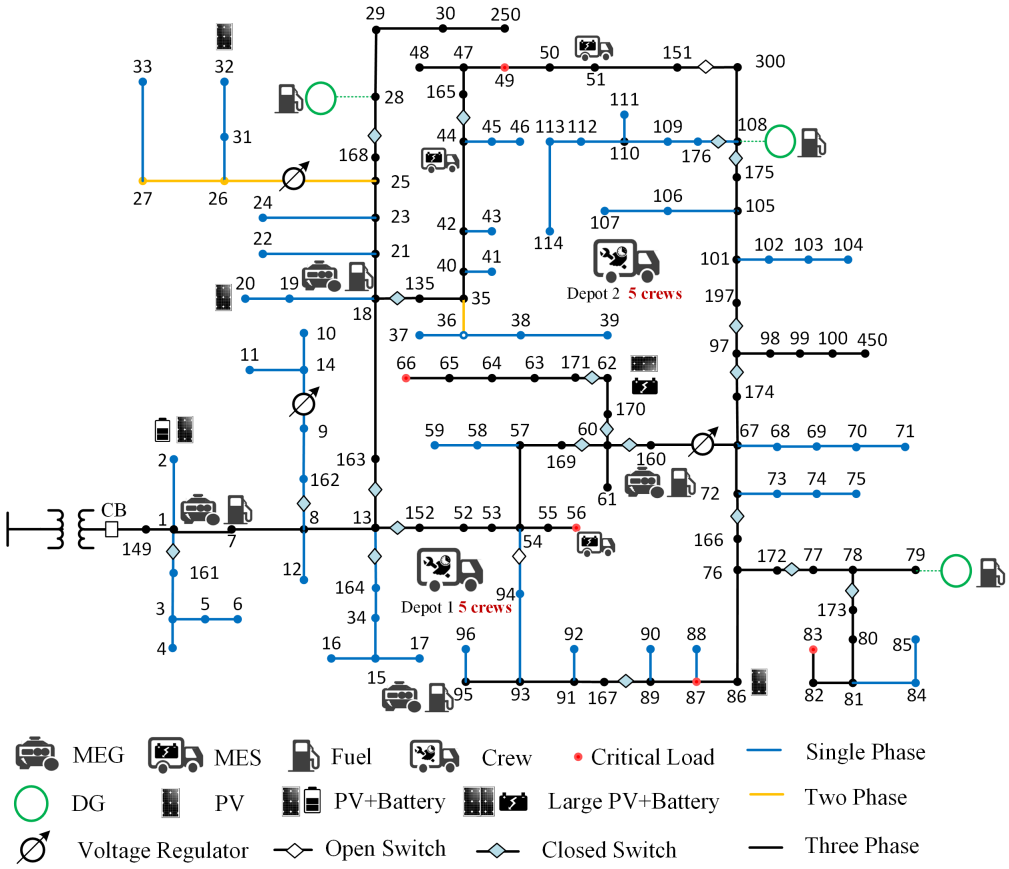

Figure 4.4 The optimal pre-event resource preparation at confidence level $\alpha = 95\%$

4.5.2 Pre-event Resource Preparation Results with $\alpha = 95\%$

The optimal pre-event resource preparation solution depends on the risk aversion. Now given the confidence level $\alpha = 95\%$, the pre-event resource preparation model, with 20 damage scenarios, is solved in 2.62 hours. The optimal first-stage decision variables (locations of mobile devices and crews) are shown in Figure 4.4. Four MEG are installed at bus 1, 18, 95, and 160 separately. Three MES are placed at bus 44, 51, and 56. Fuel is pre-delivered to buses with DG and MEG. 10 crews are even allocated to depot 1 and depot 2. To do resilience analysis and risk analysis in the following subsections, we also present optimal pre-event resource preparation at different confidence level α in Figure 4.5.

المنارة للاستشارات
www.manaraa.com

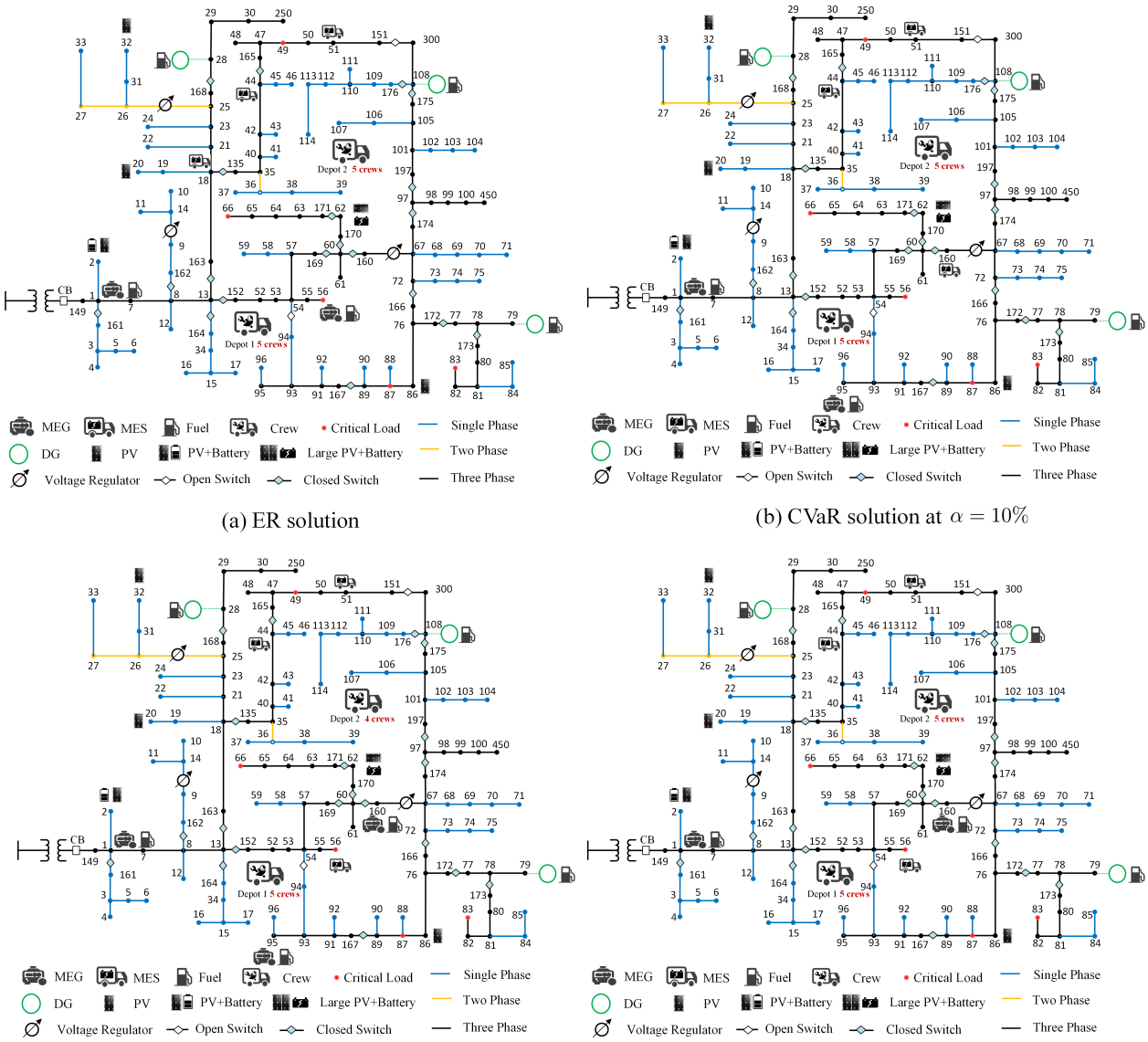

(a) ER solution

(b) CVaR solution at $\alpha = 10\%$

(c) CVaR solution at $\alpha = 30\%$

(d) CVaR solution at $\alpha = 60\%$

Figure 4.5 The optimal pre-event resource preparation at different confidence level α

4.5.3 Resilience Analysis

To evaluate the preparation results with different α, we generate an additional random scenario and test the response of the system. The generated scenario has 15 damaged lines and we assume that the substation is not receiving power from the transmission system for 12 hours starting from

المنارة للاستشارات
www.manaraa.com

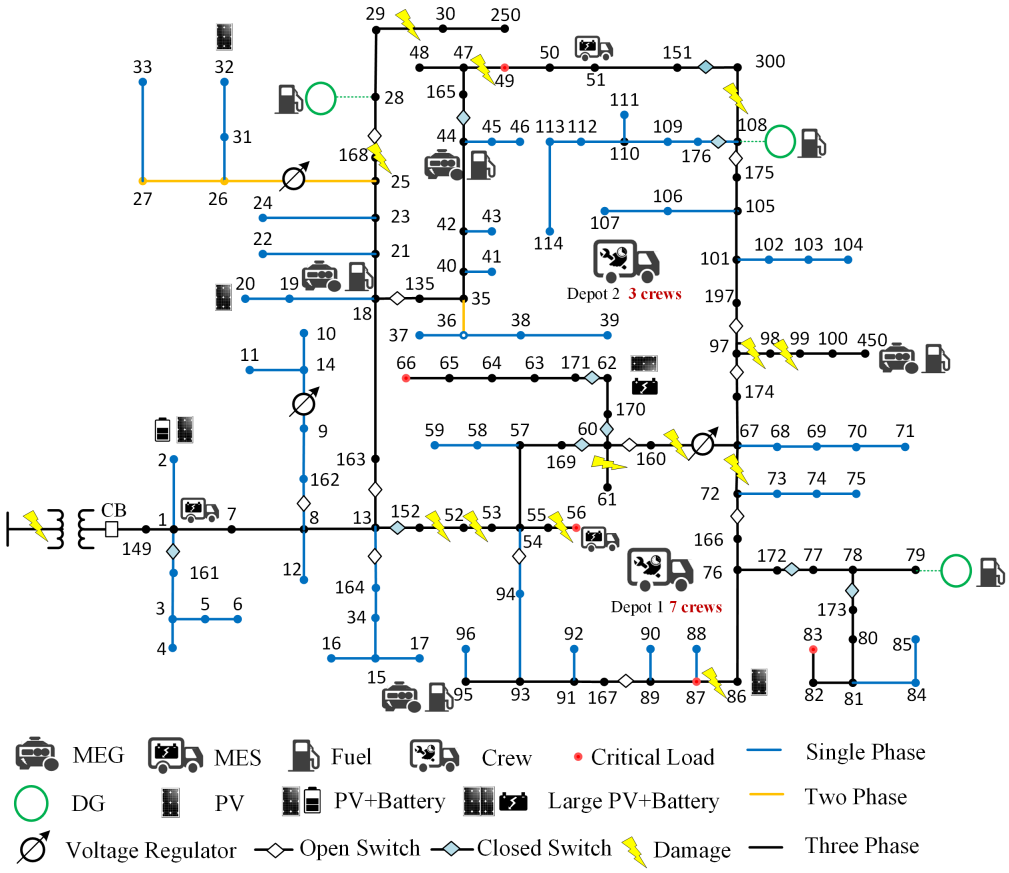

Figure 4.6 The damaged lines in the additional random scenario with $\alpha = 95\%$

8 : 00 am. Figure 4.6 presents locations of damaged lines on the pre-allocated test system at confidence level $\alpha = 95\%$. Figure 4.7 shows the comparison of the percentage of power served load during the event, and after the repair process starts with different α. Table 4.3 gives th pre-event allocation cost, the amount of load served, and average outage duration with different α. We also compare the resilience improvement percentage and outage hour decreased percentage in Table 4.3. From Table 4.3, it can be seen that the pre-event preparation solution at $\alpha = 95\%$ is the best option for utility to allocate resources before the event. Because this solution improves 13% resilience and reduces 23% outage hour, although the allocation cost is 3.28% higher than the ER solution.

المنارة للاستشارات
www.manaraa.com

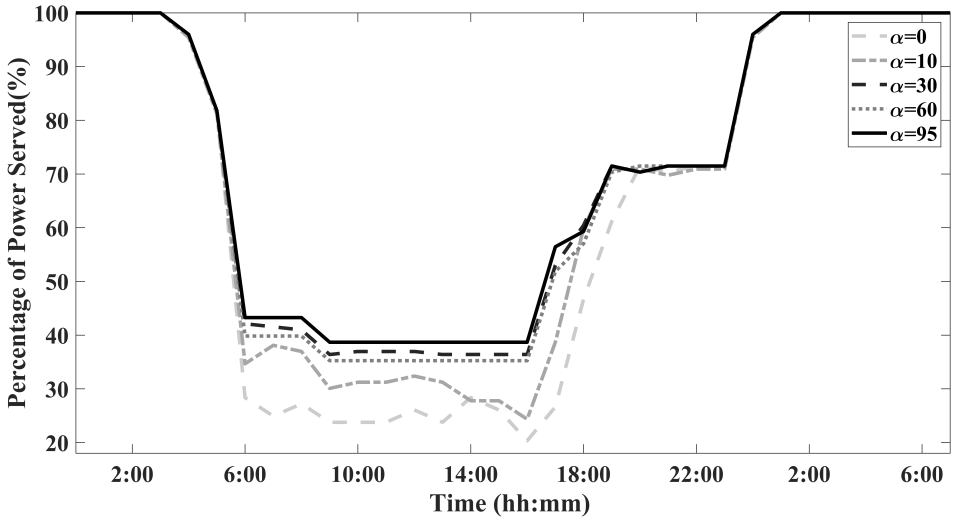

Figure 4.7 Load served percentage comparison for different confidence level α

Table 4.3 The amount of load served, average outage duration and pre-event allocation cost with different confidence level α

α	Allocation Cost ($)	Load Served (kWh)	Resilience Improved Percentage (%)	Average Outage Duration (h)	Outage Decreased Percentage(%)
0	$91,695.00$	$51,397.60$		11.38	
10%	$72,479.56$	$54,555.18$	6.14	10.24	9.93
30%	$89,488.00$	$57,482.13$	11.84	9.15	19.54
60%	$80,632.76$	$56,830.52$	10.57	9.27	18.51
95%	$94,705.00$	$58,260.10$	13.35	8.66	23.89

4.5.4 Risk Analysis

To show the value of the proposed CVaR-based model, we use the value of the CVaR solution (VCS) proposed in [74] to measure how much we gain by considering CVaR compared to expected risk (ER). VCS_α is similar to the value of stochastic solution used to compare the performance of stochastic solution with the performance of the deterministic solutions in the stochastic environment and can be written as follows:

$$\text{VCS}_\alpha = \frac{\text{CVaR}_\alpha \text{of the ER solution} - \text{Optimal CVaR}_\alpha}{\text{Optimal CVaR}_\alpha} \tag{4.86}$$

المنارة للاستشارات
www.manaraa.com

where ER solution represents the optimal first-stage allocation solution from solving the general stochastic programming model. The ER-based optimization model of pre-event preparation problem can be expressed as follows:

$$\min \sum_{i\in\Omega_{CN}} \Big(\sum_{g\in\Omega_{MES}} C_g^E x_{g,i}^{MES} + \sum_{g\in\Omega_{MEG}} C_g^G x_{g,i}^{MEG} \Big) + \sum_{i\in\Omega_G} C^F x_i^F + C^A \Big(\sum_{r\in\Omega_R} x_r^A - x_{fixed}^A \Big) + \sum_{s\in\mathcal{S}} p_r(s)\pi_s \tag{4.87}$$

$$s.t. \text{ Constraints } (4.23) - (4.28), (4.31) - (4.84)$$

Similarly, we also define the value of ER solution over CVaR solution as follows:

$$\text{VRS}_\alpha = \frac{\text{Optimal ER} - \text{ER of the CVaR}_\alpha \text{ solution}}{\text{Optimal ER}} \tag{4.88}$$

where CVaR_α solution represents the optimal first-stage allocation solution from solving the CVaR-based model.

Figure 4.8 and Figure 4.9 show VCS_α and VRS_α with various α for the pre-event preparation model respectively. From Figure 4.8 , it can be seen that when $\alpha = 0$, $\text{VCS}_\alpha = 0$, which indicates the CVaR_α is equivalent to the ER. As α increases, the value of VCS_α increases. It indicates that when $\alpha = 0$, the proposed CVaR-based model can completely represent the general stochastic optimization model, which evaluate the expected risk from the uncertain damage consequence of extreme event; when α is close to 1, it can consider the worse-consequence of an extreme event. These results illustrate the proposed CVaR-based model can capture high damage loss consequences stemming from the pre-event allocation decision as well as the nature of extreme weather events. In Figure 4.9, we observes the value α increases, the value of VRS_α also increases. It indicates that the solution with higher α has better performance and more risk-averse when we focus on low-probability but high-intense extreme weather events.

المنارة للاستشارات
www.manaraa.com

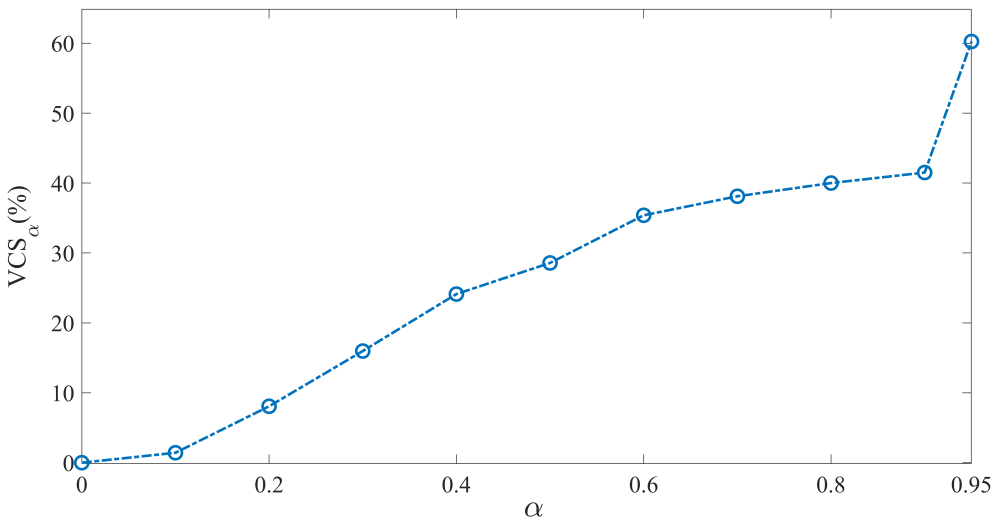

Figure 4.8 The value of CVaR$_\alpha$ solutions over ER solutions

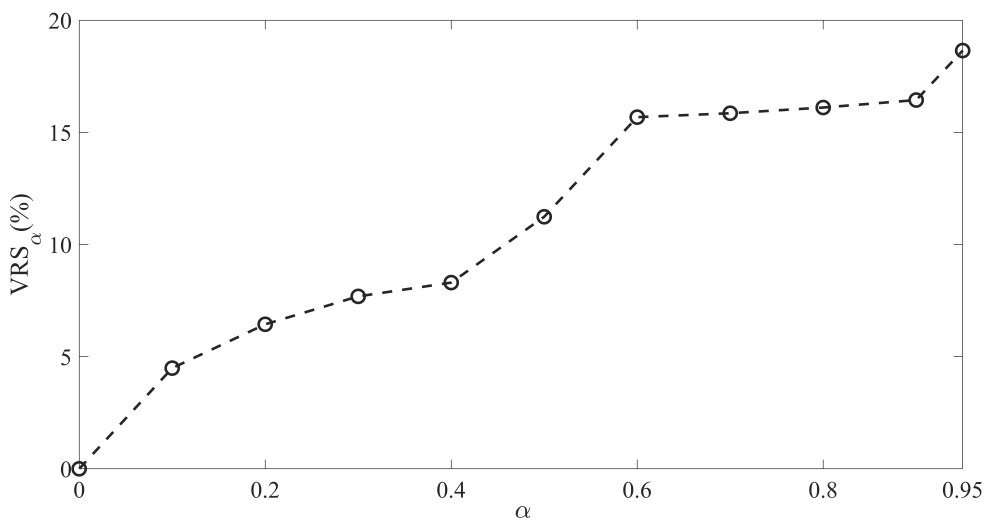

Figure 4.9 The value of ER solutions over CVaR$_\alpha$ solutions

المنارة للاستشارات
www.manaraa.com

4.6 Summary

This chapter formulates a short-term proactive energy management and preparation problem in the distribution system for an upcoming event as a two-stage stochastic mixed-integer linear program model, considering the weather-induced uncertainties and a risk-averse measure for potential damage consequence. We use CVaR as a general, coherent, and risk-averse approach to measure the probabilistic damage consequence from an extreme weather event. A modified progressive hedging algorithm is proposed for solving the proposed model. To highlight the value of our model, comparisons of the proposed model and the expected-risk model are conducted in the modified IEEE 123-bus distribution feeder with different confidence level α. When α of CVaR is small, it indicates that utility pays limited attention to sever damage loss consequence when they prepare for an upcoming event. At the same time, when the confidence level α of CVaR becomes large, the proposed model can capture high damage loss consequence stemming from the pre-event allocation decision as well as the nature of extreme weather events.

المنارة للاستشارات
www.manaraa.com

CHAPTER 5. CONCLUSIONS AND FUTURE WORK

5.1 Conclusion

Recent severe power outages caused by extreme weather events, such as hurricanes, ice storm, and flooding have highlighted the importance and urgency of enhancing the resilience of electric power distribution systems. The goal of this dissertation is to pioneer advanced optimization-based methodologies to provide actionable resilience-enhanced strategies for utility companies to upgrade power distribution systems in the long-term and prepare for the upcoming event in the short-term.

An innovative modeling and solution methodology using a stochastic framework is proposed in the chapter 3 to design a more resilient distribution systems against extreme weather event. The proposed strategy consists of three ROD measures, namely, line hardening, installing DGs, and adding automatic switches. First, the spatial-temporal correlations among ROD decisions, uncertainty space, and system operation reactions during and after extreme weather events are investigated. The structure of uncertainty space is constructed to decompose the correlations among ROD decisions and the key random variables in the uncertainty space. Then, the evolution of the system operational state during extreme weather events is estimated, and the operational cost related to extreme weather events is evaluated. A two-stage stochastic mixed-integer framework is proposed to model ROD problems, with the objective of minimizing the investment cost in the first stage and the expected cost of the loss of load, repair, and DG operation in the second stage. The framework can outline the effects of ROD decisions and uncertainty space on system response during extreme weather events. As a result, a functional relationship between ROD measures and ROD effects on system operation is successfully established. To solve this problem, a scenario-based dual composition algorithm is introduced to achieve global optimality. The numerical studies on the 123-bus distribution system demonstrate the effectiveness of implementing optimal ROD measures.

المنارة للاستشارات
www.manaraa.com

A proactive energy management and preparation strategy is presented in the Chapter 4 to reduce the grid damage consequence and decrease the restoration time in an upcoming extreme weather event. The proposed strategy manages solar energy in coordination with various flexible resources to prepare for a forthcoming extreme weather events with the objective to improve distribution system resilience during and after the event. A two-stage stochastic mixed-integer linear program model is formulated, considering the weather-induced uncertainties and a risk-averse measure for potential damage consequence. The first stage determines the pre-event resource allocation, including pre-dispatching mobile emergency generator (MEG) and mobile energy storage (MES), pre-delivering fuel, and pre-staging repair crews to different depots. The second stage operates various flexible resources with the objective to minimize the CVaR associated with damage loss. CVaR is an averse risk measure that focus on low-probability but high damage consequence from extreme weather events. A modified progressive hedging algorithm is proposed for solving the proposed CVaR minimization preparation problem. To highlight the value of our model, comparisons of the proposed model and the expected-risk model are conducted in the modified IEEE 123-bus distribution feeder with different confidence level α. When α of CVaR is small, it indicates that utility pays limited attention to sever damage loss consequence when they prepare for an upcoming event. At the same time, when the confidence level α of CVaR becomes large, the proposed model can capture high damage loss consequence stemming from the pre-event allocation decision as well as the nature of extreme weather events. The utility can decide their optimal pre-event proactive energy management and preparation strategy based on their risk preference.

In summary, the proposed methodologies can result in increased absorptive capacity and reduced recovery time and save credible physical and economic losses in facing extreme weather events.

المنارة للاستشارات
www.manaraa.com

5.2 Research Contribution

The main contributions of this dissertation are listed as follows:

5.2.1 Resilience-Oriented Design of Distribution Systems

- A hybrid independent stochastic process and deterministic causal structure is proposed to capture the spatiotemporal correlation among the various uncertainties of a ROD problem. This approach avoids establishing the high-dimension joint distribution of uncertain variables. A simulation technique based on structural engineering is presented to model the evolving impacts of hurricanes on physical infrastructures to support a more accurate uncertainty modeling.

- A two-stage SMILP is proposed to optimally implement multiple resilience-enhancing methods considering various uncertainties, thus increasing the infrastructure strength and enabling self-healing operations. Besides, this model captures the entire failure-recovery process so that both investment and restoration costs can be modeled. The self-healing operation in the second stage can mimic the outage propagation in a network until sectionalizers disconnect lines. The model sectionalizes a distribution system into multiple self-supported MGs and redispatches DGs to minimize the cost of the loss of load and DG operation in the second stage while keeping radial topologies.

- A customized DD algorithm is developed to balance optimality and solution efficiency.

5.2.2 Risk-Averse Proactive Preparedness of Distribution Systems with Conditional Value-at-Risk

- Multiple flexible resources in coordination with the integrated solar PV systems, including mobile emergency generator (MEG), mobile energy storage (MES), back-up diesel DGs, network reconfiguration, and repair crews, are considered to ensure several-day islanded operation during and after the event.

المنارة للاستشارات
www.manaraa.com

- A stochastic process is proposed to simulate line damage status before the event ends and its corresponding repair time through modeling the complex interactions among weather forecast information, grid components' structure limitation, and the repair time of the single damaged infrastructure.

- Risk is properly considered using CVaR methodology. The CVaR-constrained pre-event resource allocation problem is formulated as a SMILP to achieve the trade-off between expected allocation cost and damage loss risk. The model allows utilities to have different risk preferences to decide their optimal pre-event proactive energy management and preparation strategy.

- The modified progressive hedging algorithm is introduced to solve the proposed CVaR-constrained pre-event resource allocation problem efficiently.

5.3 Future Work

5.3.1 Resilience Assessment of Distribution Systems

In order to prevent and fast recover from extreme events, power distribution systems have been gradually equipped with state-of-art smart grid technologies to have self-healing capability. Self-healing is defined as the capability of the system to rapidly detect faults, take actions to minimize any adverse impacts, and promptly return to a stable operating state [75]. However, it is still unknown if a self-healing distribution system is resilient to extreme weather events. Because resilience is still an emerging concept that has not been adequately explored by the power engineering community [9]. TIn previous work [76], we quantify the resilience metric by the magnitude of the expected degradation in performance level over time. In the future, we can develop different resilience metrics to evaluate the resilience of the distribution system based on the real utility outage data.

المنارة للاستشارات
www.manaraa.com

5.3.2 Resilience-oriented Design of Distribution Systems Using Risk Measures

In chapter 3, we propose a resilience-oriented design methodology using stochastic programming. The general stochastic programming approach provides risk-neutral investment decisions for utilities. In future work, we can use the CVaR minimization model to design resilient distribution systems against extreme weather events, while the trade-off between the investment cost and resilience enhancement level can be balanced.

5.3.3 Proactive Preparedness

Proactive preparedness to cope with extreme weather events is significantly useful and helpful in reducing the restoration time and cost after events and in enhancing the resilience of distribution systems [13]. Chapter 4 presents a resource preparation strategy ahead of an upcoming extreme weather event considering the uncertainty of the damaged line status, solar irradiance, load demand, and crew repair time. In the future, we can make full use of advanced techniques or equipment, such as microsensor or drone, to real-time monitor the vulnerable parts of distribution systems and take some effective proactive measures to prevent damages.

5.4 Publications

Journal

1. **Shanshan Ma**, Shiyang Li, Zhaoyu Wang, Feng Qiu, "Resilience-Oriented Distribution System Design with Decision-Dependent Uncertainty," *IEEE Transactions on Power System*, accepted, 2018.
2. **Shanshan Ma**, Zhaoyu Wang, Leigh Tesfatsion, "Swing Contracts with Dynamic Reserves for Flexible Service Management," *IEEE Transactions on Power System*, accepted, 2018.
3. **Shanshan Ma**, Liu Su, Zhaoyu Wang, Feng Qiu, "Resilience Enhancement of Distribution Grids Against Extreme Weather Events," *IEEE Transactions on Power System*, accepted.
4. Anmar Arif, **Shanshan Ma**, Zhaoyu Wang, Jianhui Wang, Sarah M. Ryan, Chen Chen, "Optimizing Service Restoration in Distribution Systems With Uncertain Repair Time and Demand," *IEEE Transactions on Power System*, vol. 33, no. 6, pp. 6828-6838, Nov. 2018.

المنارة للاستشارات
www.manaraa.com

5. **Shanshan Ma**, Bokan Chen, Zhaoyu Wang, "Resilience enhancement strategy for distribution systems under extreme weather events," *IEEE Transactions on Smart Grid*, vol. PP, no. 99, p. 1, 2016.

Conference

1. **Shanshan Ma**, Nichelle'Le Carrington, Anmar Arif, Zhaoyu Wang, "Resilience Assessment of Self-healing Distribution Systems Under Extreme Weather Events," *2019 IEEE Power & Energy Society General Meeting (PESGM)*, Atlanta, GA, 2019.
2. **Shanshan Ma**, Shiyang Li, Zhaoyu Wang, Anmar Arif, Kang Ma, "A Novel MILP Formulation for Fault Isolation and Network Reconfiguration in Active Distribution Systems," *2018 IEEE Power & Energy Society General Meeting (PESGM)*, Portland, OR, 2018, pp. 1-5.
3. Chong Wang, Zhaoyu Wang, Kai Zhou, **Shanshan Ma** "Maintenance Scheduling of Integrated Electric and Natural Gas Grids with Wind Energy Integration," *2018 IEEE Power & Energy Society General Meeting (PESGM)*, Portland, OR, 2018, pp. 1-5.
4. Chong Wang, Zhaoyu Wang, **Shanshan Ma**, "SVM-Based Parameter Identification for Static Load Modeling," *2018 IEEE PES T&D Conference & Exposition (T&D)*, Denver, CO, 2018, pp. 1-5.
5. Anmar Arif, **Shanshan Ma**, Zhaoyu Wang, "Dynamic Reconfiguration and Fault Isolation for A Self-Healing Distribution System," *2018 IEEE PES T&D Conference & Exposition (T&D)*, Denver, CO, 2018, pp. 1-5.
6. Anmar Arif, **Shanshan Ma**, Zhaoyu Wang, "Online Decomposed Optimal Outage Management after Natural Disasters," *2017 IEEE Power & Energy Society General Meeting*, Chicago, IL, 2017, pp. 1-5.
7. Anmar Arif, **Shanshan Ma**, Zhaoyu Wang, "Optimization of transmission system repair and restoration with crew routing," *2016 North American Power Symposium (NAPS)*, Denver, CO, 2016, pp. 1-6.

المنارة للاستشارات
www.manaraa.com

REFERENCES

[1] A. B. Smith, "2018 us billion-dollar weather and climate disasters: a historic year in context," *NOAA Climate. gov [available online at: https://www.climate.gov/news-features/blogs/beyond-data/2018s-billion-dollar-disasters-context, accessed 7 February 2019]*, 2019.

[2] "Economic benefits of increasing electric grid resilience to weather outages," White House, Tech. Rep., Jul. 2013.

[3] A. M. Salman, Y. Li, and M. G. Stewart, "Evaluating system reliability and targeted hardening strategies of power distribution systems subjected to hurricanes," *Reliability Engineering & System Safety*, vol. 144, pp. 319–333, 2015.

[4] A. L. Tyler Hodge, "Hurricane irma cut power to nearly two-thirds of florida's electricity customers," U.S. Energy Information Administration, Tech. Rep., 2017. [Online]. Available: https://www.eia.gov/todayinenergy/detail.php?id=32992

[5] A. B. Smith, "2017 us billion-dollar weather and climate disasters: a historic year in context," *NOAA Climate. gov [available online at: https://www. climate. gov/news-features/blogs/beyond-data/2017-us-billion-dollar-weather-and-climate-disasters-historic-year, accessed 26 May 2018]*, 2018.

[6] R. E. Brown, "Hurricane hardening efforts in florida," in *Proc. IEEE Power and Energy Society General Meeting - Conversion and Delivery of Electrical Energy in the 21st Century*, Jul. 2008, pp. 1–7.

[7] A. Gholami, F. Aminifar, and M. Shahidehpour, "Front lines against the darkness: enhancing the resilience of the electricity grid through microgrid facilities," *IEEE Electrif. Mag.*, vol. 4, no. 1, pp. 18–24, 2016.

[8] M. Panteli and P. Mancarella, "The grid: Stronger, bigger, smarter?: Presenting a conceptual framework of power system resilience," *IEEE Power Energy Mag.*, vol. 13, no. 3, pp. 58–66, May 2015.

[9] M. Panteli, D. N. Trakas, P. Mancarella, and N. D. Hatziargyriou, "Power systems resilience assessment: Hardening and smart operational enhancement strategies," *Proceedings of the IEEE*, vol. 105, no. 7, pp. 1202–1213, Jul. 2017.

[10] A. Gholami, T. Shekari, M. H. Amirioun, F. Aminifar, M. H. Amini, and A. Sargolzaei, "Toward a consensus on the definition and taxonomy of power system resilience," *IEEE Access*, vol. 6, pp. 32 035–32 053, 2018.

[11] E. E. Institute, "Before and after the storm: A compilation of recent studies, programs, and policies related to storm hardening and resiliency," Edison Electric Institute, 701 Pennsylvania Avenue, N.W. Washington, D.C. 20004-2696, Tech. Rep., Mar. 2014.

المنارة للاستشارات
www.manaraa.com

[12] G. Li, P. Zhang, P. B. Luh, W. Li, Z. Bie, C. Serna, and Z. Zhao, "Risk analysis for distribution systems in the northeast u.s. under wind storms," *IEEE Transactions on Power Systems*, vol. 29, no. 2, pp. 889–898, Mar. 2014.

[13] H. Gao, Y. Chen, S. Mei, S. Huang, and Y. Xu, "Resilience-oriented pre-hurricane resource allocation in distribution systems considering electric buses," *Proc. IEEE*, vol. 105, no. 7, pp. 1214–1233, Jul. 2017.

[14] H. Gao, Y. Chen, Y. Xu, and C. C. Liu, "Resilience-oriented critical load restoration using microgrids in distribution systems," *IEEE Trans. Smart Grid*, vol. 7, no. 6, pp. 2837–2848, Nov. 2016.

[15] A. Arif and Z. Wang, "Service restoration in resilient power distribution systems with networked microgrid," in *Power and Energy Society General Meeting (PESGM)*. IEEE, 2016, pp. 1–5.

[16] Y. Xu, C.-C. Liu, K. P. Schneider, and D. T. Ton, "Placement of remote-controlled switches to enhance distribution system restoration capability," *IEEE Trans. Power Syst.*, vol. 31, no. 2, pp. 1139–1150, 2016.

[17] W. Yuan, J. Wang, F. Qiu, C. Chen, C. Kang, and B. Zeng, "Robust optimization-based resilient distribution network planning against natural disasters," *IEEE Trans. Smart Grid*, vol. PP, no. 99, pp. 1–10, 2016.

[18] S. Ma, B. Chen, and Z. Wang, "Resilience enhancement strategy for distribution systems under extreme weather events," *IEEE Trans. Smart Grid*, vol. PP, no. 99, p. 1, 2016.

[19] C. He, C. Dai, L. Wu, and T. Liu, "Robust network hardening strategy for enhancing resilience of integrated electricity and natural gas distribution systems against natural disasters," *IEEE Trans. Power Syst.*, vol. 33, no. 5, pp. 5787–5798, Sep. 2018.

[20] E. Yamangil, R. Bent, and S. Backhaus, "Resilient upgrade of electrical distribution grids," in *Twenty-Ninth AAAI Conference on Artificial Intelligence*, Austin, Texas, USA, Jan. 2015, pp. 1233–1240.

[21] A. Arab, A. Khodaei, S. K. Khator, K. Ding, V. A. Emesih, and Z. Han, "Stochastic pre-hurricane restoration planning for electric power systems infrastructure," *IEEE Trans. Smart Grid*, vol. 6, no. 2, pp. 1046–1054, Mar. 2015.

[22] A. Barnes, H. Nagarajan, E. Yamangil, R. Bent, and S. Backhaus, "Resilient design of large-scale distribution feeders with networked microgrids," *Electric Power Systems Research*, vol. 171, pp. 150–157, 2019.

[23] M. H. Amirioun, F. Aminifar, and H. Lesani, "Resilience-oriented proactive management of microgrids against windstorms," *IEEE Trans. Power Syst.*, vol. PP, no. 99, p. 1, 2017.

[24] M. Panteli, D. N. Trakas, P. Mancarella, and N. D. Hatziargyriou, "Boosting the power grid resilience to extreme weather events using defensive islanding," *IEEE Trans. Smart Grid*, vol. 7, no. 6, pp. 2913–2922, Nov. 2016.

المنارة للاستشارات
www.manaraa.com

[25] M. H. Amirioun, F. Aminifar, and H. Lesani, "Towards proactive scheduling of microgrids against extreme floods," *IEEE Trans. Smart Grid*, vol. 9, no. 4, pp. 3900–3902, Jul. 2018.

[26] A. Gholami, T. Shekari, and S. Grijalva, "Proactive management of microgrids for resiliency enhancement: An adaptive robust approach," *IEEE Trans. Sustain. Energy*, vol. 10, no. 1, pp. 470–480, Jan. 2019.

[27] K. S. A. Sedzro, A. J. Lamadrid, and L. F. Zuluaga, "Allocation of resources using a microgrid formation approach for resilient electric grids," *IEEE Trans. Power Syst.*, vol. 33, no. 3, pp. 2633–2643, May 2018.

[28] S. Lei, J. Wang, C. Chen, and Y. Hou, "Mobile emergency generator pre-positioning and real-time allocation for resilient response to natural disasters," *IEEE Trans. Smart Grid*, vol. 9, no. 3, pp. 2030–2041, 2018.

[29] A. Arif, Z. Wang, C. Chen, and B. Chen, "A stochastic multi-commodity logistic model for disaster preparation in distribution systems," *IEEE Trans. Smart Grid*, p. 1, 2019.

[30] A. Arif, Z. Wang, J. Wang, and C. Chen, "Power distribution system outage management with co-optimization of repairs, reconfiguration, and dg dispatch," *IEEE Trans. Smart Grid*, vol. 9, no. 5, pp. 4109–4118, Sep. 2018.

[31] H. Farzin, M. Fotuhi-Firuzabad, and M. Moeini-Aghtaie, "Enhancing power system resilience through hierarchical outage management in multi-microgrids," *IEEE Trans. Smart Grid*, vol. 7, no. 6, pp. 2869–2879, Nov. 2016.

[32] L. Che and M. Shahidehpour, "Adaptive formation of microgrids with mobile emergency resources for critical service restoration in extreme conditions," *IEEE Trans. Power Syst.*, vol. 34, no. 1, pp. 742–753, Jan. 2019.

[33] A. Sharma, D. Srinivasan, and A. Trivedi, "A decentralized multi-agent approach for service restoration in uncertain environment," *IEEE Trans. Smart Grid*, vol. 9, no. 4, pp. 3394–3405, Jul. 2018.

[34] C. Chen, J. Wang, F. Qiu, and D. Zhao, "Resilient distribution system by microgrids formation after natural disasters," *IEEE Trans. Smart Grid*, vol. 7, no. 2, pp. 958–966, Mar. 2016.

[35] N. Xu, S. D. Guikema, R. A. Davidson, L. K. Nozick, Z. Çağnan, and K. Vaziri, "Optimizing scheduling of post-earthquake electric power restoration tasks," *Earthquake engineering & structural dynamics*, vol. 36, no. 2, pp. 265–284, 2007.

[36] P. M. Carvalho, F. J. Carvalho, and L. A. Ferreira, "Dynamic restoration of large-scale distribution network contingencies: Crew dispatch assessment," in *2007 IEEE Lausanne Power Tech.* IEEE, 2007, pp. 1453–1457.

[37] C. Zapata, S. Silva, H. Gonzalez, O. Burbano, and J. Hernandez, "Modeling the repair process of a power distribution system," in *2008 IEEE/PES Transmission and Distribution Conference and Exposition: Latin America.* IEEE, 2008, pp. 1–7.

المنارة للاستشارات
www.manaraa.com

[38] V. J. Garcia, D. P. Bernardon, A. R. Abaide, O. A. Bassi, and G. Dhein, "Reliability assessment by coordinating maintenance vehicles in electric power distribution systems," *Procedia-Social and Behavioral Sciences*, vol. 111, pp. 1045–1053, 2014.

[39] A. Arif, S. Ma, Z. Wang, J. Wang, S. M. Ryan, and C. Chen, "Optimizing service restoration in distribution systems with uncertain repair time and demand," *IEEE Trans. Power Syst.*, vol. 33, no. 6, pp. 6828–6838, Nov. 2018.

[40] B. Chen, Z. Ye, C. Chen, J. Wang, T. Ding, and Z. Bie, "Toward a synthetic model for distribution system restoration and crew dispatch," *IEEE Trans. Power Syst.*, p. 1, 2018.

[41] S. Lei, C. Chen, Y. Li, and Y. Hou, "Resilient disaster recovery logistics of distribution systems: Co-optimize service restoration with repair crew and mobile power source dispatch," *IEEE Trans. Smart Grid*, p. 1, 2019.

[42] R. W. Wolfe and R. O. Kluge, "Designated fiber stress for wood poles," *Gen. Tech. Rep. FPL-GTR-158. Madison, WI: US Department of Agriculture, Forest Service, Forest Products Laboratory. 39 p.*, vol. 158, 2005.

[43] S. Bjarnadottir, Y. Li, and M. G. Stewart, "Hurricane risk assessment of power distribution poles considering impacts of a changing climate," *J. Infrastruct. Syst.*, vol. 19, no. 1, pp. 12–24, 2012.

[44] N. G. B. III, "ANSI-NESC update," 2005 AWPA Annual Meeting, Tech. Rep., 2005. [Online]. Available: http://woodpoles.org/portals/2/documents/ANSI_NESC_05.pdf

[45] R. Brown, "Cost-benefit analysis of the deployment of utility infrastructure upgrades and storm hardening programs," *Quanta Technology, Raleigh, NC*, 2009.

[46] Z. Wang and J. Wang, "Self-healing resilient distribution systems based on sectionalization into microgrids," *IEEE Trans. Power Syst.*, vol. 30, no. 6, pp. 3139–3149, 2015.

[47] Z. Wang, B. Chen, J. Wang, and C. Chen, "Networked microgrids for self-healing power systems," *IEEE Trans. Smart Grid*, vol. 7, no. 1, pp. 310–319, Jan. 2016.

[48] R. K. Ahuja, T. L. Magnanti, and J. B. Orlin, "Network flows: theory, algorithms, and applications," 1993.

[49] M. E. Baran and F. F. Wu, "Network reconfiguration in distribution systems for loss reduction and load balancing," *IEEE Trans. Power Deli.*, vol. 4, no. 2, pp. 1401–1407, Apr. 1989.

[50] S. Ma, S. Li, Z. Wang, A. Arif, and K. Ma, "A novel MILP formulation for fault isolation and network reconfiguration in active distribution systems," in *Proc. IEEE Power Energy Society General Meeting (PESGM)*, Portland, Oregon, USA, Aug. 2018, pp. 1–5.

[51] D. Gade, G. Hackebeil, S. M. Ryan, J.-P. Watson, R. J.-B. Wets, and D. L. Woodruff, "Obtaining lower bounds from the progressive hedging algorithm for stochastic mixed-integer programs," *Math. Program.*, vol. 157, no. 1, pp. 47–67, 2016.

المنارة للاستشارات
www.manaraa.com

[52] G. Guo, G. Hackebeil, S. M. Ryan, J.-P. Watson, and D. L. Woodruff, "Integration of progressive hedging and dual decomposition in stochastic integer programs," *Oper. Res. Lett.*, vol. 43, no. 3, pp. 311–316, 2015.

[53] G. L. Nemhauser and L. A. Wolsey, "Integer programming and combinatorial optimization," *Wiley, Chichester. GL Nemhauser, MWP Savelsbergh, GS Sigismondi (1992). Constraint Classification for Mixed Integer Programming Formulations. COAL Bulletin*, vol. 20, pp. 8–12, 1988.

[54] W. H. Kersting, "Radial distribution test feeders," in *IEEE Power Engineering Society Winter Meeting*, vol. 2. IEEE, 2001, pp. 908–912.

[55] R. E. Brown, "Hurricane hardening efforts in florida," in *Proc. IEEE Power and Energy Society General Meeting - Conversion and Delivery of Electrical Energy in the 21st Century*, Jul. 2008, pp. 1–7.

[56] A. Märkert and R. Gollmer, "User's guide to ddsip–ac package for the dual decomposition of two-stage stochastic programs with mixed-integer recourse," *Department of Mathematics, University of Duisburg-Essen, Duisburg*, 2008.

[57] G. Bayraksan and D. P. Morton, "Assessing solution quality in stochastic programs via sampling," *Tutorials in Operations Research*, vol. 5, pp. 102–122, 2009.

[58] S. Ma, S. Li, Z. Wang, and F. Qiu, "Resilience-oriented design of distribution systems," *IEEE Trans. Power Syst.*, vol. 34, no. 4, pp. 2880–2891, Jul. 2019.

[59] A. Arif, "Distribution system outage management after extreme weather events," 2019.

[60] R. Torquato, Q. Shi, W. Xu, and W. Freitas, "A Monte Carlo simulation platform for studying low voltage residential networks," in *Proc. IEEE Power Energy Society General Meeting*, Jul. 2015, p. 1.

[61] R. Rocchetta, Y. Li, and E. Zio, "Risk assessment and risk-cost optimization of distributed power generation systems considering extreme weather conditions," *Reliability Engineering & System Safety*, vol. 136, pp. 47–61, 2015.

[62] R. T. Rockafellar and S. Uryasev, "Conditional value-at-risk for general loss distributions," *Journal of banking & finance*, vol. 26, no. 7, pp. 1443–1471, 2002.

[63] ——, "Optimization of conditional value-at-risk," *Journal of risk*, vol. 2, pp. 21–42, 2000.

[64] X. Chen, W. Wu, and B. Zhang, "Robust restoration method for active distribution networks," *IEEE Trans. Power Syst.*, vol. 31, no. 5, pp. 4005–4015, Sep. 2016.

[65] A. Arif, Z. Wang, C. Chen, and J. Wang, "Repair and resource scheduling in unbalanced distribution systems using neighborhood search," *IEEE Trans. Smart Grid*, p. 1, 2019.

[66] B. Chen, C. Chen, J. Wang, and K. L. Butler-Purry, "Sequential service restoration for unbalanced distribution systems and microgrids," *IEEE Trans. Power Syst.*, vol. 33, no. 2, pp. 1507–1520, Mar. 2018.

المنارة للاستشارات
www.manaraa.com

[67] R. Dufo-López, J. L. Bernal-Agustín, J. M. Yusta-Loyo, J. A. Domínguez-Navarro, I. J. Ramírez-Rosado, J. Lujano, and I. Aso, "Multi-objective optimization minimizing cost and life cycle emissions of stand-alone pv–wind–diesel systems with batteries storage," *Applied Energy*, vol. 88, no. 11, pp. 4033–4041, 2011.

[68] B. Chen, C. Chen, J. Wang, and K. L. Butler-Purry, "Multi-time step service restoration for advanced distribution systems and microgrids," *IEEE Trans. Smart Grid*, vol. 9, no. 6, pp. 6793–6805, Nov. 2018.

[69] F. Y. Melhem, O. Grunder, Z. Hammoudan, and N. Moubayed, "Energy management in electrical smart grid environment using robust optimization algorithm," *IEEE Trans. Ind. Appl.*, vol. 54, no. 3, pp. 2714–2726, May 2018.

[70] W. Römisch and S. Vigerske, "Recent progress in two-stage mixed-integer stochastic programming with applications to power production planning," in *Handbook of Power Systems I.* Springer, 2010, pp. 177–208.

[71] R. T. Rockafellar and R. J.-B. Wets, "Scenarios and policy aggregation in optimization under uncertainty," *Math. Oper. Res.*, vol. 16, no. 1, pp. 119–147, 1991.

[72] S. M. Ryan, R. J.-B. Wets, D. L. Woodruff, C. Silva-Monroy, and J.-P. Watson, "Toward scalable, parallel progressive hedging for stochastic unit commitment," in *2013 IEEE Power & Energy Society General Meeting.* IEEE, 2013, pp. 1–5.

[73] F. D. Munoz and J.-P. Watson, "A scalable solution framework for stochastic transmission and generation planning problems," *Computational Management Science*, vol. 12, no. 4, pp. 491–518, 2015.

[74] L. Su and C. Kwon, "Risk-averse network design with behavioral conditional value-at-risk for hazardous materials transportation," 2018.

[75] S. M. Amin and B. F. Wollenberg, "Toward a smart grid: power delivery for the 21st century," *IEEE Power and Energy Magazine*, vol. 3, no. 5, pp. 34–41, Sep. 2005.

[76] S. Ma, N. Carrington, A. Arif, and Z. Wang, "Resilience assessment of self-healing distribution systems under extreme weather events," in *2019 IEEE Power & Energy Society General Meeting (PESGM)*, Aug. 2019.

المنارة للاستشارات
www.manaraa.com